SIMULATION OF SOLAR ABSORPTION AIR CONDITIONING

BY

JEFFREY CLAY BLINN

MASTER OF SCIENCE
(CHEMICAL ENGINEERING)

UNIVERSITY OF WISCONSIN-MADISON

1979

SIMULATION OF SOLAR ABSORPTION AIR CONDITIONING

BY

JEFFREY CLAY BLINN

A thesis submitted in partial fulfillment of the
requirements for the degree of

MASTER OF SCIENCE
(Chemical Engineering)

at the

UNIVERSITY OF WISCONSIN-MADISON

(1979)

ACKNOWLEDGEMENTS

I would like to thank my advisors, Professors Jack Duffie and John W. Mitchell, for their support, assistance and encouragement. I would like to thank Tom Freeman, John C. Mitchell, Pat Hughes and Warren Buckles for their amazing patience in answering my questions on TRNSYS and programming in general. The ideas, suggestions and support provided by my fellow grad students and the rest of the Solar Lab staff are greatly appreciated. The people of the Solar Energy Applications Laboratory at Colorado State University were also very helpful.

A special measure of thanks goes to my wife Cindy for her patience, love and encouragement during my graduate school career, and to my son Mike just for being himself. Finally, I thank my parents for all they have done to bring me this far.

This work was supported by the Solar Heating and Cooling Research and Development Branch, Office of Conservation and Solar Applications, U.S. Department of Energy under contract E (11-1)-2588.

TABLE OF CONTENTS

List of Figures

List of Tables

Nomenclature

A	Collector Area
b_n	Wall transfer function Coefficient
C_e	Cost of electricity
C_f	Cost of backup fuel
C_g	Thermal Capacitance of generator and solution
C_m	Room moisture capacitance
C_p	Specific Heat
C_s	Solution thermal capacitance
COP or COP_a	Coefficient of performance of absorption chiller
COP_b	Coefficient of performance of backup chiller
d_n	Wall transfer function coefficient
f	Fraction by solar
F'	Collector efficiency factor
F_R	Collector heat removal factor
G	Mass flow rate per unit collector area
H_T	Insolation on tilted surface
$\dot{m}_{cond}$	Rate of water vapor removal by condensation
$\dot{m}_{gen}$	Rate of water vapor addition by internal generation
$\dot{m}_{ch}$	Mass flow rate of chilled water
$\dot{m}_{hw}$	Mass flow rate of firing water
$\dot{m}_{ss}$	Mass flow rate of strong solution
$\dot{m}_{ws}$	Mass flow rate of weak solutin
$\dot{m}_w$	Mass of moisture present in conditioned space
Q	Integrated heat flow
$\dot{Q}$	Instantaneous heat flow

SUBSCRIPTS ON Q OR $\dot{Q}$

coil	at cooling coil
cool	into evaporator
cool,a	into evaporator of absorption chiller
cool,b	into evaporator of backup chiller

	dump	dumped by relief valve
	gen	into generator
	lat	latent
	sens	sensible
	shg	sensible heat gains
	u	useful collected
T	Temperature	

SUBSCRIPTS ON T

a	at absorber exit
aux	auxiliary supply
c	condensing water inlet
ch	chilled water delivery
ch,in	chilled water exit
cmax	maximum condensing water temperature
cmin	minimum condensing water temperature
cr	changeover temperature
e	effective sol-air temperature
env	temperature of surroundings
g	generator temperature
g,avg	generator averaged over timestep
g,avg	generator averaged over period when $T_g > T_{gmin}$
gmin	minimum generator temperature to produce cooling
g,ss	steady state generator temperature
hw	firing water inlet temperature
hw,ret	firing water return temperature
i	coil inlet temperature
o	coil outlet temperature
r	room temperature
rd	room design temperature
s	coil surface temperature
smin	minimum solar source temperature
stor	storage temperature
wb	wet bulb temperature
2	generator inlet solution temperature

t	time
U	Overall heat transfer coefficient
U_L	Collector loss coefficient
$(UA)_{fc}$	Chiller free convection loss coefficient
$(UA)_o$	Generator heat transfer coefficient
$\dot{V}_{inf}$	Volume infiltration rate
W_{amb}	Ambient humidity ratio
W_r	Room humidity ratio
W_s	Saturation humidity ratio at coil surface
x_w or x_{ws}	Weight fraction LiBr in weak solution
x_s or x_{ss}	Weight fraction LiBr in strong solution
α	Absorptivity
$\gamma-$	Thermostat state of previous timestep
$\gamma+$	Thermostat state of current timestep
Δh_{vap}	Heat of vaporization of water
Δt	Timestep
ε	Emissivity
ε_g	Generator heat exchange effectiveness
ε_s	Sensible heat exchanger effectiveness
η_{ah}	Auxiliary boiler efficiency
η_c	Collector efficiency
ϕ	Fraction of timestep in which $T_g > T_{gmin}$
ρ_{air}	Density of air
τ_c	Chiller cooldown time constant
τ_h	Chiller startup time constant

Abstract

A model of the transient and steady-state performance of a single-effect lithium bromide-water absorption chiller has been developed. All startup transients are assumed to be accounted for by the thermal storage of the solution and hardware in the generator. The generator is treated as a single node thermal capacitance, leading to a model in which the temperature of solution in the generator exponentially approaches its steady-state value. When the chiller is idle the solution temperature decays exponentially towards the temperature of the surroundings. The generator temperature transients are characterized by two time constants, one applying to startup and one applying to cooldown. The instantaneous performance during transient operation is a function of the instantaneous generator and condensing water temperatures.

TRNSYS simulations of residential air-conditioning systems were in Miami, FL, Charleston, SC and Columbia, MO and were run using this model, with performance data and time constants for a commercially available three-ton absorption chiller. Over the course of a cooling season, chiller transients were found to lead to reductions of approximately 5-8% in COP and air conditioning load met by solar. The effect of the transients was most pronounced during the months in which the cooling load was lowest and was less noticeable in months with high cooling loads. Increasing the room thermostat deadband decreased the frequency of chiller cycling and significantly improved system performance.

Four different auxiliary strategies were also examined and compared. In three cases, auxiliary was provided in the form of heat to operate the absorption chiller. Heat was either added directly to the generator with no solar contribution in the auxiliary mode (parallel heat auxiliary), to the firing water stream between storage and generator (series heat auxiliary). One mode (series-parallel heat auxiliary) chooses between series and parallel heat auxiliary based on storage tank temperature. The fourth mode uses a separate vapor-compression air conditioner as a backup.

Series heat auxiliary required 9-10% more auxiliary energy than did parallel heat or series-parallel heat auxiliary. Vapor compression auxiliary led to a slightly higher fraction by solar than any of the heat auxiliary modes. Any choice between heat and vapor compression auxiliary would have to be made on economic grounds.

When heat auxiliary was used, the optimum auxiliary supply temperature was found to be approximately 90°C for the particular chiller simulated. This corresponds to the temperature at which the chiller shows the highest steady state COP.

The optimum value of the minimum solar source temperature on chiller operation was found to be 77°C, which is very close to the minimum firing water supply temperature for chiller operation. The value of the optimum minimum temperature was not affected by collector U_L.

CHAPTER I

Introduction

1.1. Objectives

The objectives of the work leading to this thesis were twofold. The first goal was the development of a model for simulating solar powered absorption air conditioning which accounted for startup transients in the absorption chiller. This phase of the project is described in Chapters 2 and 3.

After developing the absorption air conditioner model, the next objective was to simulate residential solar air conditioning systems. Topics investigated included the effects of chiller start-up transients, room thermostat deadband and auxiliary control strategy on system performance. The simulation phase of this project is described in Chapters 4, 5 and 6.

1.2 Previous Work

There has been significant research and development effort on the design, construction and testing of absorption air conditioning units. The report of Farber et al. (1) contains an extensive data base and bibliography for absorption air conditioning. The report of Auh (2) of Brookhaven National Laboratory provides a description of the principles of absorption air conditioning and a survey of research in solar absorption air conditioning as of July, 1977. The reports by Farber et al. and Auh provide a good overview of past research in solar absorption air conditioning.

In 1959 Chung, Löf and Duffie (3) proposed using solar energy to operate a lithium bromide-water absorption air conditioner. They simulated, on an hourly basis, a system comprising a collector, storage tank and absorption air conditioner for one clear and one cloudy day and concluded that solar absorption air conditioning was technically feasible.

In 1973, Butz (4) simulated the performance of a residential solar heating and air conditioning system in Albuquerque, New Mexico. The air conditioning system used a lithium bromide-water absorption chiller controlled by a room thermostat. A quasi-steady chiller model was used, i.e. the chiller responded instantly when it was turned on or when operating conditions changed. Butz found that solar energy could provide a significant fraction of the cooling needed in the residence simulated. An economic analysis was performed to determine the combinations of collector, fuel and electricity costs under which a solar heating-cooling system was economically justifiable.

Allen, Moore, et al. (5) performed a simulation study of a solar air conditioning system comprising an ammonia-water absorption chiller, collectors and a storage tank for chilled water (cold side storage). Effects of non-idealities in the absorption cycle (i.e. finite temperature differences across heat exchangers, and pressure drops in fluid flow paths) were evaluated. In addition, results obtained using high and low performance flat plate collectors were compared. This study, like the Butz study, used a quasi-steady

chiller model. The ratio of heat taken up in the evaporator (cooling produced) to insolation on the collectors ranged from 0.1 for the low performance collectors to 0.5 for the high performance collectors.

Experimental studies of a solar absorption air conditioning system have been in progress since 1973 at Colorado State University Solar House I in Fort Collins, CO (2,6,7,8,9). Initially (6) an Arkla-Servel lithium bromide-water air conditioner (modified for solar operation) and flat plate collectors were used. Later an advanced lithium bromide-water chiller (Arkla model WF-36) and Corning evacuated tubular collectors were added (7).

It was found that a significant fraction of the cooling load could be met by solar. As an example, in August, 1977 the Arkla WF-36 chiller and Corning evacuated tubular collectors met 43% of the house cooling load for the month (9).

It was observed at CSU that the average coefficient of performance of the chiller was degraded significantly when the chiller was cycled on and off frequently by the room thermostat during periods of low cooling load (2,8,9). For example, the Arkla-Servel chiller gave a COP of 0.37 during September, 1974, a month of low cooling load. This compares unfavorably to a 1974 seasonal average COP of 0.59. Figure 1.2.1 shows the effect of cycling on the cooling capacity and COP of the Arkla-Servel chiller during one day. (As of this writing no similar data has been published for the Arkla WF-36 chiller in CSU House I.)

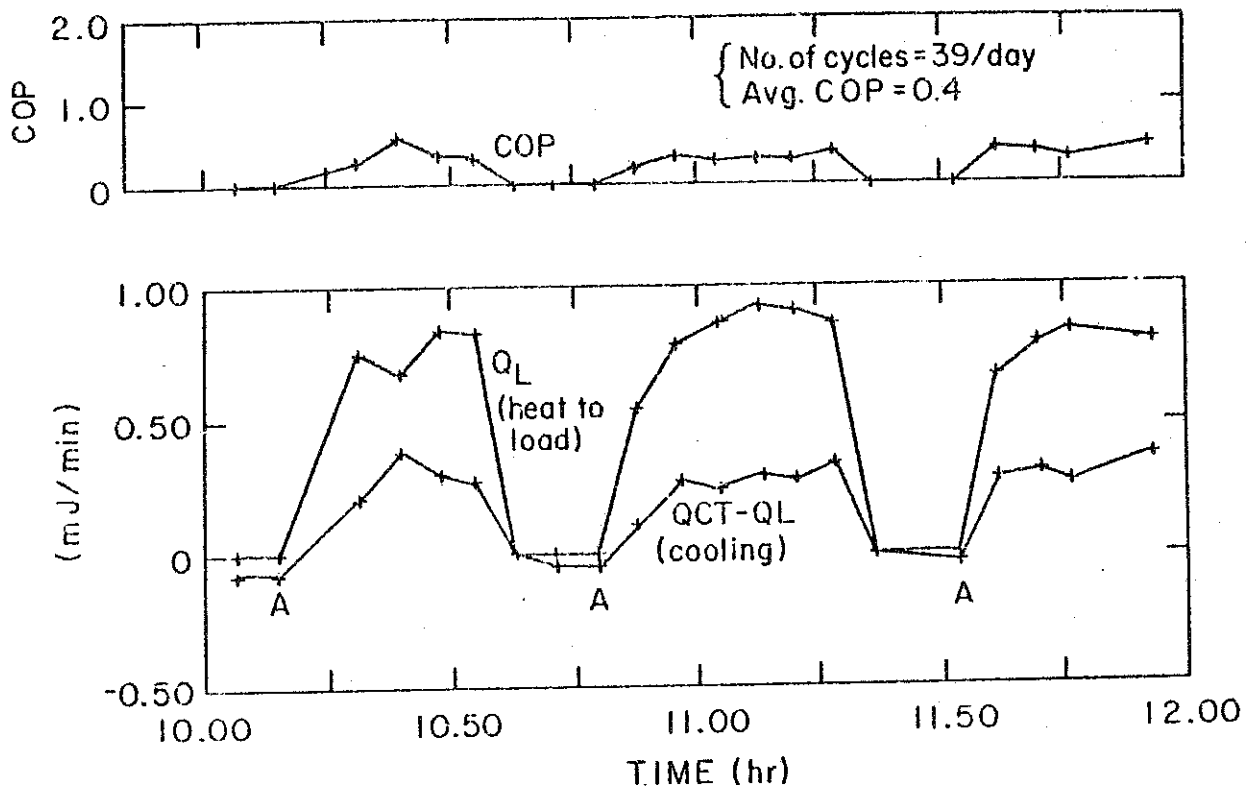

FIGURE 1.2.1: TRANSIENT PERFORMANCE OF AN ARKLA-SERVEL CHILLER AT CSU HOUSE I (2)

Hoover, Ochs and Bradley (10) have simulated the transient performance of an Arkla WF-36 chiller using an empirical relation between the chiller idle time and the initial reduction in COP and capacity over a specified time interval following startup. A chiller used to cool a laboratory building in Boulder City, Nevada was simulated on an hourly basis for the month of June, 1976. Chiller cycling during the first half of the month led to a 7% reduction in chiller capacity. Significant improvements in system performance were observed when cold side storage was added to reduce chiller cycling.

In light of the experience of the researchers at CSU House I and the work of Hoover et al., further study of the transient performance of solar absorption chillers is needed. In this thesis a simple theoretical model is developed to describe the operational transients of a single-effect absorption chiller. The model is then applied to simulations of residential solar air conditioning systems.

CHAPTER II

Transient Modeling of a Single-Effect Absorption Chiller

2.1 The Absorption Refrigeration Cycle

A simple single-effect lithium bromide-water refrigeration machine is shown schematically in Figure 2.1.1 The corresponding thermodynamic cycle is sketched on a pressure-temperature-composition (PTX) diagram in Figure 2.1.2.

Heat is supplied to the generator to boil off water vapor from a solution of lithium bromide and water. Solution enters the generator at concentration x_w and leaves at point G on Figure 2.1.2.

The water vapor evolved in the generation is condensed in the condenser (point C on Figure 2.1.2) and sent through a pressure reducing device to the evaporator (point E in Figure 2.1.2) where it boils at a low temperature and pressure to provide the refrigeration effect.

The solution leaving the generator (the so-called "strong solution") travels through a sensible heat exchanger (SHX in Figure 2.1.1) where it is cooled and the weak solution entering the generator is preheated. The strong solution enters the absorber, where it is contacted with water vapor from the evaporator. The water vapor is absorbed into the strong solution, and the resulting weak solution (point A, Figure 2.1.2) is pumped to the generator through the sensible heat exchanger.

Heat is rejected from the absorber to some low-temperature sink (e.g. cooling water) to remove the heat of mixing and the

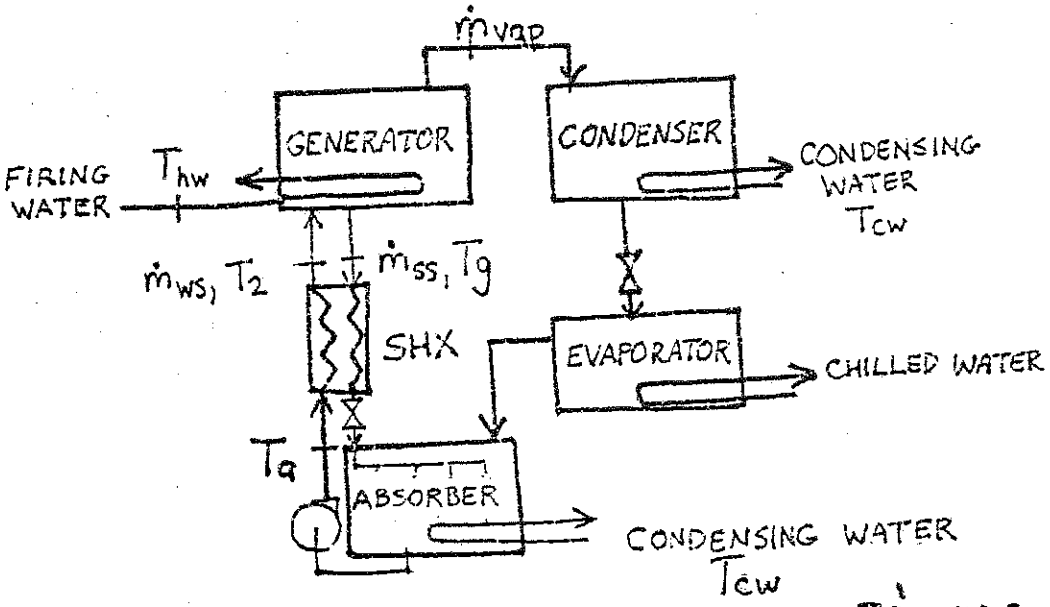

FIGURE 2.1.1 SINGLE EFFECT LITHIUM BROMIDE - WATER ABSORPTION CHILLER.

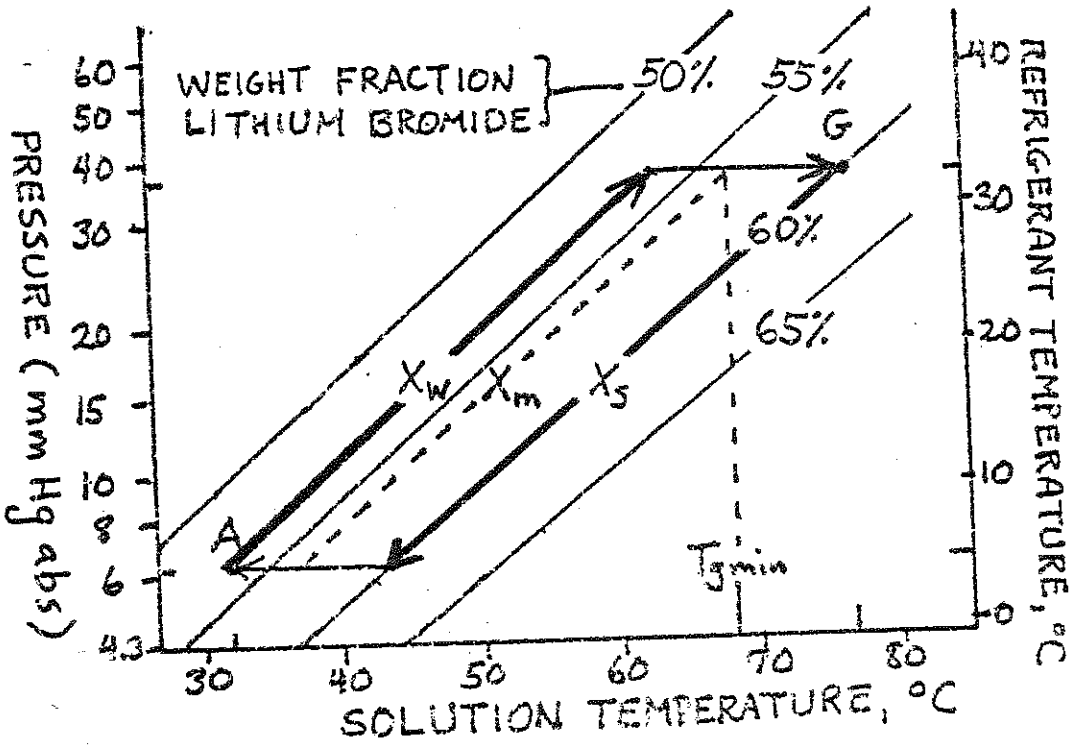

FIGURE 2.1.2 PTX DIAGRAM FOR LITHIUM BROMIDE AND WATER

sensible heat transported in by the strong solution.

The rate of cooling is approximately proportional to the rate at which the water vapor is evolved in the generator. The rate at which water vapor is evolved can be shown to be a function of the ratio of x_w to x_s. A material balance on lithium bromide flow through the generator yields:

$$\dot{m}_{ws} x_w = \dot{m}_{ss} x_s \qquad (2.1.1)$$

which may be rearranged to

$$\dot{m}_{ss} = \dot{m}_{ws} \frac{x_w}{x_s} \qquad (2.1.2)$$

An overall mass balance for the generator yields:

$$\dot{m}_{vap} = \dot{m}_{ws} - \dot{m}_{ss} \qquad (2.1.3)$$

Inserting 2.1.2 into 2.1.3 gives

$$\dot{m}_{vap} = \dot{m}_{ws} (1 - \frac{x_w}{x_s}) \qquad (2.1.4)$$

If $\dot{m}_{ws}$ is fixed by the solution pump, it follows that the refrigeration effect is proportional to $(\frac{x_s - x_w}{x_s})$.

Chiller cooling capacity can be increased by increasing x_s or decreasing x_w. An increase in x_s may be achieved by lowering the generator pressure (which is set by the condenser temperature) or by raising the generator temperature. A decrease in x_w may be obtained by raising the absorber pressure (which is set by the

condenser temperature) or by raising the generator temperature. A decrease in x_w may be obtained by raising the absorber pressure (which is set by raising the evaporator temperature) or by lowering the absorber temperature. Thus, cooling capacity will depend on evaporator, absorber, generator and condenser temperatures.

When the chiller is not operating, the lithium bromide and water charge in the chiller will form a solution of concentration x_m (Figure 2.1.2). If the chiller has been idle for a long time, the solution will have cooled to a temperature near that of its surroundings. If heat is then added at the generator, the generator temperature T_g will begin to rise. The pressure in the generator will rise until it reaches a value at which vapor begins to condense in the condenser. Up to this point, no liquid water has left the condenser to be boiled in the evaporator, and therefore there has been no refrigeration effect.

As the generator temperature is increased further, the generator pressure does not increase due to the fact that generator pressure is now determined by the vapor pressure in the condenser. To maintain equilibrium, x_s must increase. Water vapor must be evolved in the generator as per equation 2.1.4, and heat will began to be taken up in the evaporator.

Thus it can be seen that there is a minimum value of T_g below

which no cooling will occur and that this value is fixed by the initial lithium bromide concentration and the equilibrium vapor pressure in the condenser.

2.2 Transient Modeling of Absorption Chiller

It is possible to rigorously model the steady-state performance of an absorption chiller by solving all of the appropriate thermodynamic and heat-transfer equations that apply to the cycle, for all operating conditions of interest. This approach would probably be taken in designing a chiller to meet a known set of performance objectives.

An easier approach to simulating the steady state performance of an absorption chiller is to use an empirical or "black box" model. The performance of the chiller at steady state is expressed as a function of operating conditions, often by a curve fit of experimental operating data. This approach has been used by Butz et al. to simulate solar-operated absorption air conditioning.

Unfortunately, in a residential application, the chiller often does not operate at steady state. This is a result of the control strategy most commonly employed, in which a room thermostat calls for cooling when the room temperature rises above a set point, and shuts the chiller off when the room temperature drops below this point. If the chiller's cooling capacity is significantly greater than the building cooling load, the thermostat will cycle fairly frequently and the chiller will spend most of its operating time in

a transient mode. Because of this, it is desirable to have some way of evaluating the effect of cycling on chiller performance.

The model described below was developed for use in TRNSYS (11), a transient simulation program. In a TRNSYS simulation, system conditions are calculated at timesteps on the order of 0.25-1.0 hours apart. Thus, a monthly simulation can include several thousand timesteps. Since the chiller model subroutine in a TRNSYS simulation will be called so often, it is definitely desirable to make it as computationally simple as possible.

A rigorous heat-transfer and thermodynamic approach to chiller transient modeling was rejected as being computationally too complicated. A purely empirical approach was unpromising because of the scarcity of transient-mode chiller performance data. The model that was finally developed combines elements of both of these approaches.

Consider the lithium bromide-water chiller diagrammed in Figures 2.1.1 and 2.1.2. The key variables, as discussed in Section 2.1, are condenser temperature (which fixes the condenser and generator pressures), evaporator temperature (which fixes the evaporator and absorber pressures), the generator temperature (which, with condensing pressure, fixes the strong solution concentration) and absorber temperature (which, in conjunction with the evaporator pressure, fixes the concentration of the weak solution going to the generator). The rate of water vapor evolution in the generator is fixed by the difference between the weak and strong solution concentrations.

To model the transient behavior of the chiller, the following assumptions are made:

1. The generator behaves as a single node system with effective thermal capacitance Cg.
2. The absorber, sensible heat exchanger and generator may be characterized as constant effectiveness heat exchangers when T_g is below T_{gmin} and $\dot{m}_{vap}$ is zero.
3. The absorber and sensible heat exchanger respond very rapidly to changes in temperature.
4. The thermal capacitance rate of the firing water supplied to the generator is greater than the thermal capacitance rate of the weak solution.

Consider the chiller shown in Figure 2.1.1, in the case where heat is being supplied to the generator but water vapor is not being generated (i.e. T_g is less than T_{gmin}). From the assumptions above, the rate at which heat is supplied to the generator is given by

$$\dot{Q}_{gen} = \varepsilon_g (\dot{m}C_p)_{ws} (T_{hw} - T_2) \qquad (2.2.1)$$

A transient energy balance on the generator yields:

$$C_g \frac{dT_g}{dt} = \varepsilon_g (mC_p)_{ws} (T_{hw}-T_2)-(mC_p)_{ws}(T_g-T_2) \qquad (2.2.2)$$

For the sensible heat exchanger

$$\varepsilon_s (T_g-T_a) = T_2-T_a \qquad (2.2.3)$$

which rearranges to

$$T_2 = \varepsilon_s T_g + (1-\varepsilon_s)T_a \qquad (2.2.4)$$

Inserting 2.2.4 into 2.2.2 and rearranging,

$$\frac{dT_g}{dt} = \frac{(\dot{m}C_p)_{ws}}{C_g} = [\varepsilon_g T_{hw} + (1-\varepsilon_s)(1-\varepsilon_g)T_a - (1-\varepsilon_s(1-\varepsilon_g))T_g] \qquad (2.2.5)$$

which may be further rearranged to yield

$$\frac{dT_g}{dt} = \frac{(\dot{m}C_p)_{ws}(1-\varepsilon_s)(1-\varepsilon_g)}{C_g} \left[\frac{\varepsilon_g T_{hw} + (1-\varepsilon_s)(1-\varepsilon_g)T_a}{1-\varepsilon_s(1-\varepsilon_g)} - T_g\right] \qquad (2.2.6)$$

The steady-state generator temperature is obtained by setting the right hand side equal to zero:

$$T_{g,ss} = \frac{\varepsilon_g T_{hw} + (1-\varepsilon_s)(1-\varepsilon_g)\ T_a}{1-\varepsilon_s(1-\varepsilon_g)} \qquad (2.2.7)$$

Defining the startup time constant, τ_h, as

$$\tau_h = \frac{C_g}{(\dot{m}C_p)_w\ (1-\varepsilon_s(1-\varepsilon_g))} \qquad (2.2.8)$$

equation 2.2.6 may be rewritten as

$$\frac{dT_g}{dt} = \frac{T_{g,ss} - T_g}{\tau_h} \qquad (2.2.9)$$

If the chiller is at a temperature $T_{g,o}$ at time τ_o, the solution to 2.2.9 is

$$T_g(t) = T_{g,ss} + (T_{g,o} - T_{g,ss})\exp\left(-\frac{(t-t_o)}{\tau_h}\right) \qquad (2.2.10)$$

When the chiller is shut off, solution will drain to the lowest part of the chiller and cool down by conduction and free convection. A transient energy balance on the solution shutdown yields

$$C_s \frac{dT_s}{dt} = (UA)_{fc}\ (T_{env} - T_s) \qquad (2.2.11)$$

If at $t=t_o$, $T_s=T_{s,o}$, equation 2.2.11 has the solution

$$T_s(t) = T_{env} + (T_{s,o} - T_{env}) \exp\left(-\frac{(t-t_o)}{\tau_c}\right) \qquad (2.2.12)$$

where the cooldown time constant τ_c is defined as

$$\tau_c = \frac{C_s}{(UA)_{fc}} \qquad (2.2.13)$$

To complete the transient model, it is assumed that the condenser, evaporator and absorber respond to changes in temperature much more rapidly than the generator, and that the instantaneous performance of the chiller is a unique function of generator temperature, cooling water inlet temperature (which fixes condenser and absorber temperatures) and chilled water delivery temperature (which fixes evaporator temperature). These assumptions are justified by noting that the largest temperature swings occur in the generator (the absorber, evaporator and condensor operate fairly close to ambient temperature, while the generator operates some 50°C higher) and that the thermal capacitance of the solution in the generator-absorber loop is much greater than that of the vapor in the condensor and evaporator.

Additionally, although equation 2.2.9 was derived for the situation in which T_g is less than T_{gmin}, we assume that it is approximately valid over the entire range of operating temperatures encountered. The difference between room temperature and T_{gmin} is usually considerably greater than the difference between T_{gmin} and the maximum generator temperature. It will be shown in Chapter 4

that equation 2.2.9 provides a good fit to an observed generator temperature history for T_g both above and below T_{gmin}.

When T_g is above T_{gmin}, cooling and generator heat uptake are expressed as functions of T_g and T_c, with the chilled water temperature assumed constant:

$$\dot{Q}_{cool} = f_1 (T_g, T_c) \tag{2.2.14}$$

$$Q_{gen} = f_2 (T_g, T_c) \tag{2.2.15}$$

The function f_1 and f_2 may have any convenient form. For the simulations to be described in this thesis, f_1 and f_2 were expressed as quadratic functions of T_g and T_c

$$f_1(T_g,T_c) = (\text{Rated chiller capacity}) \times CAPY(T_g,T_c) \tag{2.2.16}$$

$$\begin{aligned} CAPY(T_g,T_c) = {} & a_{11}+a_{12}T_c+a_{13}T_c^2 + \\ & (a_{21}+a_{22}T_c+a_{23}T_c^2)T_g + \\ & (a_{31}+a_{32}T_c+a_{33}T_c^2)T_g^2 \end{aligned} \tag{2.2.17}$$

$$f_2(T_g,T_c) = \frac{f_1(T_g,T_c)}{COP(T_g,T_c)} \tag{2.2.18}$$

$$\begin{aligned} COP(T_g,T_c) = {} & b_{11}+b_{12}T_c+b_{13}T_c^2 + \\ & (b_{21}+b_{22}T_c+b_{23}T_c^2)T_g + \\ & (b_{31}+b_{32}T_c+b_{33}T_c^2)T_g^2 \end{aligned} \tag{2.2.19}$$

Values of a_{ij} and b_{ij}, and graphs of $f_1(T_g,T_c)$ and $COP(T_g,T_c)$ for the specific chiller simulated appear in Chapter 4.

When the generator temperature is below T_{gmin},

$$\dot{Q}_{cool} = 0 \tag{2.2.20}$$

$$\dot{Q}_{gen} = (UA)_o(T_{hw}-T_g) \tag{2.2.21}$$

where $(UA)_o$ is the heat exchange parameter for the generator under conditions in which no water vapor is evolved (i.e. non-boiling conditions).

Equations 2.2.7 through 2.2.21 make it possible to calculate the generator or solution temperature at any time, and to calculate chiller performance as a function of generator temperature.

CHAPTER III

Computer Modeling of Solar Absorption Air Conditioning

3.1 The Transient Simulation Program

A solar air conditioning system consists of a number of hardware components (including the building, collectors, storage, controls and the absorption chiller) connected by pipes and wires and driven by time-varying forcing functions (insolation and other meteorological conditions).

TRNSYS is a transient simulation program written at the University of Wisconsin specifically for the purpose of simulating solar energy systems. TRNSYS is a FORTRAN program which models individual components with FORTRAN subroutines. The transfer of information which is accomplished by pipes and wires in a real system is accomplished through input and output arrays in the FORTRAN subroutines. Weather or other forcing data is read in from cards or tape. TRNSYS iteratively solves the simultaneous differential and algebraic equations in the component subroutines using a modified Euler algorithm with a fixed timestep.

The TRNSYS program is discussed in much greater detail by Klein, Beckman and Duffie (11) and in the TRNSYS User's Manuel (12). The User's Manual, in particular, gives detailed mathematical descriptions of existing standard TRNSYS components. The remainder of this chapter is devoted to discussing non-standard TRNSYS components used in simulating solar absorption air conditioning systems.

3.2 TRNSYS Component For Transient Chiller Model

3.2.1 Absorption Chiller Transients

The transient chiller model described in Chapter 2 was incorporated into a component subroutine for use in TRNSYS. In this subroutine, firing water and condensing water temperatures are assumed constant throughout a given timestep. The generator temperature varies through the timestep as per equations 2.2.10 and 2.2.12, i.e. when chiller is operating:

$$T_g^+ = T_{g,ss} + (T_g^- - T_{g,ss}) \exp(^-\Delta t/\tau_h) \qquad (3.2.1)$$

and when chiller is idle:

$$T_g^+ = T_{env} + (T_g^- - T_{env}) \exp(^-\Delta t/\tau_c) \qquad (3.2.2)$$

There are several cases which must be considered when the chiller is operating. If over the entire timestep the generator temperature is below T_{gmin}, no cooling is delivered. The cooling capacity is given by

$$\dot{Q}_{cool} = 0 \qquad (3.2.3)$$

and, by analogy with equation 2.2.19, the average rate of heat uptake at the generator is

$$\dot{Q}_{gen} = (UA)_o (T_{hw} - T_{gavg}) \qquad (3.2.4)$$

The average generator temperature over the timestep, T_{gavg}, is calculated as

$$T_{gavg} = T_{g,ss} + \left(\frac{\tau_h}{\Delta t}\right)(T_g^- - T_{g,ss})\left(1 - \exp\left(\frac{-\Delta t}{\tau_h}\right)\right) \qquad (3.2.5)$$

If T_g is above T_{gmin} throughout the entire timestep, the average rate of cooling and heat uptake at the generator are calculated by analogy to equations 2.2.14 and 2.2.15 as

$$\dot{Q}_{cool} = f_1 (T_{gavg}, T_c) \tag{3.2.6}$$

$$\dot{Q}_{gen} = f_2 (T_{gavg}, T_c) \tag{3.2.7}$$

where f_1 and f_2 are empirical functions described in Chapter 2.

A third case which must be considered occurs when T_g^- is below T_{gmin} and T_g^+ is above T_{gmin}, or vice versa. In this case, T_g will be above T_{gmin} for a fraction of the timestep, ϕ, calculated as

$$\phi = 1 - \frac{\tau_h}{\Delta t} \log \left(\frac{T_{g,ss} - T_g^-}{T_{g,ss} - T_{gmin}}\right) \tag{3.2.8}$$

when T_g^- is below T_{gmin}, or

$$\phi = 1 - \frac{\tau_h}{\Delta t} \log \left(\frac{T_{g,ss} - T_g^+}{T_{g,ss} - T_{gmin}}\right) \tag{3.2.9}$$

when T_g is below T_{gmin}. The average generator temperature over the period in which T_g is above T_{gmin} is calculated:

$$T'_{gavg} = T_{g,ss} + \left(\frac{\tau_h}{\bar{\phi}\Delta t}\right)(T_{gmin} - T_{g,ss})\left(1 - \exp\left(\frac{-\bar{\phi}\Delta t}{\tau_h}\right)\right) \tag{3.2.10}$$

The cooling delivered over the timestep is

$$\dot{Q}_{cool} = \phi f_1 (T'_{gavg}, T_c) \tag{3.2.11}$$

and the heat uptake at the generator is

$$\dot{Q}_{gen} = (1-\phi)(UA)_o (T_{hw} - T_{gavg}) + \phi f_2 (T'_{gavg}, T_c) \tag{3.2.12}$$

Equations 3.2.1 through 3.2.12 make it possible to calculate the generator temperature history and chiller performance within any timestep.

3.2.2 Firing Water Pump and Cooling Tower

The firing water pump delivers a constant flowrate whenever the chiller operates. The TRNSYS component outputs the firing water flowrate and return temperature whenever the chiller is operating in a mode in which firing water is withdrawn from storage.

The cooling tower is modeled by assuming that the return cooling water is delivered at a constant increment above ambient wet bulb temperature. A thermostatically controlled cooling tower fan is modeled so that the cooling tower never returns water below a set minimum temperature, $T_{cmin.}$ Another thermostatic switch shuts off the chiller if the condensing water temperature exceeds a set maximum value, T_{cmax}.

3.2.3 Auxiliary Heater and Controls

Auxiliary energy is needed to run the chiller if the solar source temperature is too low to operate the chiller, or if the chiller capacity is too low to meet the cooling load imposed on it with firing water at the solar source temperature.

In the TRNSYS component, chiller operation is called for by an on-off signal input from an external controller (e.g. a room thermostat). Auxiliary is called for either by an external input (e.g. the second stage of a room thermostat) or by a signal from

an internal controller which makes its decision based on the solar source temperature.

The internal controller will call for auxiliary heat (or shut off the chiller, if no auxiliary heat is provided for) when the solar source temperature, T_{stor}, falls below a set value T_{smin}. This control is necessary to prevent attempted chiller operation under conditions where $T_{g,ss}$, as given by equation 3.2.2, would be less than T_{gmin}. In this situation, in accord with equations 3.2.4 and 3.2.3, heat would be supplied to the generator and rejected into the cooling water circuit at the absorber without any cooling being delivered.

Four auxiliary modes are provided. In three of the modes, an auxiliary heater is included which provides firing water at a set temperature T_{aux} whenever auxiliary is called for and T_{stor} is below T_{aux}. The heater is modeled as responding instantly with no standby losses on startup transients. In the fourth mode, no auxiliary is provided, and the internal minimum-solar-source-temperature controller shuts the chiller off if T_{stor} falls below T_{smin}.

In all four modes, if the chiller is operating from solar source, firing water is returned to storage at a temperature given by

$$T_{hw,ret} = T_{hw} - \frac{\dot{Q}_{gen}}{(\dot{m}C_p)_{hw}} \qquad (3.2.13)$$

If auxiliary is called for, the firing water return temperature and flow rate will depend on the auxiliary mode selected. These differences will now be explained.

The first mode will be referred to as series heat auxiliary. In this mode, as shown in Figure 3.2.1, when auxiliary is called for firing water circulates from storage to the auxiliary heater where it is heated to T_{aux}, then to the absorption chiller. Firing water is returned from the absorption chiller to the storage tank.

When auxiliary is operating

$$\dot{Q}_{aux} = (\dot{m}C_p)_{hw} (T_{aux}-T_{stor}) \tag{3.2.14}$$

and

$$T_{hw,ret} = T_{stor} - \frac{\dot{Q}_{gen}-\dot{Q}_{aux}}{(\dot{m}C_p)_{hw}} \tag{3.2.15}$$

It is possible, if T_{stor} is sufficient low, that $\dot{Q}_{aux}$ will exceed $\dot{Q}_{gen}$, in which case equation 3.2.15 shows that firing water can be returned to storage at a higher temperature than when it was removed.

A second scheme for providing auxiliary heat to operate the chiller is diagrammed in Figure 3.2.2. When auxiliary is called for, firing water circulates between the absorption chiller and the auxiliary heater, bypassing storage completely. In this case

$$\dot{Q}_{aux} = \dot{Q}_{gen} \tag{3.2.16}$$

and

$$\dot{m}_{hw} \text{ (from storage)} = 0 \tag{3.2.17}$$

This will be referred to as parallel heat auxiliary.

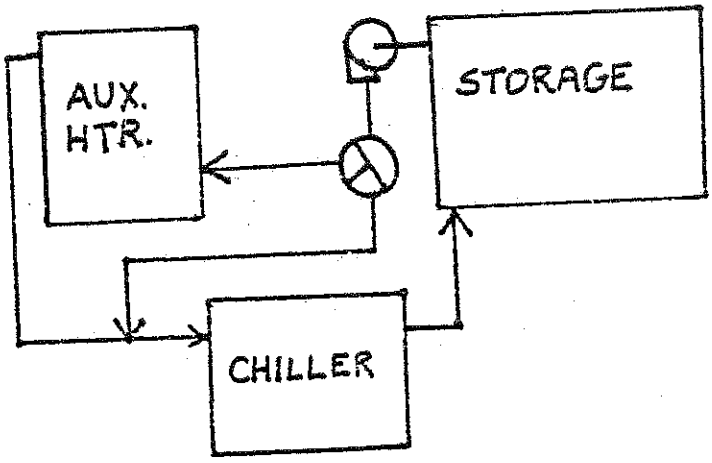

FIGURE 3.2.1 SYSTEM WITH SERIES HEAT AUXILIARY

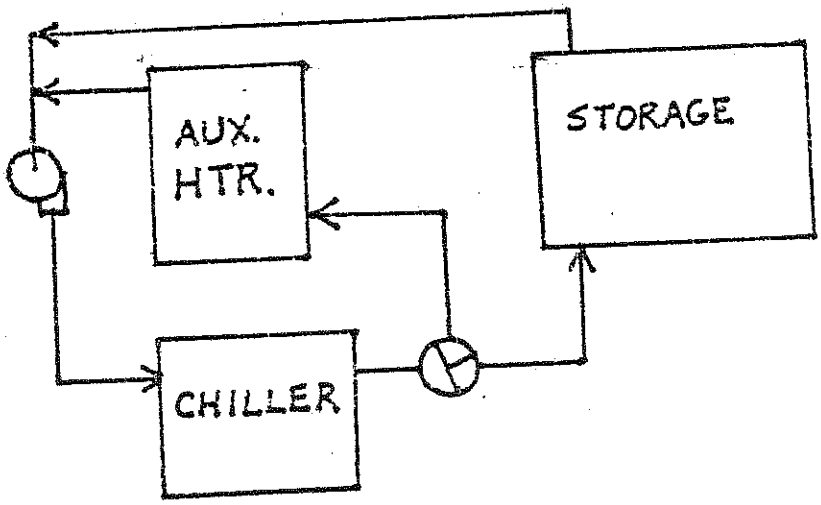

FIGURE 3.2.2 SYSTEM WITH PARALELL HEAT AUXILIARY

A third scheme for providing auxiliary heat is shown in Figure 3.2.3. This mode is referred to as series-parallel heat auxiliary. A controller causes the system to operate in series heat auxiliary mode if the solar source temperature is above a set changeover temperature T_{cr}, and in parallel heat auxiliary if the solar source is below T_{cr}.

The fourth mode (which strictly speaking, is not an auxiliary mode) dispenses with the auxiliary heater entirely. The chiller is shut off if the solar source temperature falls below T_{smin}. Back-up cooling, if needed, must be provided by some other means, e.g. by a vapor compression air conditioner. This mode is diagrammed in Figure 3.2.4.

3.3 Air Conditioning Load Model

The building cooling load is simulated using existing TRNSYS Type 17 and 18 wall and roof models. The wall models are based on the ASHRAE transfer function method (13).

An existing TRNSYS building load component, Type 19, uses the ASHRAE (14) method for the time-distribution of instantaneous sensible heat gains and losses. Type 19 calculates an instantaneous space heating or cooling load and a floating room temperature. This load component provides a very detailed treatment of sensible cooling loads, but does not provide any treatment of latent loads or of dehumidification. The Type 19 subroutine was therefore modified to calculate latent loads and model dehumidification as described below.

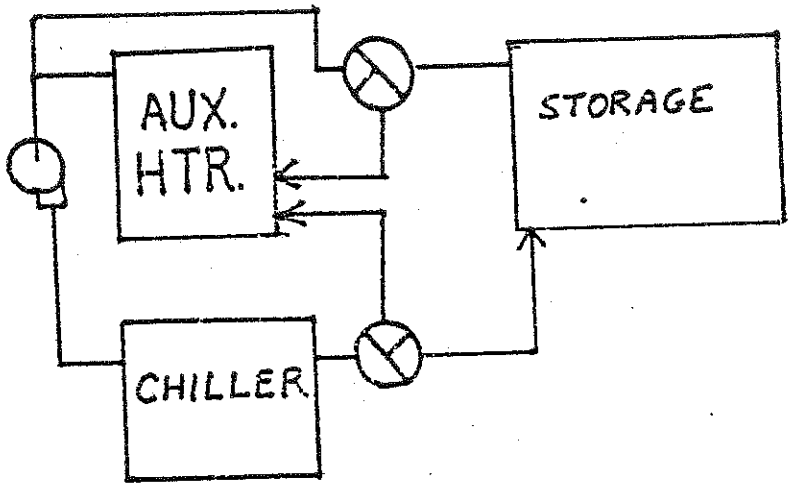

FIGURE 3.2.3 SYSTEM WITH SERIES-PARALLEL HEAT AUXILIARY

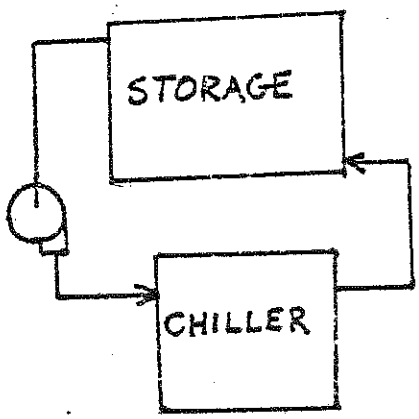

FIGURE 3.2.4 SYSTEM WITHOUT HEAT AUXILIARY

Performing a mass balance on the moisture in the room:

$$\frac{dm_w}{dt} = \dot{V}_{inf}\rho_{air}\,(W_{amp}-W_r) + \dot{m}_{gen}-\dot{m}_{cond} \qquad (3.3.1)$$

Moisture gain by diffusion through the building envelope is usually much less than the moisture gain due to infiltration, and is neglected.

The room moisture capacitance, C_m, is defined as the ratio of the moisture present in the structure (including room air, building envelope, and contents) to the humidity ratio of the room air. The humidity ratio is expressed as a mass of water vapor per mass of dry air. Therefore C_m expresses the room moisture capacitance as an equivalent quantity of dry air.

If it is assumed that the moisture content of the building structure and contents is in equilibrium with the humidity of the room air, equation 3.3.1 may be rewritten as

$$C_m\frac{dW_r}{dt} = \dot{V}_{inf}\rho_{air}\,(W_{amb}-W_r)+ \dot{m}_{gen}-\dot{m}_{cond} \qquad (3.3.2)$$

Performing an energy balance on the same space yields

$$(\Sigma mC_p)_{space}\frac{dT_r}{dt} = \Sigma\dot{Q}_{shg}-(\dot{Q}_{cool}-\dot{m}_{cond}\,\Delta h_{vap}) \qquad (3.3.3)$$

The quantity $(\Sigma mC_p)_{space}$ is the thermal capacitance of the space. The quantity $(\dot{Q}_{cool}-\dot{m}_{cond}\Delta h_{vap})$ is the difference between the heat removed from the space at the cooling coil and the heat released in the condensation process. Thus, this quantity is equal to the net rate of sensible heat removal from the space, i.e.

$$\dot{Q}_{lat} = \dot{m}_{cond}\Delta h_{vap} \tag{3.3.4}$$

$$\dot{Q}_{sens} = \dot{Q}_{cool} - \dot{Q}_{lat} \tag{3.3.5}$$

Equation 3.3.3 may be rewritten as

$$(\Sigma mC_p)_{space}\frac{dT_r}{dt} = \Sigma\dot{Q}_{shg} - \dot{Q}_{sens} \tag{3.3.6}$$

Equations 3.3.2 and 3.3.6 are coupled by the $\dot{m}_{cond}$ term. To estimate the rate of moisture removal it is necessary to model the processes which occur at the cooling coil.

The coil is modeled based on a method suggested by Stoecker (15). The temperature and humidity ratio of the air leaving the coil satisfy the relation

$$\frac{T_{out}-T_s}{T_{in}-T_s} = \frac{W_{out}-W_s}{W_{in}-W_s} \tag{3.3.7}$$

where the subscript "in" refers to the condition of air entering the coil, the subscript "out" refers to conditions at coil exit and the subscript "s" refers to saturation conditions at the coil surface temperature. This is equivalent to saying that the exit conditions lie on a straight line on a W-T psychrometric chart between the room condition point and a point on the saturation curve at T_s, as shown on Figure 3.3.1.

Equation 3.3.7 may be rearranged to give

$$T_{in}-T_{out} = (T_s-T_{in})\left(\frac{W_{out}-W_{in}}{W_{in}-W_s}\right) \tag{3.3.8}$$

The sensible heat removal per unit mass of air is equal to $C_p(T_{in}-T_{out})$ and the latent heat removal per unit mass of air is equal to $\Delta h_{vap}(W_{in}-W_{out})$, so from equation 3.3.8 it follows that

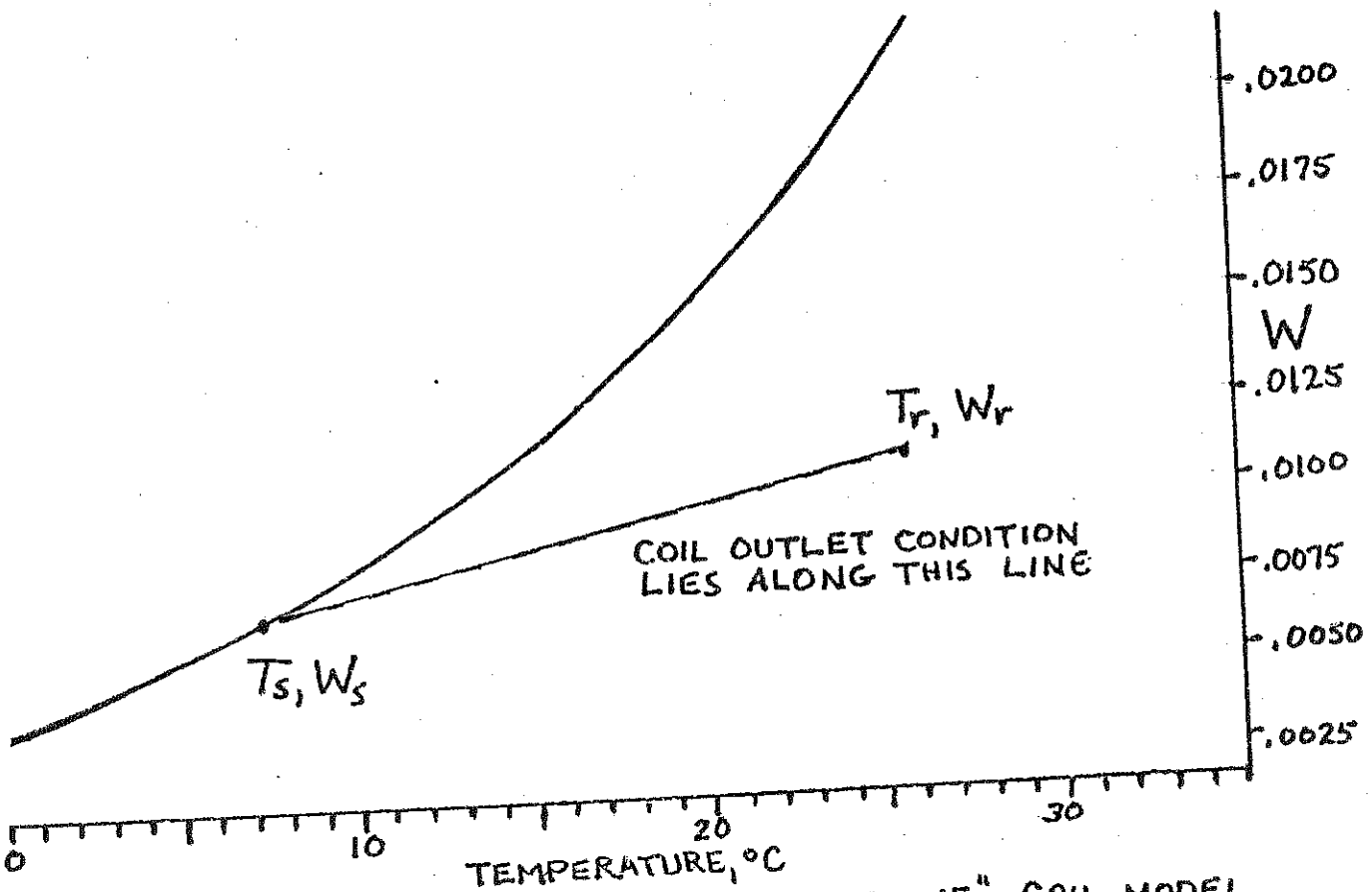

FIGURE 3.31 PSYCHROMETRIC CHART SHOWING "STRAIGHT LINE" COIL MODEL

$$\frac{\dot{Q}_{sens}}{C_p} = \frac{\dot{Q}_{lat}}{\Delta h_{vap}} \left(\frac{T_{in}-T_s}{W_{in}-W_s}\right) \tag{3.3.9}$$

This may be rearranged to give

$$\frac{\dot{Q}_{sens} + \dot{Q}_{lat}}{\dot{Q}_{lat}} = \frac{(T_{in}-T_s)\, C_p + (W_{in}-W_s)\Delta h_{vap}}{(W_{in}-W_s)\Delta h_{vap}} \tag{3.3.10}$$

Inserting equation 3.3.5 into 3.3.10 and rearranging yields

$$\dot{Q}_{lat} = \dot{Q}_{cool} \frac{(W_{in}-W_s)\Delta h_{vap}}{(W_{in}-W_s)\Delta h_{vap} + (T_{in}-T_s)C_p} \tag{3.3.11}$$

and

$$\dot{Q}_{sens} = \dot{Q}_{cool} \frac{C_p(T_{in}-T_s)}{(W_{in}-W_s)\Delta h_{vap} + (T_{in}-T_s)C_p} \tag{3.3.12}$$

Inserting 3.3.11 into 3.3.2, and 3.3.12 into 3.3.6 gives the two coupled ordinary differential equations which describe room temperature and humidity:

$$(\Sigma m C_p)_{space} \frac{dT_r}{dt} = \Sigma \dot{Q}_{shg} - \dot{Q}_{cool} \frac{C_p(T_{in}-T_s)}{(W_m-W_s)\Delta h_{vap}+(T_{in}-T_s)C_p} \tag{3.3.13}$$

and

$$C_m \frac{dW_r}{dt} = \dot{V}_{mf\ air}(W_{amb}-W_r) + \dot{m}_{gen} - \dot{Q}_{cool} \frac{(W_{in}-Q_s)\Delta h_{vap}}{(W_m-W_s)\Delta h_{vap} + (T_{in}-T_s)C_p} \tag{3.3.14}$$

The ambient humidity ratio, W_{amb}, is calculated from the ambient temperature and relative humidity using an algorithm provided by ASHRAE (16). The ASHRAE algorithm is basically an empirical curve fit which describes the saturation curve. The saturation humidity ratio at the coil, W_s, is calculated from T_s using the same algorithm with a relative humidity of 100%.

Equations 3.3.16 and 3.3.17 are readily solved by TRNSYS to give timestep-by-timestep values of T_r and W_r.

CHAPTER IV

Description of System Simulated

4.1 Building

4.1.1 General Description

The same house was modeled in all simulations described below. A sketch of this house is presented in Figure 4.1.1. The two-story building is 9.1 m on a side, with a total floor area of 167 m^2. There is no basement, and the attic is insulated and outside the conditioned space of the house.

The roof has a pitch of 25° and faces north and south. The north and south walls are 4.9 m high. The east and west are 6.1 m high at the centers and 4.9 m high at the edges. The total roof area is 92.1 m^2, divided equally between the north and south faces. The east and west walls have areas of 53.4 m^2 and the north and south walls have areas of 44.6 m^2 each.

4.1.2 Walls

The walls are of frame construction, consisting of 1 inch wood siding, 1 inch insulation between 2 by 4 inch (nominal) studs on 16 inch centers, a 3 inch air space and 0.75 inch plaster on the inside surface. The U-value of this wall construction is reported by ASHRAE as 3.64 kJ/hr m^2°C (.178 BTU/hr ft^2°F). The walls are painted white ($\varepsilon = 0.8$, $\alpha = 0.3$).

Window area in each wall amounts to 12% of the total wall area. The windows are of single-pane clear glass without shading, and

have a U-value of 21.7 kJ/hrm^2°C and a transmittance of 0.8.

The walls are simulated using the TRNSYS Type 17 transfer-function wall subroutine developed by Pawelski (17) based on the method of Mitalas and Stephenson (18). Detailed explanations of the transfer function method are given elsewhere (13). A brief description of the model is presented below.

The instantaneous heat flux into the conditioned space is related to the past history of heat flux and temperature difference across the wall:

$$q_{e,t} = \sum_{n=0} b_n (T_{e,t-n\Delta} - T_{rc}) - \sum_{n=1} d_n q_{e,t-n\Delta} \qquad (4.1.1)$$

Usually all b_n and d_r coefficients for n greater than about 6 are negligible. The ASHRAE 1977 Handbook of Fundamentals (13) contains values of d_n and b_n for a number of wall types.

The advantage of using a transfer function wall model is that the time dependence of heat conduction through the wall is accurately calculated with considerably less computational effort than would be required for a finite-element unsteady state heat flow calculation.

Transfer function coefficients for the wall simulated (ASHRAE wall type 38) are given in Table 4.1.1.

4.1.3 Roof and Attic

The roof and attic are simulated using the TRNSYS Type 18 transfer function pitched roof and attic subroutine developed by

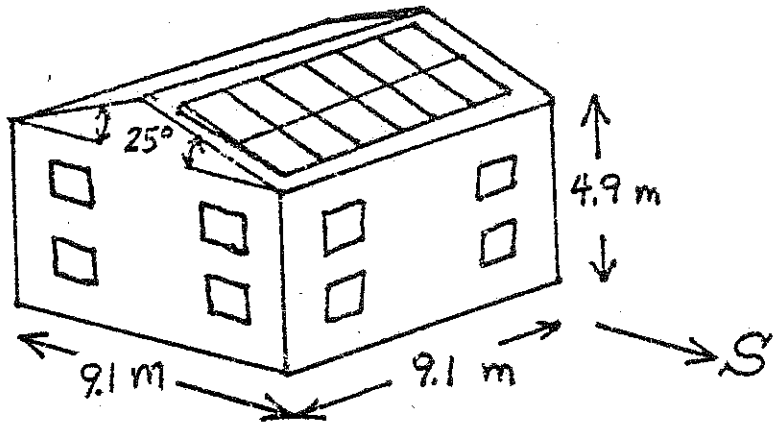

FIGURE 4.1.1 HOUSE SIMULATED

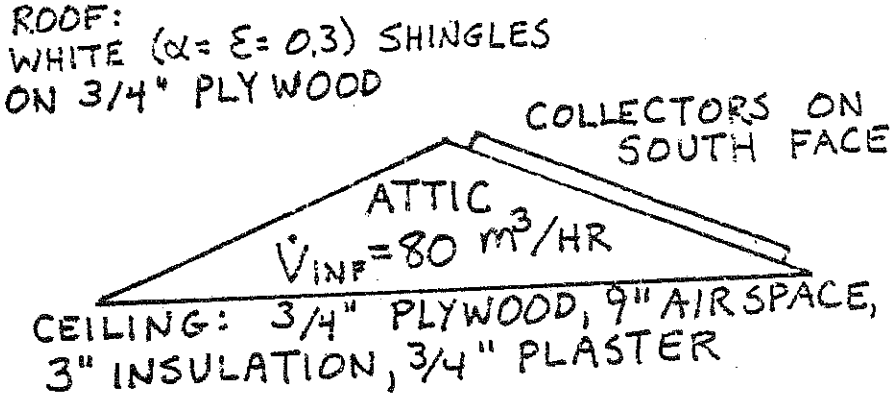

FIGURE 4.1.2 ROOF AND ATTIC CONSTRUCTION

Pawelski. The subroutine calculates the conduction heat gain to the conditioned space through the ceiling using an approach similar to that described above for the walls. Transfer function coefficients for an attic of the construction illustrated in Figure 4.1.2 are stored in the TRNSYS subroutine.

4.1.4 Room Load

The space cooling load is calculated using a modified version of TRNSYS Type 19. The modifications, as set forth in Chapter 3, deal with calculations of the rate of moisture gain into the space, the rate of moisture and sensible heat removal from the space at the air conditioning coil, and determination of the temperature and humidity of the air in the conditioned space.

Sensible heat gains occur via conduction through the walls and ceiling, by radiation through fenestration, by infiltration, and by internal generation. The conduction and infiltration gains appear instantaneously as components of the space cooling load. Solar heat gains and the radiant portion of internally generated heat gains do not contribute instantly to the space cooling load: the radiant contribution must first be absorbed by the building structure or contents and then be transferred into the room air by conduction and convection. The Type 19 subroutine includes an algorithm which calculates this time delay.

The infiltration rate way calculated assuming a constant rate of 0.5 air changes per hour. The volume of the conditioned space is 408 m^3, and thus the volume infiltration rate is 204 m^3/hour.

The building thermal capacitance, $(\Sigma mC_p)_{space}$ in equation 3.3.3, was set equal to 15,000 kJ/°C. The building moisture capacitance, C_m, was set equal to 5000 kg dry air, or approximately 10 times the room air mass, as suggested by Mitchell(19). The cooling coil surface temperature, T_s, was set equal to 7.5°C. (The absorption chiller was modeled as delivering chilled water to the coil at 7.2°C.)

4.1.5 Room Thermostat

The control configuration used to command air conditioning and heating was not identical in all simulations. In general, however, solar source heating was commanded by a Type 8 thermostat when the room temperature fell below 20°C. Cooling was commanded either by a Type 8 thermostat or a Type 2 controller. Cooling auxiliary (in the form of heat from the auxiliary heater, or cooling from a backup air conditioner if no auxiliary heat was provided) was commanded by a Type 2 controller.

Unless otherwise specified, first stage cooling was called for when the room temperature exceeded 24.5°C and second stage cooling was commanded for room temperatures above 25.5°C.

4.2 Collector and Storage

4.2.1 Collector

The collector is simulated with the TRNSYS Type 1 Mode 1 collector component. The TRNSYS component is based on the model of Hottel, Whillier and Bliss (23,24).

The rate of useful energy collection is defined as

$$\dot{Q}_u = AGC_p\ (T_o - T_i) \qquad (4.2.1)$$

The Hottel-Whillier-Bliss analysis leads to an expression relating $\dot{Q}_u$ to solar irradiation, ambient and fluid inlet temperatures, fluid flowrate, and certain collector properties:

$$\dot{Q}_u = AF_R\ [H_t\ (\tau\alpha)_e\ -\ U_L\ (T_i - T_a)] \qquad (4.2.2)$$

where

$$F_R = \frac{GC_p}{U_L}\ [1-\exp\ (\frac{-F'U_L}{GU_p})] \qquad (4.2.2)$$

In the simplest form of the Hottel-Whillier-Bliss model, U_L, $(\tau\alpha)_e$ and F_R are assumed constant for a given collector flow rate. From equation 4.2.2, this leads to a simple two-parameter expression for collector efficiency:

$$\frac{\dot{Q}_u}{AH_\tau} = F_R\ (\tau\alpha)_e - F_R U_L\ (\frac{T_i - T_a}{H_t}) \qquad (4.2.3)$$

Values of F', $(\tau\alpha)_e$ and U_L were chosen to simulate a fairly high-performance double-glazed flat plate collector with a selectively coated absorber, using water as the working fluid. The values of $F_R(\tau\alpha)_e$, $F_R U_L$ and U_L were:

$$F_R(\tau\alpha)_e = 0.785$$

$$F_R U_L = 12.2\ \text{kJ/hr m}^{2\circ}\text{C}$$

$$U_L = 14.4\ \text{kJ/hr m}^{2\circ}\text{C}$$

Collectors were mounted facing due south at a tilt angle equal to the latitude of the site being simulated.

4.2.2 Radiation Processor

Radiation data was provided in the form of hourly integrated insolation on a horizontal surface. This was converted to radiation on a tilted surface using the TRNSYS Type 16 radiation processor. The daily correlation of Liu and Jordan was used to divide insolation into beam and diffuse components.

4.2.3 Storage, Pump and Relief Valve

The collector uses water as the working fluid. The storage tank is unpressurized, and water circulates directly from storage to collector with no intermediate heat exchanger.

The tank is modelled using the TRNSYS Type 4 tank subroutine. The tank is divided into two modes to simulate the effect of thermal stratification. The tank is 1.5 m high and is insulated for a loss coefficient of 1.0 kJ/hr m^2°C (approximately R-20 hr ft^2/BTU). Unless otherwise noted, the tank was sized at 75 liters per square meter of collector. The storage tank is located outside the conditioned space of the building.

A pump (TRNSYS Type 3) operates at a flowrate equal to 50 kilograms of water per hour per square meter of collector when commanded by the pump controller. The pump controller (TRNSYS Type 2) commands pump operation when the collector outlet temperature exceeds the collector inlet temperature. A relief valve

(TRNSYS Type 13) dumps energy from the fluid stream leaving the collector so that the top node of storage never exceeds 100°C.

4.3 Absorption Air Conditioning System

4.3.1 Absorption Chiller

The model used to simulate the absorption chiller is described in general terms in Chapters 2 and 3. The specific chiller simulated is a three ton rated capacity lithium bromide-water unit whose steady state performance matches that of a commercially available chiller (Arkla model WF-36, Arkla Industries Inc., Evansville, Indiana). Figures 4.3.1 and 4.3.2 show the steady state capacity and coefficient of performance (COP) of the Arkla Chiller as a function of firing water and condensing water temperatures (20).

Parameters needed to describe the transient performance of the chiller were estimated from measurements taken on an Arkla model WF-36 chiller located at Colorado State University and on calculations for a hypothetical chiller. Table 4.3.1 lists the parameters used to describe the steady-state and transient performance of the chiller.

The steady state generator temperature is related to the firing water temperature by equation 2.2.7. It is assumed that T_a is approximately equal to T_c, and the effectiveness of the generator and sensible heat exchanger are arbitrarily assigned values of 0.65. Inserting these values into equation 2.2.7 gives an expression for the steady state generator temperature:

Table 4.3.1

Parameters to Simulate Arkla WF-36 Absorption Chiller

Rated Capacity = 37980 kJ/hr

τ_h = 0.133 hr	τ_c = 1.05 hr	$(UA)_o$ = 1900 kJ/hr
T_{gmin} = 68.2°C	$\dot{m}_{hw}$ = 2420 kg/hr	
a_{11} = 1.405	a_{12} = -3.602844	a_{13} = .100965
a_{21} = 1.044028	a_{22} = 1.883088×10^{-2}	a_{23} = 1.37682×10^{-3}
a_{31} = -1.40384×10^{-2}	a_{32} = 4.01284×10^{-4}	a_{33} = 0
b_{11} = 5.048	b_{12} = -1.921	b_{13} = 4.290611×10^{-2}
b_{21} = .4264	b_{22} = 1.522715×10^{-2}	b_{23} = -5.696471×10^{-4}
b_{31} = -6.250574×10^{-3}	b_{32} = 1.304397×10^{-4}	b_{33} = 0

Cooling Tower Parameters

Approach = 5.5°C	T_{cmin} = 23.1°C	T_{cmax} = 32.2°C

$$T_{g,ss} = 0.83\ T_{hw} + 0.17\ T_c \tag{4.3.1}$$

The empirical functions describing CAPY (T_g,T_c) and COP (T_g,T_c) were obtained from steady state performance data for the Arkla model WF-36 chiller as shown in Figures 4.3.1 and 4.3.2. Performance data shown as functions of T_{hw} and T_c were converted to functions of T_g and T_c using equation 4.3.1. The coefficients a_{ij} and b_{ij} were obtained by fitting the curves for CAPY and COP to functions of the form 2.2.17 and 2.2.19 using MINITAB (21), a statistical program of the Madison Academic Computing Center. The resulting functions were:

a) $68.2°C < T_g < 85.3°C$

$$\begin{aligned} CAPY\ (T_g,T_c) &= 1.405-3.602844\ T_c + .100965\ T_c^2 \\ &+(1.044028+1.883088\times10^{-2}T_c-1.376819\times10^{-3}T_c^2)T_g \\ &+(-1.403839\times10^{-2}+4.01284\times10^{-4}T_c)T_g^2 \end{aligned} \tag{4.3.2}$$

$$\begin{aligned} COP\ (T_g,T_c) &= 5.048-1.921\ T_c + 4.290611\times10^{-2}T_c^2 \\ &+(.4264+1.522715\times10^{-2}T_c-5.696471\times10^{-4}T_c^2)T_g \\ &+(-6.250574\times10^{-3}+1.304397\times10^{-4}T_c)T_g^2 \end{aligned} \tag{4.3.3}$$

b) $T_g < 68.2°C$

$$\dot{Q}_{cool} = 0 \tag{4.3.4}$$

$$COP = 0 \tag{4.3.5}$$

The quantity $(UA)_o$ referred to in equation 2.2.21, which characterizes heat transfer to the solution during the part of the startup process in which T_g is below T_{gmin}, was calculated using Arkla data and equation 4.3.1. Equation 4.3.1 may be rearranged to give

$$T_{hw} - T_{g,ss} = 0.17\ (T_{hw}-T_c) \tag{4.3.6}$$

Therefore

$$(UA)_o = \frac{\dot{Q}_{gen}}{0.17\ (T_{hw}-T_c)} \tag{4.3.7}$$

The heat transfer coefficient, U, increases as the rate of boiling increases. To estimate UA under conditions in which the boiling rate is low, the operating point reported by Arkla at which the chiller has the lowest cooling capacity is considered:

$$T_{hw} = 76.7°C$$

$$T_c = 29.4°C$$

$$\dot{Q}_{gen} = 15300\ kJ/hour$$

From equation 4.3.7, $(UA)_o$ equals 1900 kJ/hr °C.

The startup time constant, τ_h, was estimated from transient-mode generator temperature data reported by Leflar et al. (8) for the Arkla WF-36 chiller at Colorado State University Solar House I. The cooldown time constant, τ_c, was estimated from measurements made on the same chiller.

Time-temperature data from chiller startup were fitted to an expression of the form

$$\ell n\ (T_{g,ss}-T_g(t)) = \ell n\ (T_{g,ss}-T_g(t_o)) - \frac{t-t_o}{\tau_h} \qquad (4.3.8)$$

Data from chiller cooldown were fitted to an expression of the form

$$\ell n\ (T_g(t)-T_{env}) = \ell n\ (T_g(t_o) - T_{env}) - \frac{t-t_o}{\tau_c} \qquad (4.3.9)$$

When the quantity $(\ell n\ (T_{g,ss}-T_g(t))$ is plotted against $(t-t_o)$, equation 4.3.8 predicts a straight line of slope $-1/\tau_h$. Similarly, equation 4.3.9 predicts a slope of $-1/\tau_c$ when $(\ell n\ (T_g(t)-T_{env}))$ is plotted against $(t-t_o)$. MINITAB was used to evaluate τ_c and τ_h. The values of τ_h and τ_c which gave the best fit to the experimental data were:

$$\tau_h = 0.133 \text{ hr}$$

$$\tau_c = 1.05 \text{ hr}$$

Measured and predicted generator time-temperature histories are plotted in Figures 4.3.3 and 4.3.4.

4.3.2 Cooling Tower, Pumps, Chiller Controls and Auxiliary Heater

As described in Chapter 3, the cooling tower was modeled as delivering condensing water at a constant increment above the ambient wet bulb temperature. For the simulations described below, the approach to wet bulb was 5.5°C, i.e.

$$T_c = T_{wb} + 5.5 \qquad (4.3.10)$$

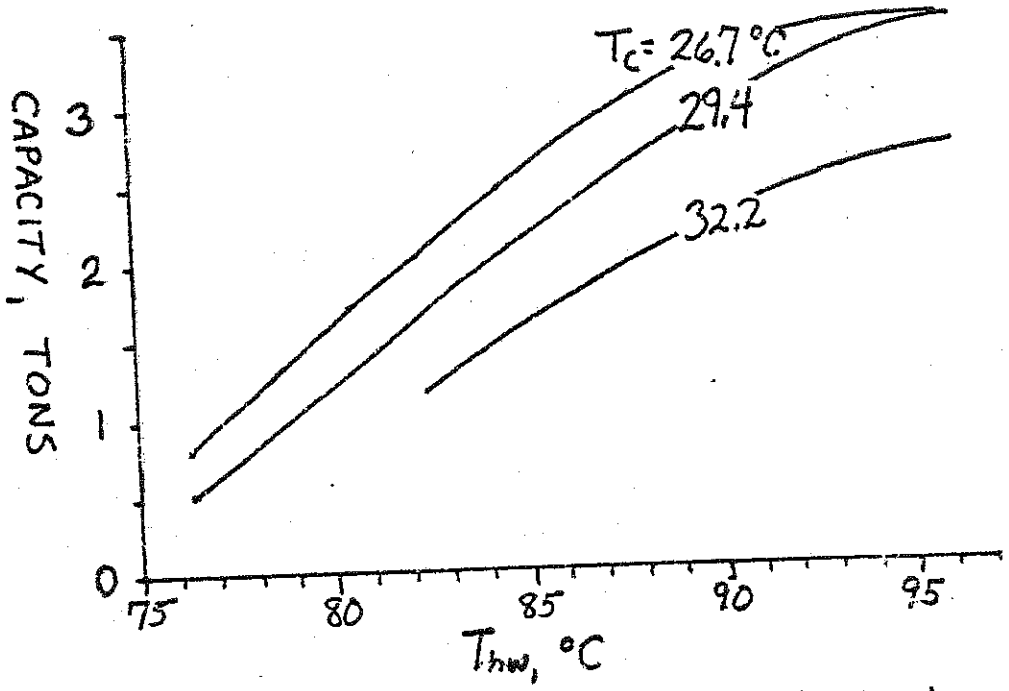

FIGURE 4.3.1 STEADY STATE CAPACITY OF ARKLA WF-36 ABSORPTION CHILLER

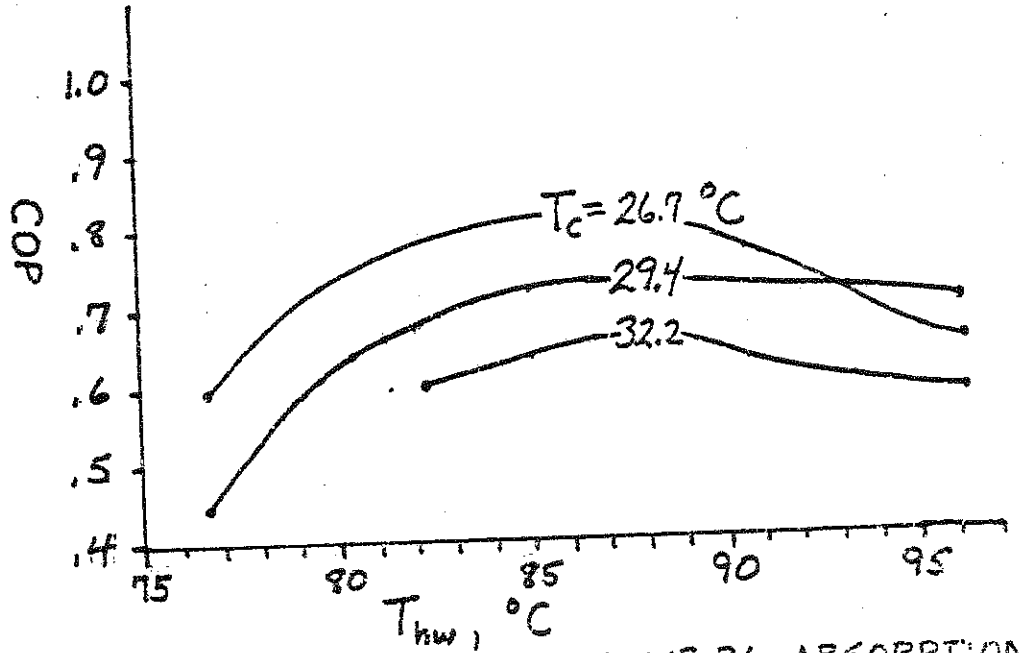

FIGURE 4.3.2 COP OF ARKLA WF-36 ABSORPTION CHILLER

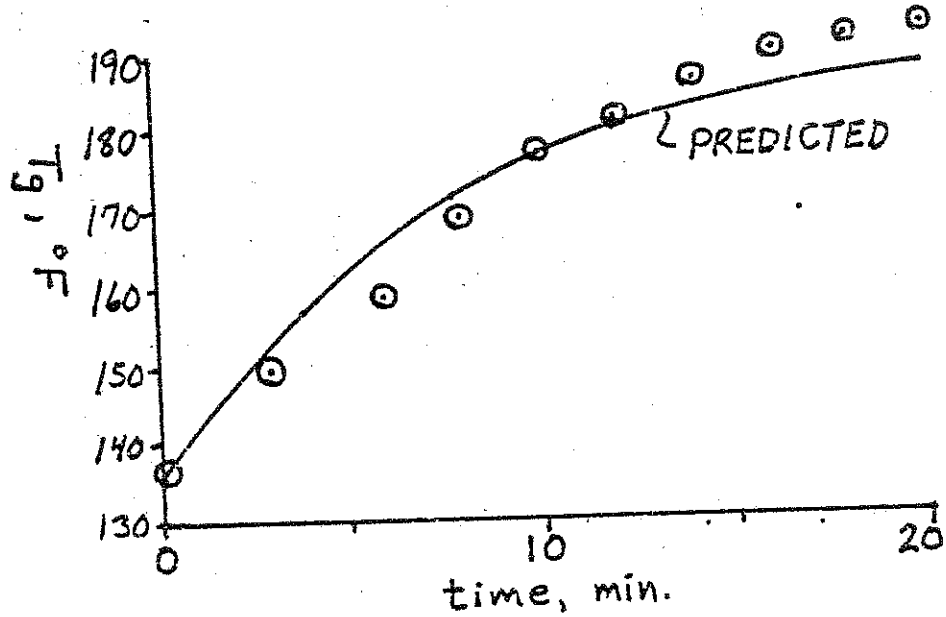

FIGURE 4.3.3 STARTUP GENERATOR TEMPERATURE HISTORY OF ARKLA WF-36 AT CSU HOUSE I

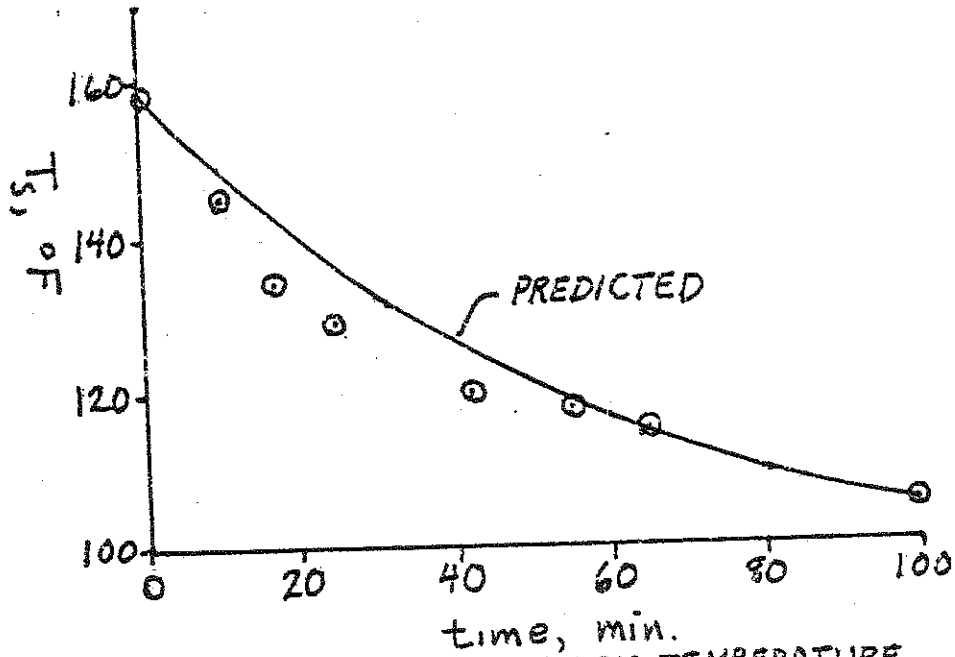

FIGURE 4.3.4 COOLDOWN SOLUTION TEMPERATURE HISTORY OF ARKLA WF-36 AT CSU HOUSE I

The minimum cooling water temperature, T_{cmin}, was set at 23.1°C, and the maximum temperature, T_{cmax}, was set at 32.2°C.

The firing water pump delivered 2440 kg/hr (approximately 12 gpm) when the chiller was operating. Firing water supplied above 96°C was automatically tempered to 96°C.

The minimum solar source temperature T_{smin} described in Chapter 3.2.3 was set at 77°C in most simulations. (A series of simulations in which T_{smin} was varied is described in Chapter 6.) To facilitate numerical convergence during a TRNSYS simulation, a deadband was set on the controller. Usually the deadband was set at 3°C, i.e. the controller would call for auxiliary when the storage temperature fell below 77°C, and keep the chiller on auxiliary until the temperature of storage rose above 80°C. It was sometimes necessary to use larger deadbands in conjunction with small storage tanks.

In simulations in which auxiliary heat was to be provided, the auxiliary heater set temperature T_{aux} was usually set at 95°C. A series of simulations in which T_{aux} was varied is described in Chapter 6.

4.4 Preliminary Simulations

4.4.1 Seasonal Cooling Load Distribution

System simulations were run on the house described above in Columbia, Mo., Charleston, S.C. and Miami Fl. using weather data from April 1 to November 1, 1975 (22). Sensible, latent and total

loads were calculated based on a room temperature of 25°C and a room humidity ratio of 0.012.

Month-by-month integrated sensible, latent and total loads are listed in Tables 4.4.1-3, and plotted in Figures 4.4.1-3.

In Miami and Charleston, the latent loads are a major fraction of the total cooling load. In Miami, the latent load amounts to about 24.5% of the total. In Charleston, the latent load contributes about 22% of the total cooling load over the season. In Columbia the latent load contribution is much smaller--approximately 7.7% of the total.

4.4.2 Fraction Solar vs. Collection Area

A series of simulations were run to determine the fraction of air conditioning load met by solar as a function of collector area. The house, collectors, storage and chiller were as described above. First stage cooling was called for at a room temperature of 24.5°C, and auxiliary cooling from a 3.2 ton vapor compression backup unit was commanded at 25.5°C. Simulations were performed for collector areas of 30, 60 and 90 m^2.

Monthly curves of f vs. A for Miami, Charleston and Columbia are shown in Figures 4.4.4, 4.4.5 and 4.4.6 respectively. The fraction by solar, f, is defined by

$$f = \frac{\dot{Q}_{cool,a}}{\dot{Q}_{cool,a} + \dot{Q}_{cool,b}} \qquad 4.4.1$$

where $\dot{Q}_{cool,a}$ and $\dot{Q}_{cool,b}$ are the monthly integrated total cooling

Table 4.4.1

House Cooling Loads: Miami, FL

T_r = 25°C W_r = .012

MONTH	Q_{sens} (GJ)	Q_{lat} (GJ)	Q_{total} (GJ)
April	9.26	1.71	10.97
May	8.95	2.81	11.76
June	9.03	3.24	12.27
July	9.76	3.44	13.20
August	10.94	4.27	15.21
September	9.68	3.61	13.29
October	9.08	2.56	11.64
Season	66.71	21.63	88.34

Table 4.4.2

House Cooling Load: Charleston, SC

T_r = 25°C W_r = .012

MONTH	Q_{sens} (GJ)	Q_{lat} (GJ)	Q_{total} (GJ)
April	3.23	0.37	3.60
May	6.82	1.63	8.45
June	7.74	1.91	9.65
July	7.68	2.74	10.42
August	9.32	3.01	12.33
September	5.54	2.08	7.62
October	3.93	0.80	4.73
Season	44.26	12.53	56.79

Table 4.4.3

House Cooling Load: Columbia, MO

T_r = 25°C W_r = .012

MONTH	Q_{sens} (GJ)	Q_{lat} (GJ)	Q_{total} (GJ)
April	2.24	0.02	2.26
May	5.02	0.29	5.31
June	7.31	0.95	8.26
July	9.30	0.80	10.10
August	8.43	0.77	9.20
September	3.35	0.33	3.68
October	2.84	0.03	2.87
Season	38.48	3.20	41.68

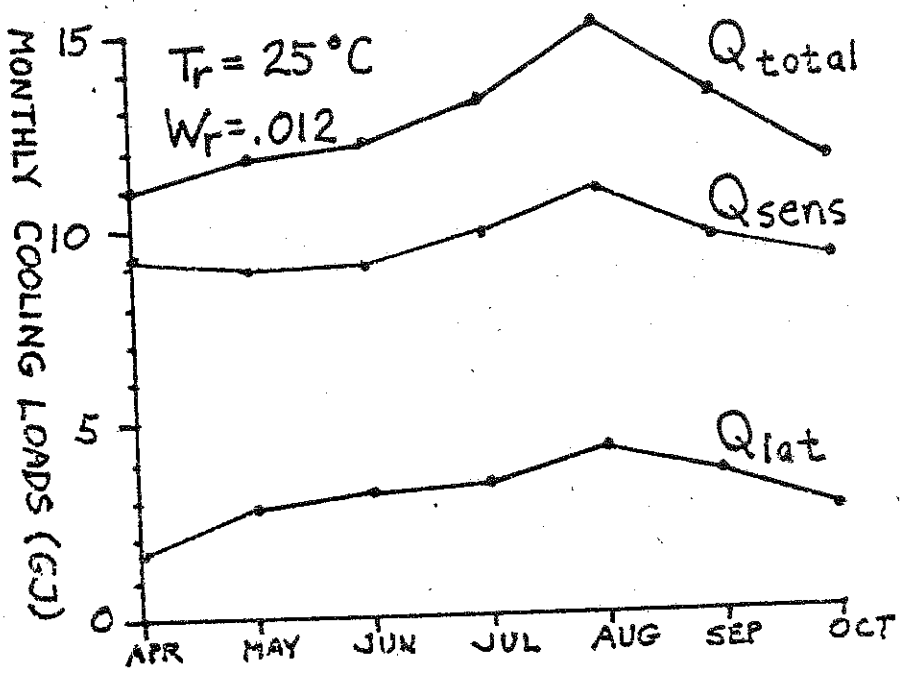

FIGURE 4.4.1 MONTHLY COOLING LOADS: MIAMI, FL

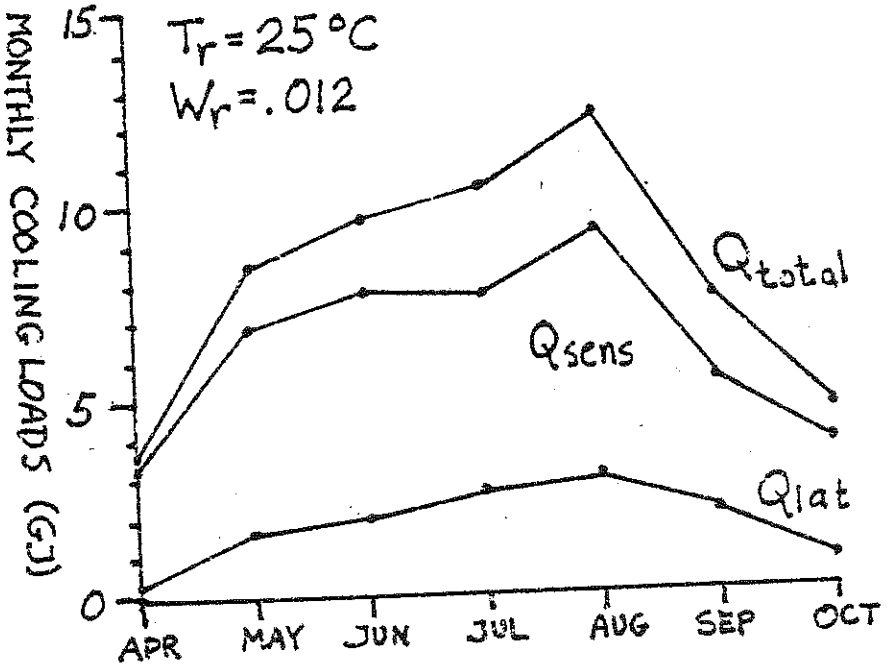

FIGURE 4.4.2 MONTHLY COOLING LOADS: COLUMBIA, MO

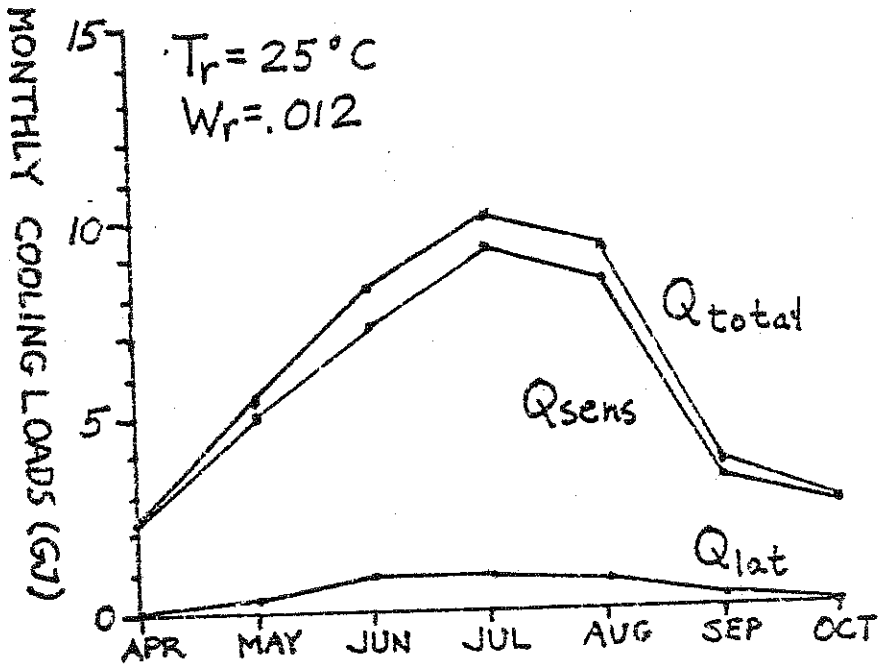

FIGURE 4.4.3 MONTHLY COOLING LOADS: CHARLESTON, SC

delivered by the absorption and backup chillers, respectively.

In Miami during June, July, August and September, and in Charleston during July and August, the f vs. A curves are nearly straight. This suggests that during these months the storage tank temperature was nearly constant. This was apparently due to the fact that the storage temperature rarely got very far above 77°C, and that the absorption chiller was using energy from storage almost as rapidly as it could be collected.

On the curves for Columbia, it often happens that the fraction by solar at 30 m^2 is very high. Simulations were not run at lower collector areas because the difficulty and expense of obtaining numerical convergence in a small tank coupled to a large chiller did not seem justified.

The most striking conclusion that can be drawn is that, during the peak cooling months in Miami and Charleston, the fraction by solar is almost directly proportional to the collector area.

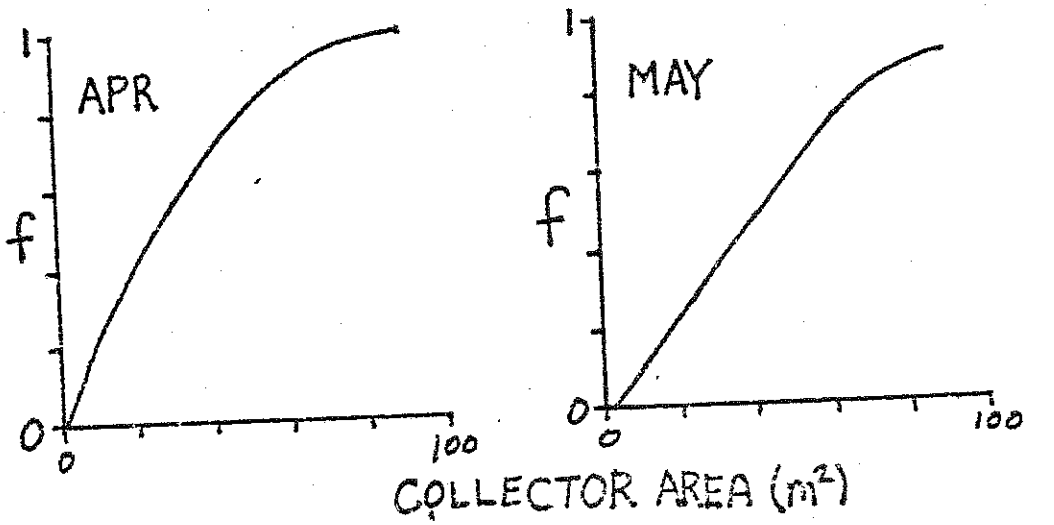

FIGURE 4.4.4 FRACTION SOLAR VS COLLECTOR AREA: MIAMI, FL

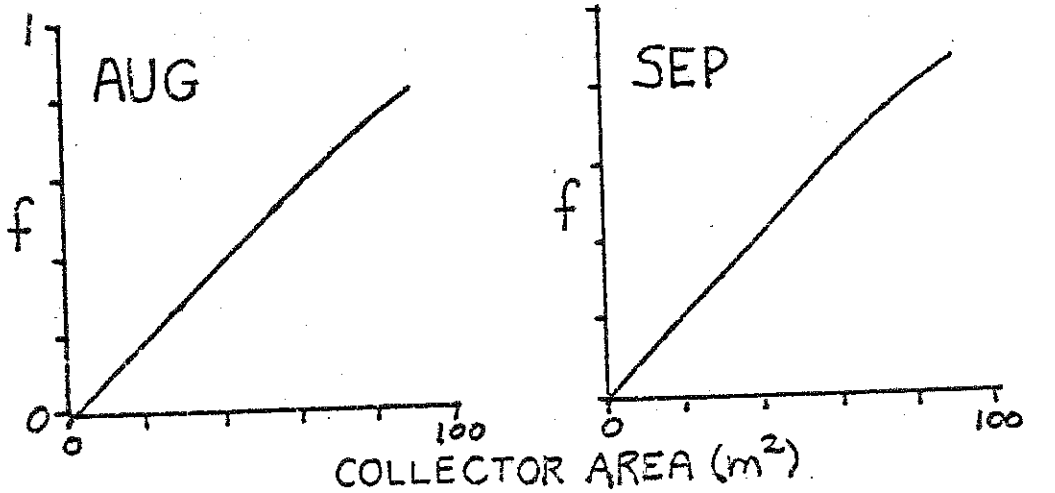

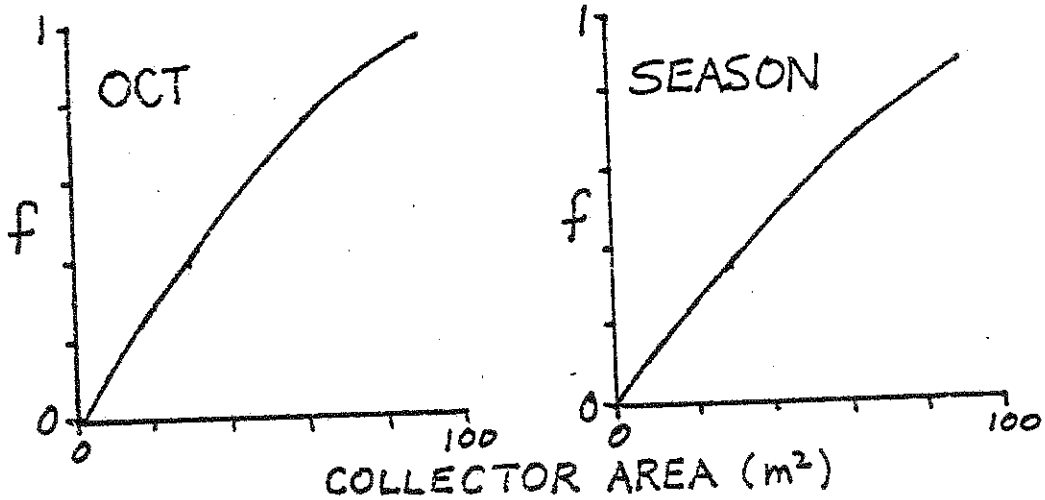

FIGURE 4.4.4 CONTINUED

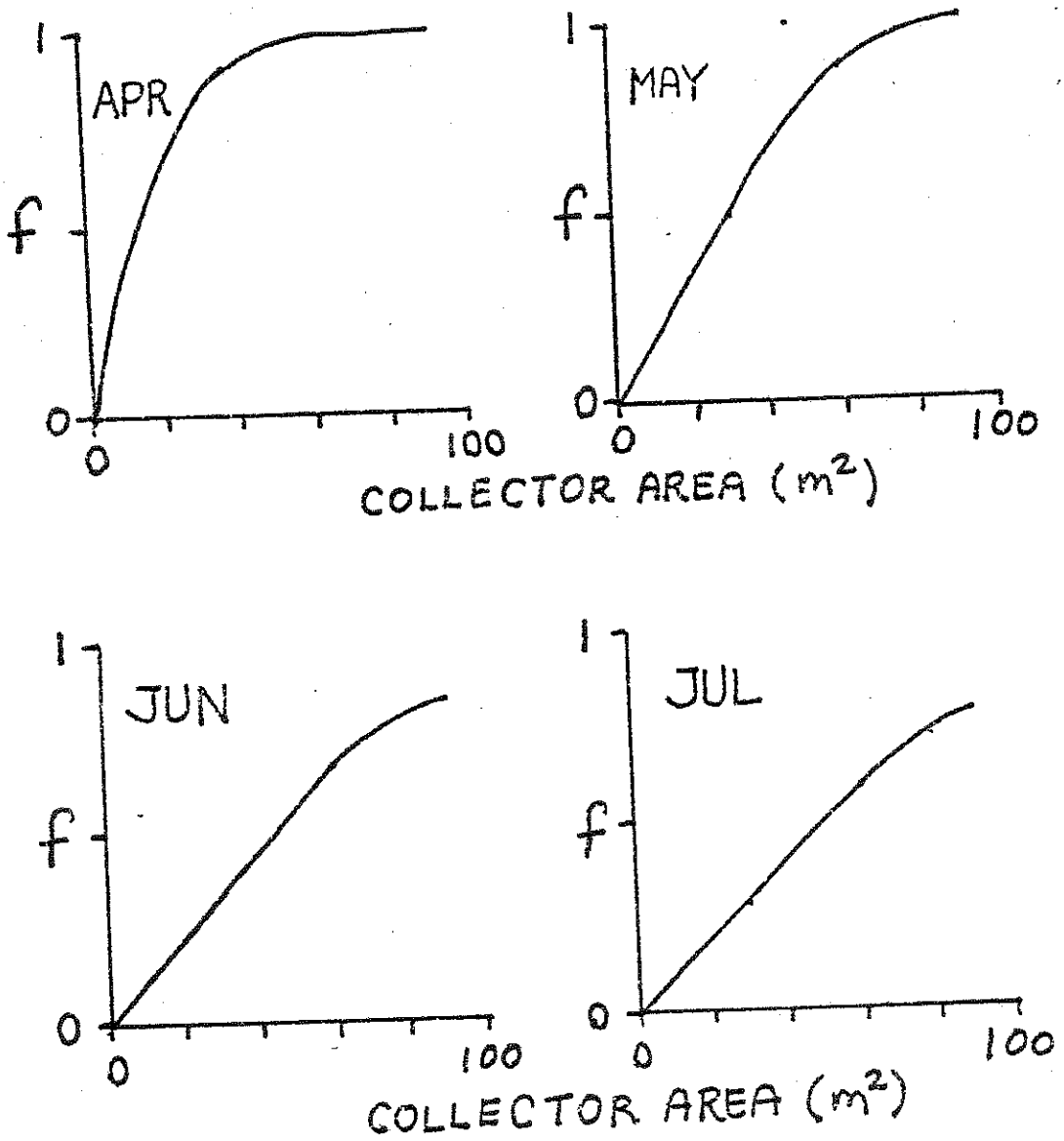

FIGURE 4.4.5 FRACTION SOLAR VS COLLECTOR AREA: CHARLESTON, SC

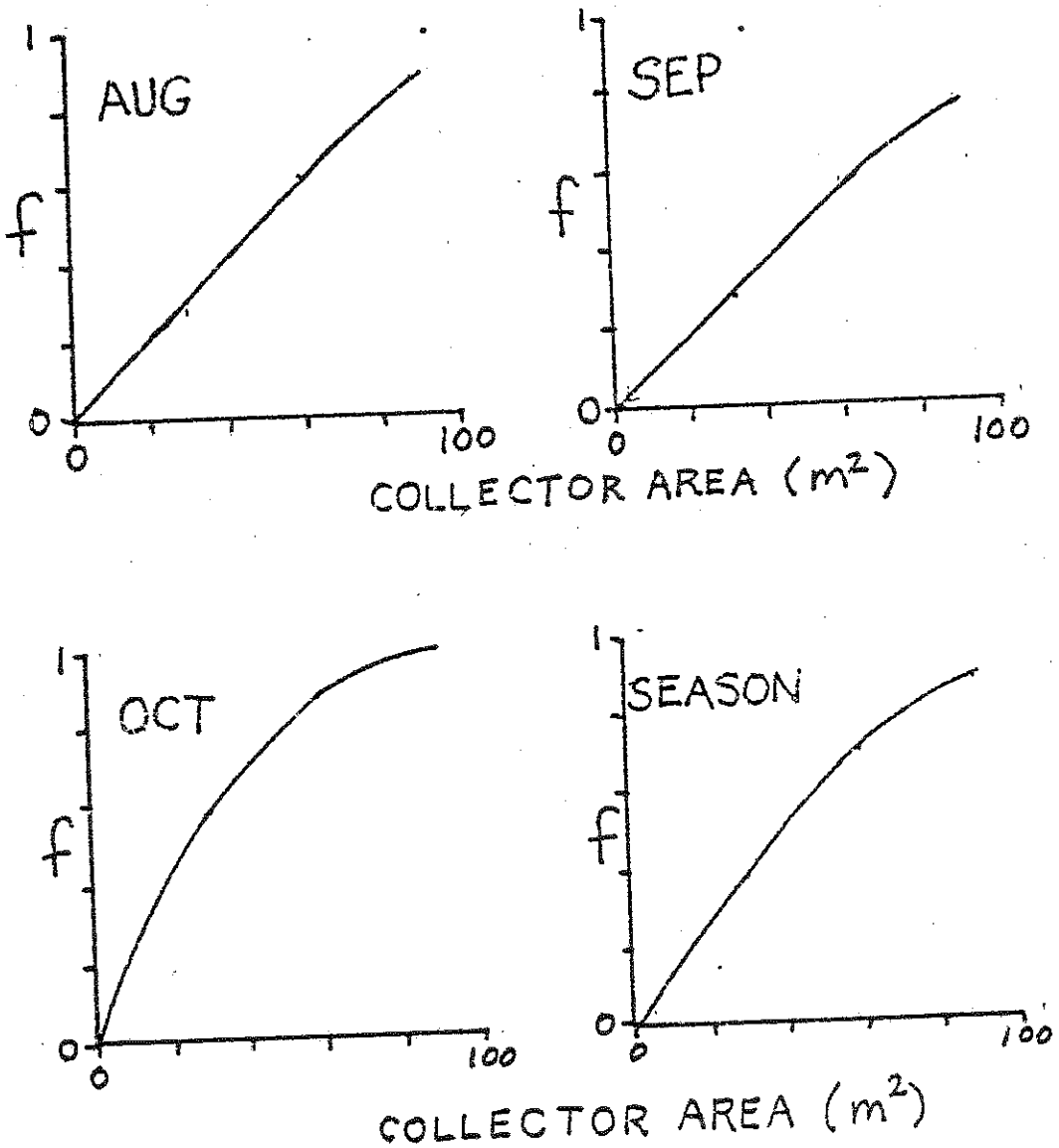

FIGURE 4.4.5, CONTINUED

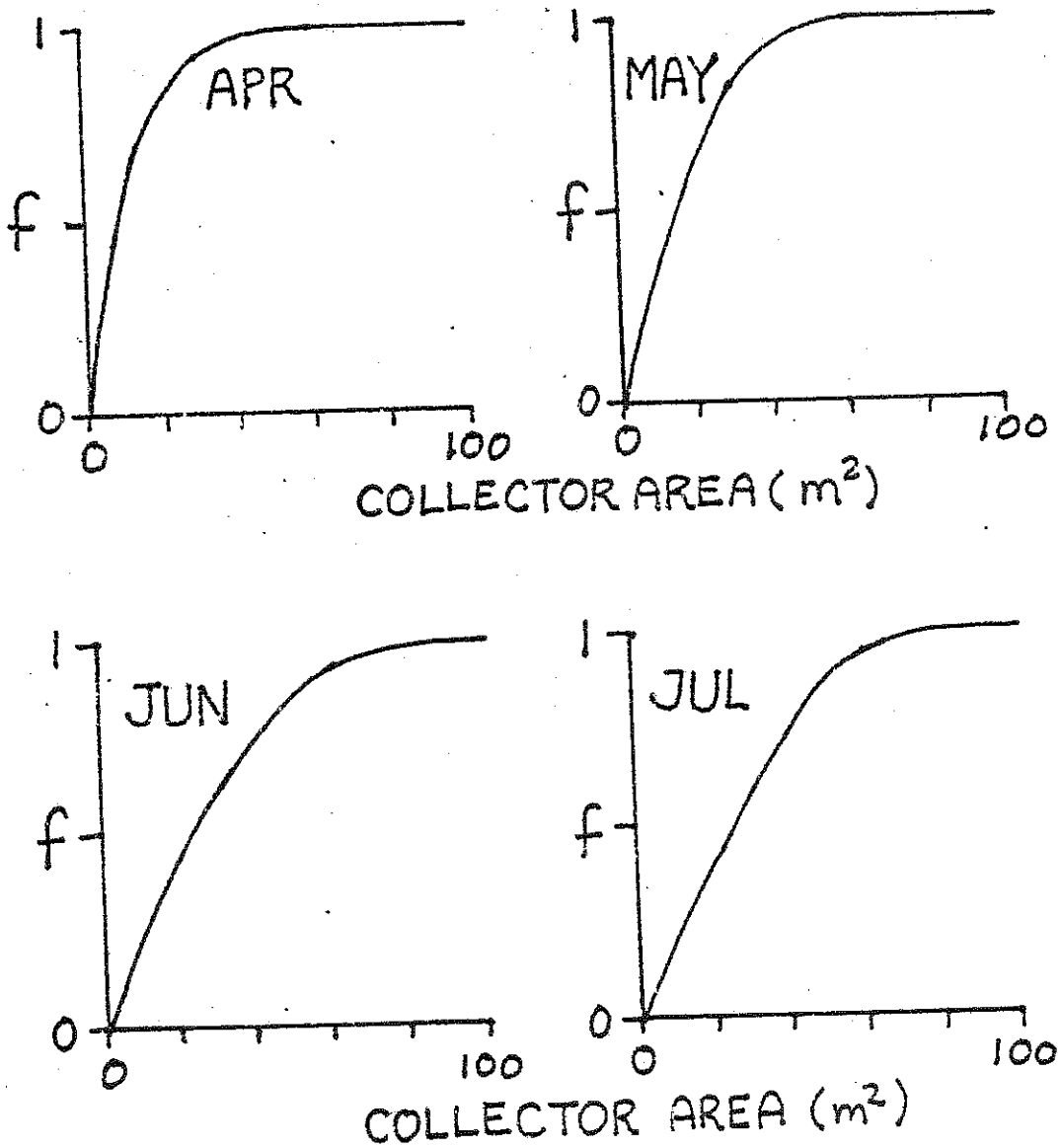

FIGURE 4.4.6 FRACTION SOLAR VS COLLECTOR AREA: COLUMBIA, MO

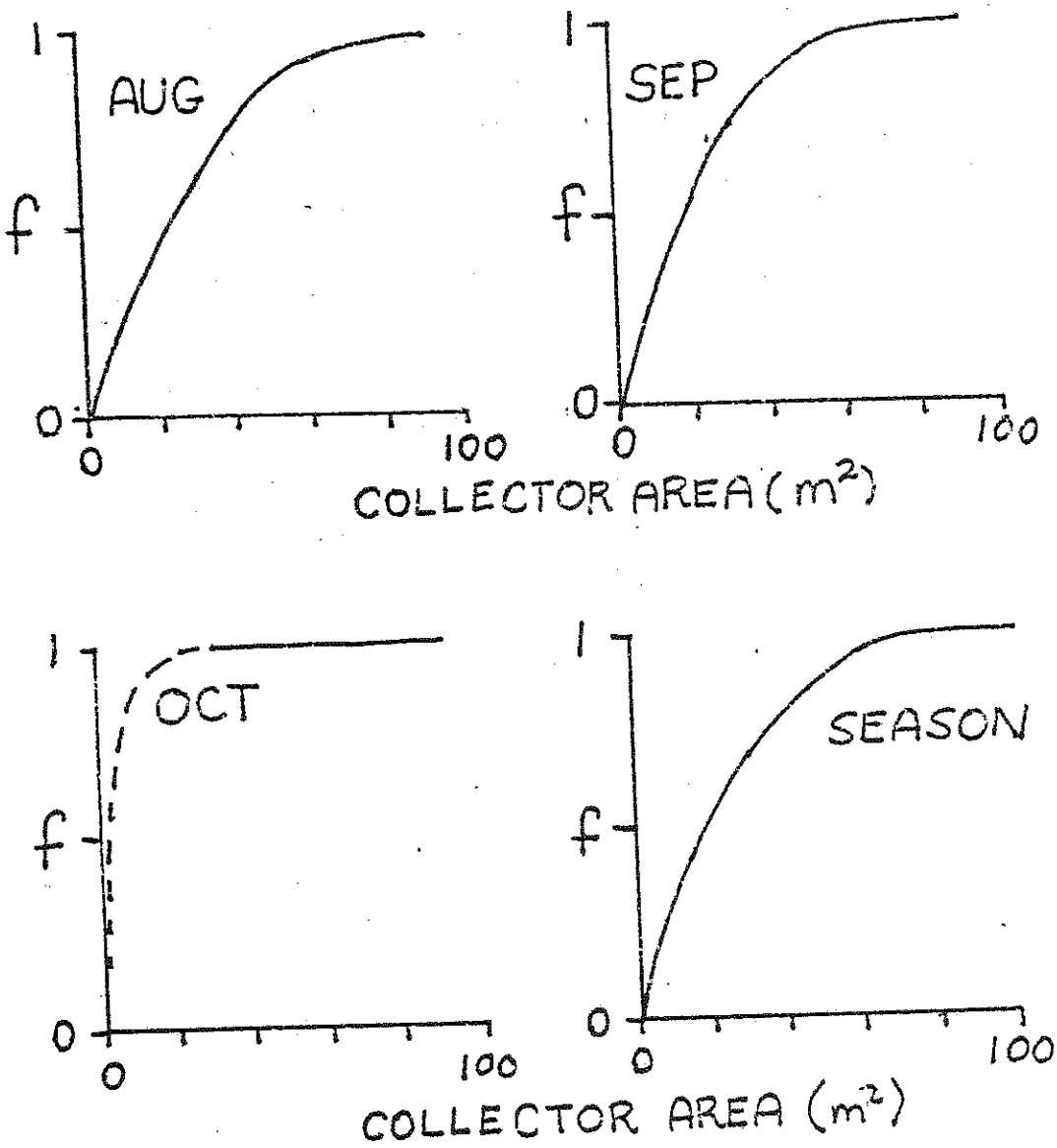

FIGURE 4.4.6, CONTINUED

CHAPTER V

Effect of Chiller Transients on Air Conditioning System Performance

5.1 Comparison of Instantaneous and Transient Response

Simulations were run to evaluate the effect of chiller transients on system performance. These simulations used the house, collector-storage system and air conditioning systems described in Chapter 4 and weather data from Miami and Charleston.

The house in Miami was simulated with collector arrays of 30 and 60 m^2. The Charleston house was simulated with 60 m^2 of collector. In these simulations, the absorption chiller used parallel heat auxiliary. The auxiliary set temperature, T_{aux}, was 95°C. The minimum solar source temperature was 77°C. First stage cooling was called for by the room thermostat when the room temperature exceeded 24.5°C, and second stage cooling was called for when the room temperature exceeded 25.5°C. The simulations were run with quarter-hour timesteps, and the state of the room thermostat (on or off) remained constant throughout the timestep.

Two cases were simulated for each location and collection area. In the first case, which will be referred to as the "instantaneous-response" case, the chiller startup and cooldown time constants were set equal to 0.001 hr. (Time constants equal to zero could not be used without causing a "division-by-zero" error in the chiller algorithm.) In the second case, which will be referred to as the "transient-response" case, values of 0.133 hr for τ_h and 1.05 hr for τ_c were used.

Table 5.1.1

Comparison of Transient and Instantaneous Chiller Response

Miami, FL $A = 60\ m^2$

All quantities expressed in GJ

	Transient	Instantaneous		Transient	Instantaneous
April			August		
Q_{cool}	12.24	12.24	Q_{cool}	16.33	16.33
Q_{gen}	19.47	18.44	Q_{gen}	26.72	26.39
Q_{aux}	2.42	1.42	Q_{aux}	11.69	11.40
May			Sept.		
Q_{cool}	13.14	13.13	Q_{cool}	14.44	14.48
Q_{gen}	20.51	19.23	Q_{gen}	23.05	22.40
Q_{aux}	6.19	5.03	Q_{aux}	8.74	8.33
June			Oct.		
Q_{cool}	13.74	13.75	Q_{cool}	13.63	13.63
Q_{gen}	21.50	20.77	Q_{gen}	21.14	20.05
Q_{aux}	9.48	8.76	Q_{aux}	5.75	4.78
July			Season		
Q_{cool}	14.38	14.40	Q_{cool}	97.9	98.0
Q_{gen}	22.65	21.92	Q_{gen}	155.0	149.2
Q_{aux}	9.50	8.67	Q_{aux}	53.8	48.4

Table 5.1.2

Comparison of Transient and Instantaneous Chiller Response

Miami, FL $A = 30\ m^2$

All quantities expressed in GJ

	Transient	Instantaneous		Transient	Instantaneous
April			August		
Q_{cool}	12.18	12.15	Q_{cool}	16.28	16.30
Q_{gen}	18.11	17.26	Q_{gen}	26.29	25.99
Q_{aux}	8.33	7.43	Q_{aux}	18.58	18.25
May			Sept.		
Q_{cool}	13.08	13.06	Q_{cool}	14.42	14.41
Q_{gen}	20.05	19.01	Q_{gen}	22.78	22.19
Q_{aux}	12.60	11.50	Q_{aux}	15.75	15.12
June			Oct.		
Q_{cool}	13.74	13.73	Q_{cool}	13.55	13.54
Q_{gen}	21.50	20.72	Q_{gen}	20.80	19.77
Q_{aux}	15.42	14.62	Q_{aux}	12.77	11.68
July			Season		
Q_{cool}	14.39	14.39	Q_{cool}	97.6	97.6
Q_{gen}	22.51	21.80	Q_{gen}	152.0	146.7
Q_{aux}	15.82	15.07	Q_{aux}	99.3	93.7

Table 5.1.3

Comparison of Transient and Instantaneous Chiller Response

Charleston, SC $A = 60\ m^2$

All quantities expressed in GJ

	Transient	Instantaneous		Transient	Instantaneous
April			August		
Q_{cool}	3.75	3.70	Q_{cool}	13.45	13.40
Q_{gen}	6.52	6.28	Q_{gen}	21.08	19.97
Q_{aux}	0	0	Q_{aux}	8.92	6.95
May			Sept.		
Q_{cool}	9.74	9.73	Q_{cool}	8.77	8.71
Q_{gen}	15.09	13.74	Q_{gen}	14.28	12.80
Q_{aux}	2.34	1.36	Q_{aux}	6.58	5.23
June			Oct.		
Q_{cool}	11.24	11.24	Q_{cool}	5.78	5.72
Q_{gen}	17.51	15.84	Q_{gen}	9.42	8.27
Q_{aux}	6.09	4.51	Q_{aux}	1.43	0.65
July			Season		
Q_{cool}	11.57	11.54	Q_{cool}	64.30	64.03
Q_{gen}	18.31	16.90	Q_{gen}	102.2	93.80
Q_{aux}	8.05	6.68	Q_{aux}	32.57	25.37

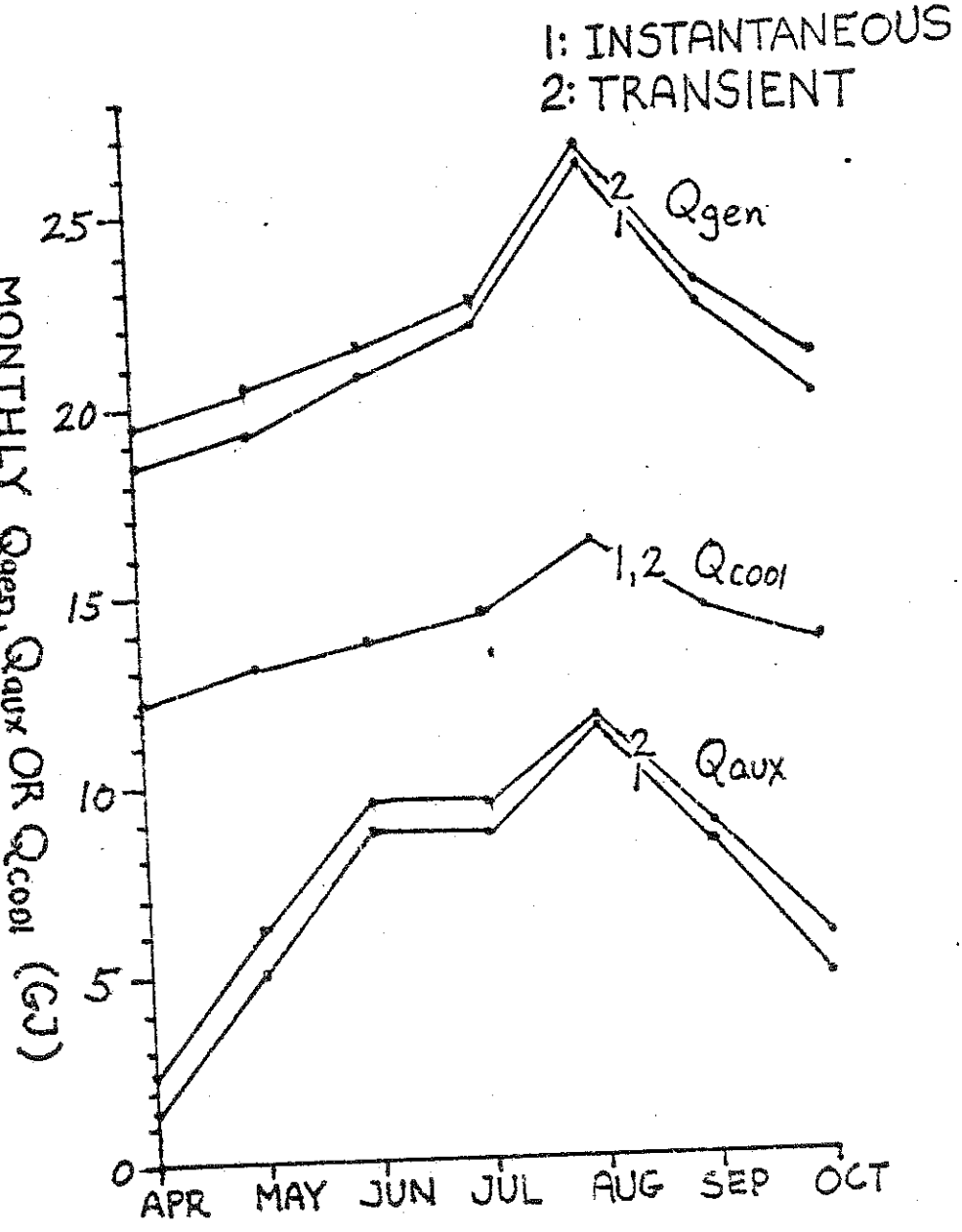

FIGURE 5.1.1 COMPARISON OF TRANSIENT AND INSTANTANEOUS CASES, MIAMI, FL $A = 60\ m^2$

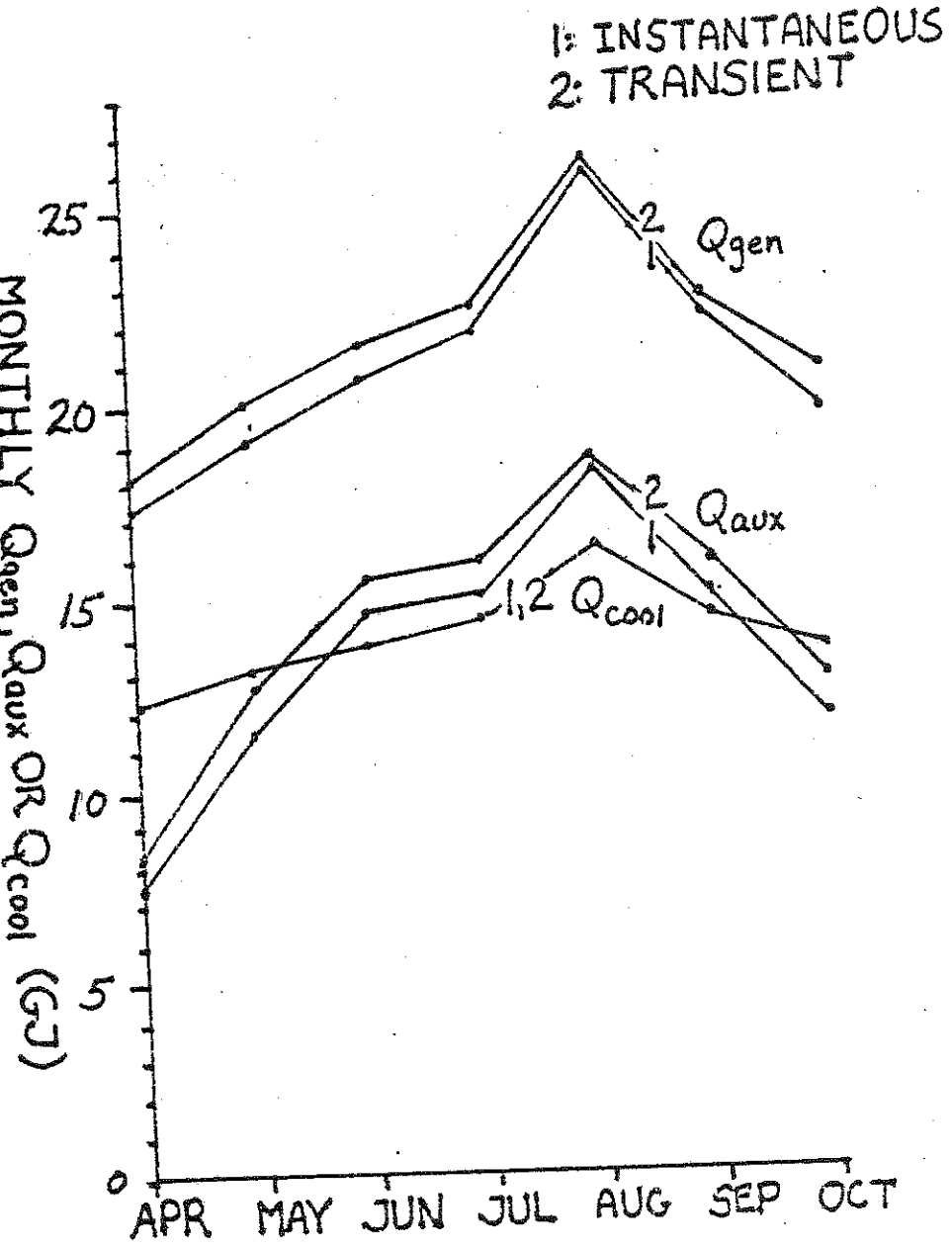

FIGURE 5.1.2 COMPARISON OF TRANSIENT AND INSTANTANEOUS CASES, MIAMI, FL $A = 30\ m^2$

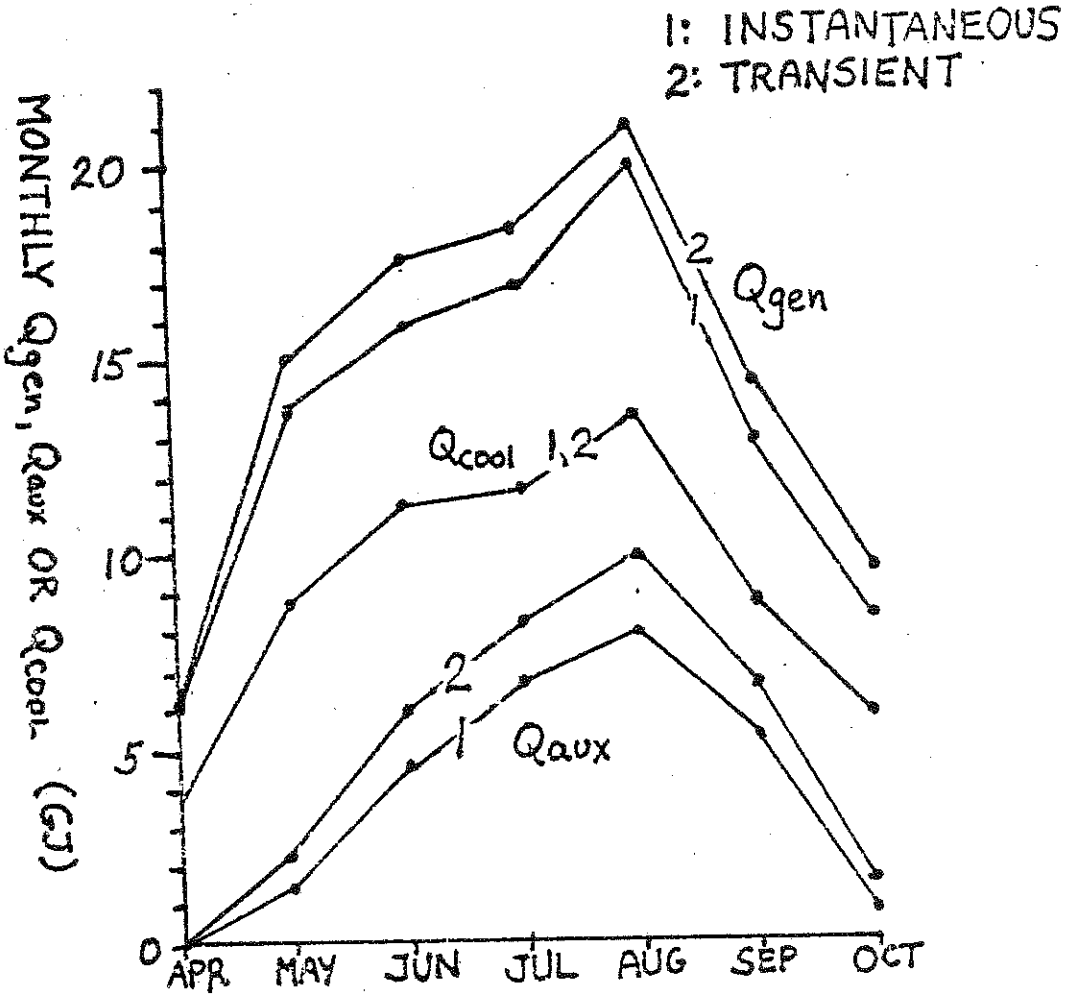

FIGURE 5.1.3 COMPARISON OF TRANSIENT AND INSTANTANEOUS CASES, CHARLESTON, SC
$A = 60\ m^2$

Table 5.1.4

Comparison of Transient and Instantaneous Chiller Response

Miami, FL A = 60 m^2

	Transient	Instantaneous		Transient	Instantaneous
April			August		
f	.876	.923	f	.563	.568
COP	.629	.675	COP	.611	.619
May			Sept.		
f	.698	.736	f	.621	.628
COP	.641	.686	COP	.626	.646
June			Oct.		
f	.559	.578	f	.728	.762
COP	.639	.662	COP	.645	.680
July			Season		
f	.581	.604	f	.653	.676
COP	.635	.657	COP	.632	.657

Table 5.1.5

Comparison of Transient and Instantaneous Chiller Response

Miami, FL A = 30 m^2

	Transient	Instantaneous		Transient	Instantaneous
April			August		
f	.540	.570	f	.293	.298
COP	.673	.704	COP	.619	.627
May			Sept.		
f	.372	.395	f	.309	.319
COP	.652	.687	COP	.633	.649
June			Oct.		
f	.283	.294	f	.386	.409
COP	.639	.663	COP	.651	.685
July			Season		
f	.297	.309	f	.347	.361
COP	.639	.660	COP	.642	.665

Table 5.1.6

Comparison of Transient and Instanteneous Chiller Response

Charleston, SC A = 60 m^2

	Transient	Instantaneous		Transient	Instantaneous
April			August		
f	1.00	1.00	f	.616	.652
COP	0.575	0.589	COP	.638	.671
May			Sept.		
f	.845	.901	f	.539	.591
COP	.645	.708	COP	.614	.680
June			Oct.		
f	.652	.734	f	.849	.921
COP	.642	.710	COP	.614	.692
July			Season		
f	.561	.605	f	.681	.730
COP	.632	.683	COP	.629	.683

Tables 5.1.1 and 5.1.2 list seasonal and monthly integrated energy quantities for the Miami simulations. Figures 5.1.1 and 5.1.2 show month-by-month plots of Q_{gen}, Q_{cool} and Q_{aux} for the transient and instantaneous cases in Miami. Comparing the transient and instantaneous case, it can be noted that in both cases total cooling provided was essentially identical. The greatest differences occurred in the total energy input to the generator, Q_{gen}, and in the auxiliary energy consumption Q_{aux}. For the 60 m^2 array, the transient case required 3.7% more energy to operate the chiller than was required in the instantaneous case over the cooling season.

Table 5.1.3 lists seasonal and monthly integrated energy flows for the Charleston simulations. Figure 5.1.3 shows month-by-month plots of Q_{gen}, Q_{cool} and Q_{aux} for Charleston. The differences between the transient and instantaneous cases are much more pronounced in Charleston than in Miami: the difference in Q_{gen} between the two cases was approximately 8.2% over the season in Charleston. Presumably this is because the chiller cycled on and off more frequently in Charleston, due to the lower cooling loads encountered.

Tables 5.1.4 and 5.1.5 list the monthly and seasonal fractions by solar and average coefficients of performance for the Miami simulations. These are calculated as

$$f = \frac{Q_{gen} - Q_{aux}}{Q_{gen}} \qquad (5.1.1)$$

$$COP = \frac{Q_{cool}}{Q_{gen}} \qquad (5.1.2)$$

Note that the above definition of f is not the same definition as was given in equation 4.4.1. Equation 5.1.1 will be used to define fraction by solar when heat auxiliary is provided, and equation 4.4.1 will apply when auxiliary is provided by a backup vapor compression unit.

The monthly values of f and COP are consistently higher for the instantaneous cases. The differences are most pronounced during months with a relatively low cooling load, such as April, May and October. Again this is presumably because the thermostat cycles on and off more frequently during these months. During months with a high cooling load, such as August, there tends to be less difference between the two cases.

Table 5.1.6 lists monthly and seasonal integrated values of f and COP for the Charleston simulations. Predictably, the differences between the transient and instantaneous cases are greater in Charleston than in Miami, and the greatest differences occur in months with lower cooling loads.

The general conclusions that can be drawn are that:

1. Chiller transients can significantly degrade the average chiller COP, and

2. The degradation of performance is greatest when the loads are lowest and the chiller cycles most frequently.

5.2 Effect of Room Thermostat Deadband

The results presented in Section 5.2.1 indicate a relationship between frequency of thermostat cycling and absorption chiller COP. Decreasing the frequency of thermostat cycling should improve the performance of the air conditioning system.

In the simulations described in Section 5.1, the room thermostat could change state as frequently as once per timestep (i.e. at 15 minute intervals). One possible means of reducing the cycling frequency is through the addition of a deadband on the room thermostat so that the thermostat would turn the chiller on at a set temperature and off at a somewhat lower temperature.

Mathematically this is described as follows:

a) If $\gamma^- = 0$ and $T_r > T_{rd} + \frac{\Delta T_{db}}{2}$

$$\gamma^+ = 1 \tag{5.2.1}$$

If $\gamma^- = 0$ and $T_r < T_{rd} + \frac{\Delta T_{db}}{2}$

$$\gamma^+ = 0 \tag{5.2.2}$$

b) If $\gamma^+ = 1$ and $T_r < T_{rd} - \frac{\Delta T_{db}}{2}$

$$\gamma^- = 0 \tag{5.2.3}$$

If $\gamma^+ = 1$ and $T_r < T_{rd} - \frac{\Delta T_{db}}{2}$

$$\gamma^- = 0 \tag{5.2.4}$$

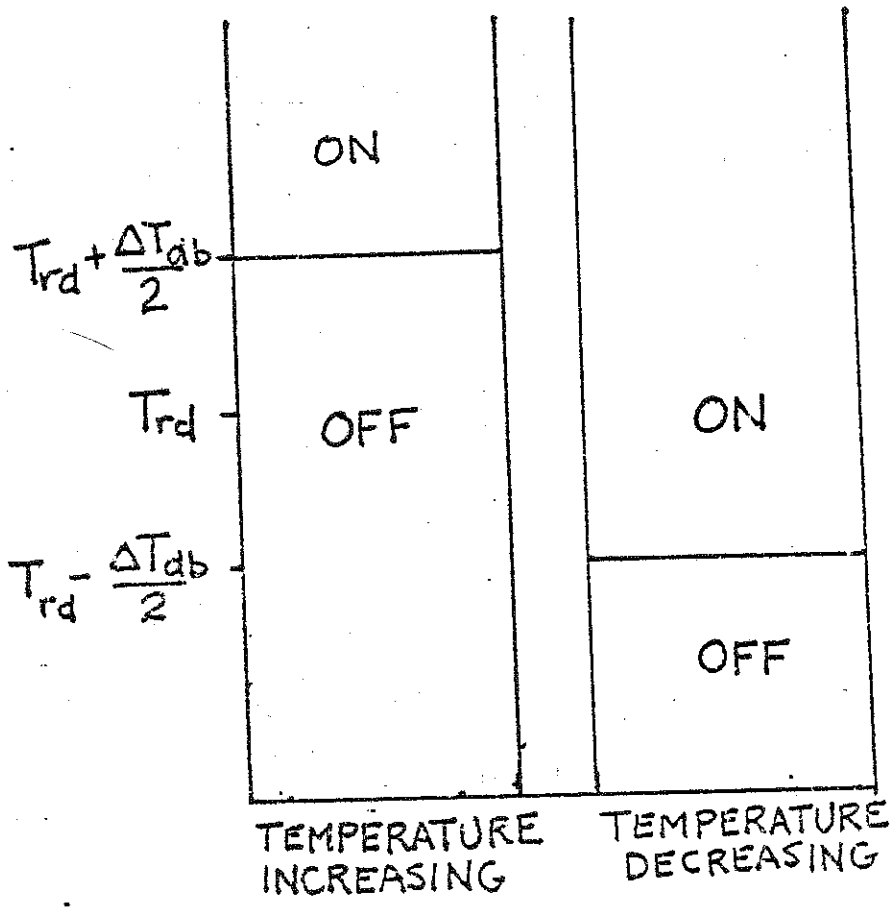

FIGURE 5.2.1 SCHEMATIC OF ROOM THERMOSTAT OPERATION WITH DEADBAND

Table 5.2.1

Effect of Room Thermostat Deadband

Charleston, SC A = 60 m^2

All energy quantities in GJ

Deadband, °C:		0	0.66	1.30	2.60	Instantaneous
APRIL:	Q_{cool}	3.75	3.73	3.73	3.77	3.70
	Q_{gen}	6.52	6.52	6.57	6.48	6.28
	Q_{aux}	0	0	0	0.04	0
MAY:	Q_{cool}	9.74	9.67	9.63	9.70	9.73
	Q_{gen}	15.09	14.72	14.43	14.12	13.74
	Q_{aux}	2.34	1.82	1.61	1.51	1.36
JUNE:	Q_{cool}	11.24	11.18	11.11	11.07	11.24
	Q_{gen}	17.51	17.07	16.65	16.14	15.84
	Q_{aux}	6.09	5.43	5.00	4.61	4.51
JULY	Q_{cool}	11.57	11.49	11.47	11.38	11.54
	Q_{gen}	18.31	17.99	17.67	17.11	16.90
	Q_{aux}	8.05	7.58	7.27	6.79	6.68

Table 5.2.1, continued

Deadband, °C:		0	0.66	1.30	2.60	Instantaneous
AUGUST:	Q_{cool}	13.45	13.33	13.30	13.27	13.40
	Q_{gen}	21.08	20.84	20.51	20.07	19.97
	Q_{aux}	8.92	7.79	7.44	7.03	6.95
SEPT:	Q_{cool}	8.77	8.72	8.63	8.57	8.71
	Q_{gen}	14.28	13.88	13.47	12.99	12.80
	Q_{aux}	6.58	6.14	5.74	5.33	5.23
OCT:	Q_{cool}	5.78	5.69	5.66	5.67	5.72
	Q_{gen}	9.42	9.03	8.76	8.46	8.27
	Q_{aux}	1.43	1.06	0.82	0.71	0.65
SEASON:	Q_{cool}	64.30	63.81	63.53	63.42	64.03
	Q_{gen}	102.20	100.0	98.04	95.37	93.80
	Q_{aux}	32.57	29.81	27.88	26.02	25.37

Table 5.2.2

Effect of Room Thermostat Deadband

Charleston, SC A = 60 m^2

fxQ_{cool} in GJ

Table 5.2.2

Deadband, °C:		0	0.66	1.30	2.60	Instantaneous
APRIL:	f	1.00	1.00	1.00	0.994	1.00
	fxQ_{cool}	3.75	3.73	3.73	3.75	3.70
	COP	0.575	0.572	0.568	0.582	0.589
MAY:	f	0.845	0.876	0.888	0.893	0.901
	fxQ_{cool}	8.23	8.47	8.55	8.66	8.77
	COP	0.645	0.657	0.667	0.687	0.708
JUNE:	f	0.652	0.682	0.700	0.714	0.734
	fxQ_{cool}	7.32	7.63	7.77	7.90	8.25
	COP	0.642	0.655	0.667	0.686	0.710
JULY:	f	0.561	0.578	0.589	0.603	0.605
	fxQ_{cool}	6.49	6.64	6.76	6.86	6.98
	COP	0.632	0.639	0.649	0.665	0.683

Table 5.2.2, continued

Deadband, °C:		0	0.66	1.30	2.60	Instantaneous
AUGUST:	f	0.616	0.626	0.637	0.650	0.652
	fxQ_{cool}	8.29	8.34	8.47	8.63	8.74
	COP	0.638	0.640	0.648	0.661	0.671
SEPT.:	f	0.539	0.558	0.574	0.590	0.591
	fxQ_{cool}	4.73	4.87	4.95	5.06	5.15
	COP	0.614	0.628	0.641	0.660	0.680
OCT:	f	0.849	0.883	0.906	0.916	0.921
	fxQ_{cool}	4.91	5.02	5.13	5.19	5.27
	COP	0.614	0.630	0.646	0.670	0.692
SEASON:	f	0.681	0.702	0.716	0.727	0.730
	fxQ_{cool}	43.79	44.79	45.49	46.11	46.74
	COP	0.629	0.638	0.648	0.665	0.683

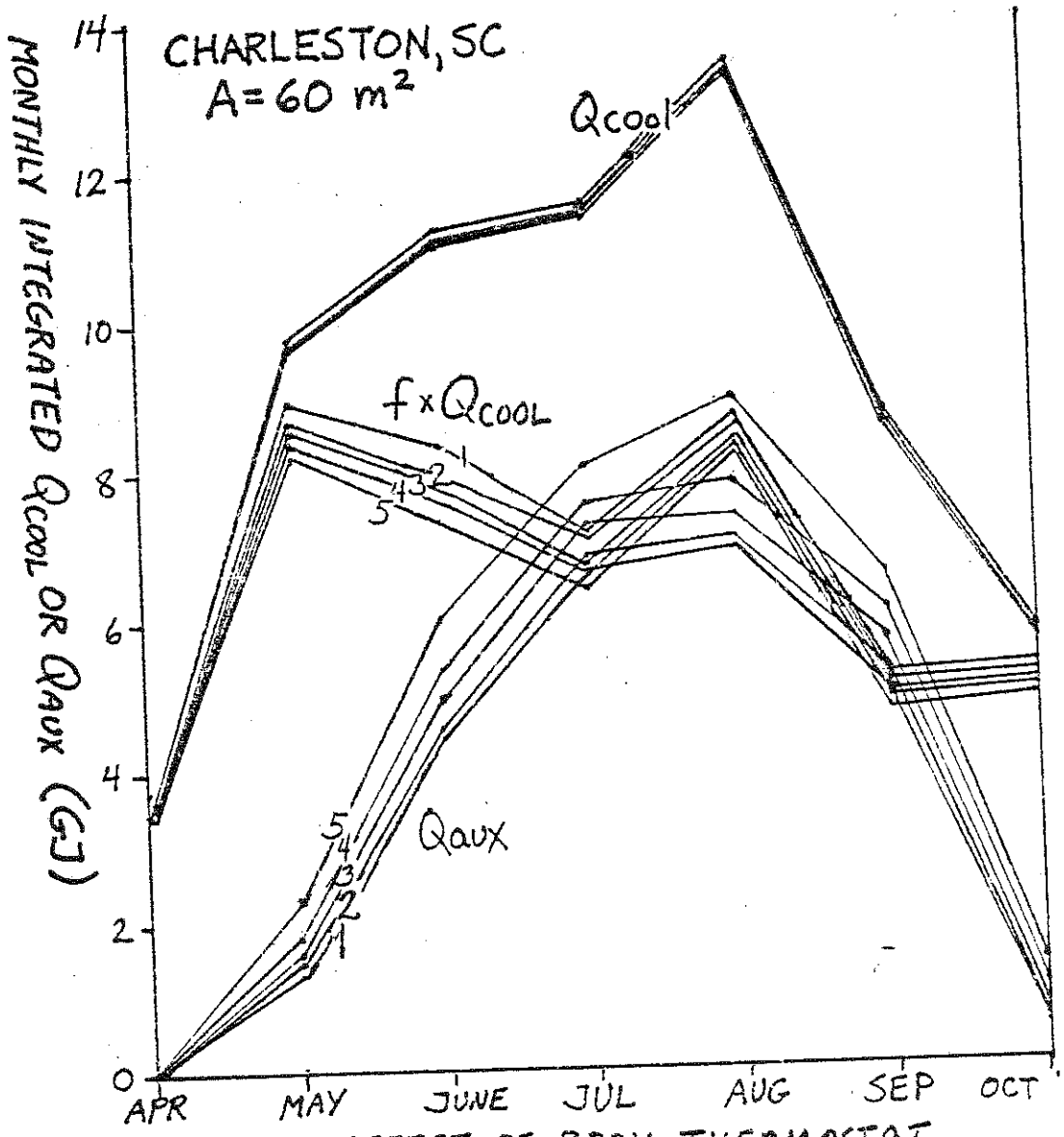

FIGURE 5.2.2 EFFECT OF ROOM THERMOSTAT DEADBAND (CHARLESTON, SC)

This behavior is shown schematically in Figure 5.2.1.

Simulations were performed using Charleston weather data from April 1 to November 1 with a collector area of 60 m^2. The absorption chiller used parallel heat auxiliary, with T_{aux} set at 95°C and T_{smin} set at 77°C.

To examine the effects of varying room thermostat deadbands, simulations were performed with thermostat deadbands of 0, 0.66, 1.30 and 2.60°C. The deadband center temperature, T_{rd}, was 24.5°C in all cases. Auxiliary was called for when the room temperature exceeded 26°C. No deadband was provided on the second stage of the room thermostat.

Tables 5.2.1 and 5.2.2 show the effect of thermostat deadband on system performance. The quantity (fQ_{cool}) in Table 5.2.2 is an approximate measure of the cooling provided by solar. Monthly values of Q_{cool}, Q_{aux} and fQ_{cool} are plotted in Figure 5.2.2.

An increase in deadband leads to a slight decrease in cooling load, as can be seen from Table 5.2.1. This is probably caused by energy stored in the building structure and contents over the course of the day being released to the ambient air at night when the ambient temperature is lower. A larger deadband allows more energy to be carried through the day in the building thermal capacitance without requiring cooling.

This effect is not very large. Over the course of a season the difference in load between the building with zero thermostat

deadband and the building with a 2.6°C thermostat deadband is only 0.88 GJ, or about 1.4% of the total load.

From Table 5.2.1 it can be seen that an increase in room thermostat deadband also led to a decrease in Q_{gen}, the energy supplied to the generator of the chiller. This cannot be entirely attributed to the accompanying decrease in cooling load. Over the season Q_{gen} was equal to 102.2 GJ with zero deadband and 95.37 GJ with a deadband of 2.5°C: a decrease of approximately 6.7%. The corresponding decrease in cooling load was only about 1.4%, which is not sufficient to entirely account for the decrease in Q_{gen}.

The auxiliary energy requirement was significantly decreased. The seasonal value of Q_{aux} was 32.6 GJ with zero deadband and 26.0 GJ with a 2.6°C deadband--a decrease of 6.6 GJ, or approximately 20%. Since auxiliary heat and parasitic power for pumps and fans are the only purchased energy requirements of the air conditioning system, a 20% reduction in auxiliary energy requirement represents a substantial reduction in chiller operating costs.

5.3 Summary

The COP of the absorption air conditioning system is significantly lowered by thermostat cycling. This effect is most significant under conditions of low cooling load, or where the absorption chiller is oversized for the cooling load.

Use of an appropriate deadband on the room thermostat will lessen the impact of chiller cycling on COP. The optimum choice

of thermostat deadband will be dictated by a compromise between energy savings and occupant comfort.

CHAPTER VI

Control of Auxiliary

6.1 Detailed Description of Auxiliary Modes

The TRNSYS chiller component described in Chapter 3 offers a choice of four auxiliary modes. These were described briefly in Chapter 3 and will be discussed in more detail here. Three of the four modes provide for auxiliary heat to be supplied to operate the absorption chiller. The fourth mode provides no auxiliary energy for the chiller; auxiliary cooling, if needed, must be provided by a separate backup unit.

In the three auxiliary-heat modes, the control system will call for auxiliary heat if chiller operation is called for by the first stage of the room thermostat and either a) storage is below T_{smin} or b) the room temperature rises sufficiently to actuate the second stage of the room thermostat. The differences between these three modes lie in the flow path of firing water during operation on auxiliary.

Series heat auxiliary is diagrammed in Figure 6.1.1. Auxiliary is called for by controller C1 when T_{stor} is below T_{smin}, or by the second stage of the room thermostat. When auxiliary is not called for, the three way valve V1 diverts firing water around the auxiliary heater. When auxiliary is called for, V1 routes firing water through the auxiliary heater, into the generator of the absorption chiller, and back to storage.

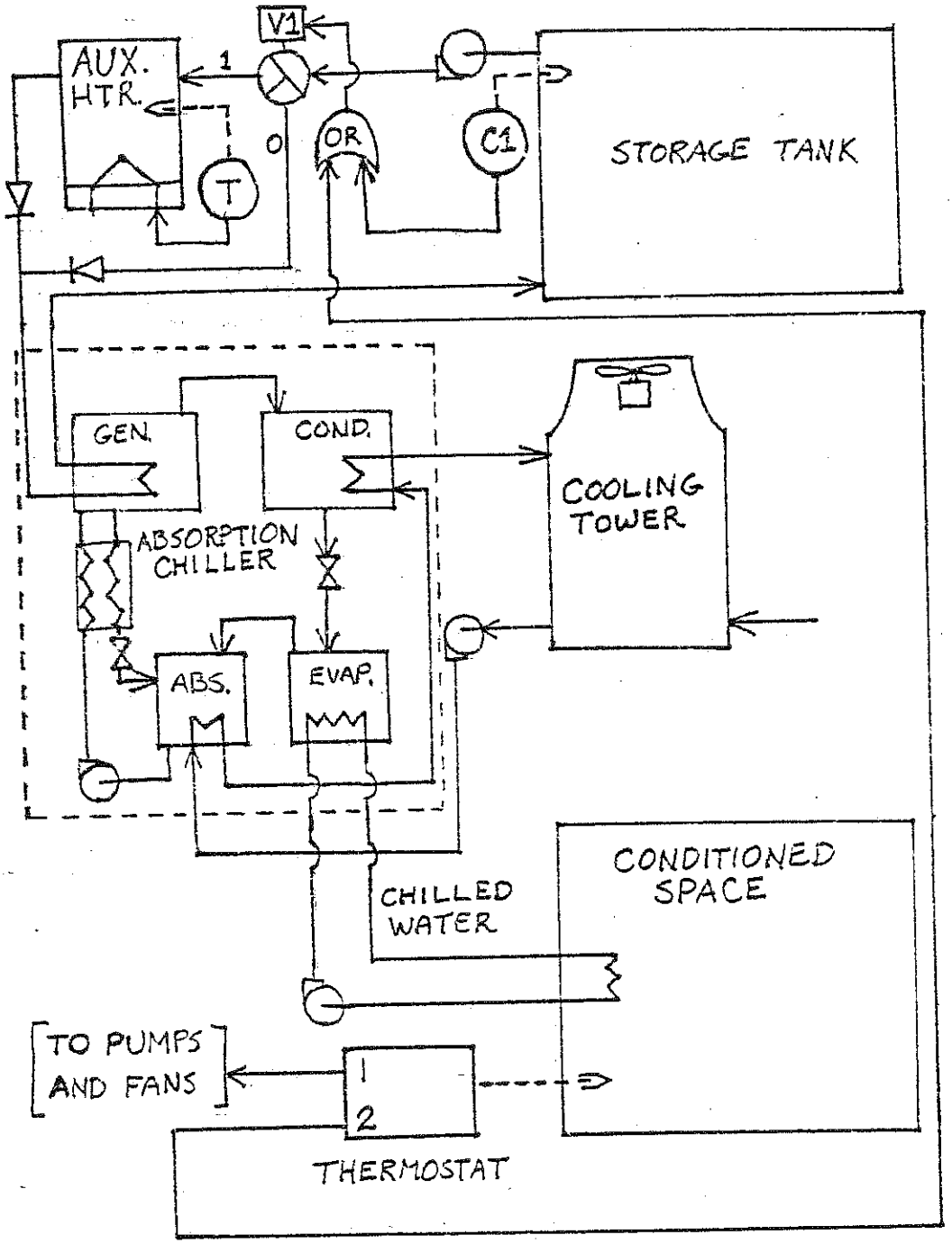

FIGURE 6.1.1 DETAILED SCHEMATIC OF SYSTEM WITH SERIES HEAT AUXILIARY

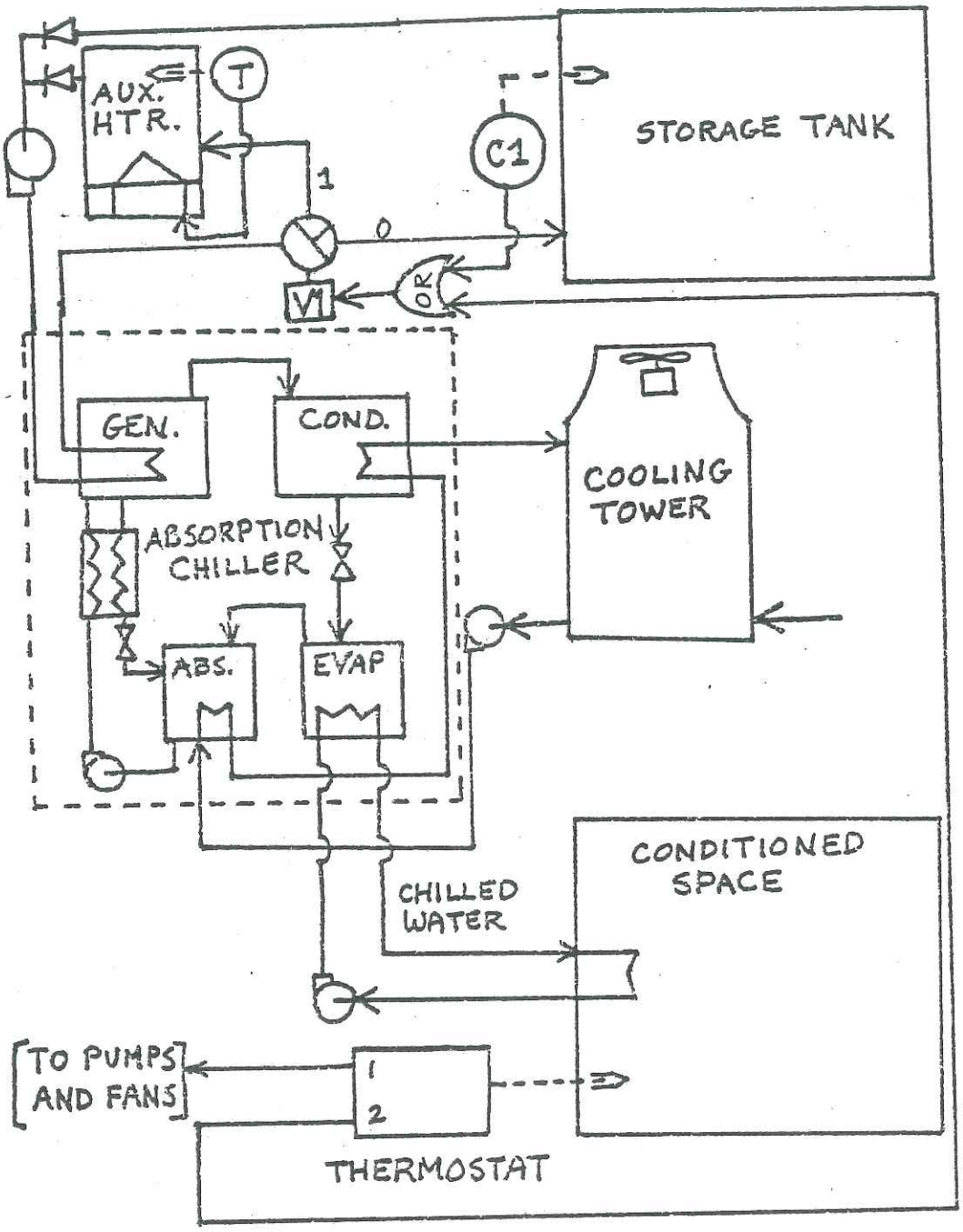

FIGURE 6.1.2 DETAILED SCHEMATIC OF SYSTEM WITH PARALLEL HEAT AUXILIARY

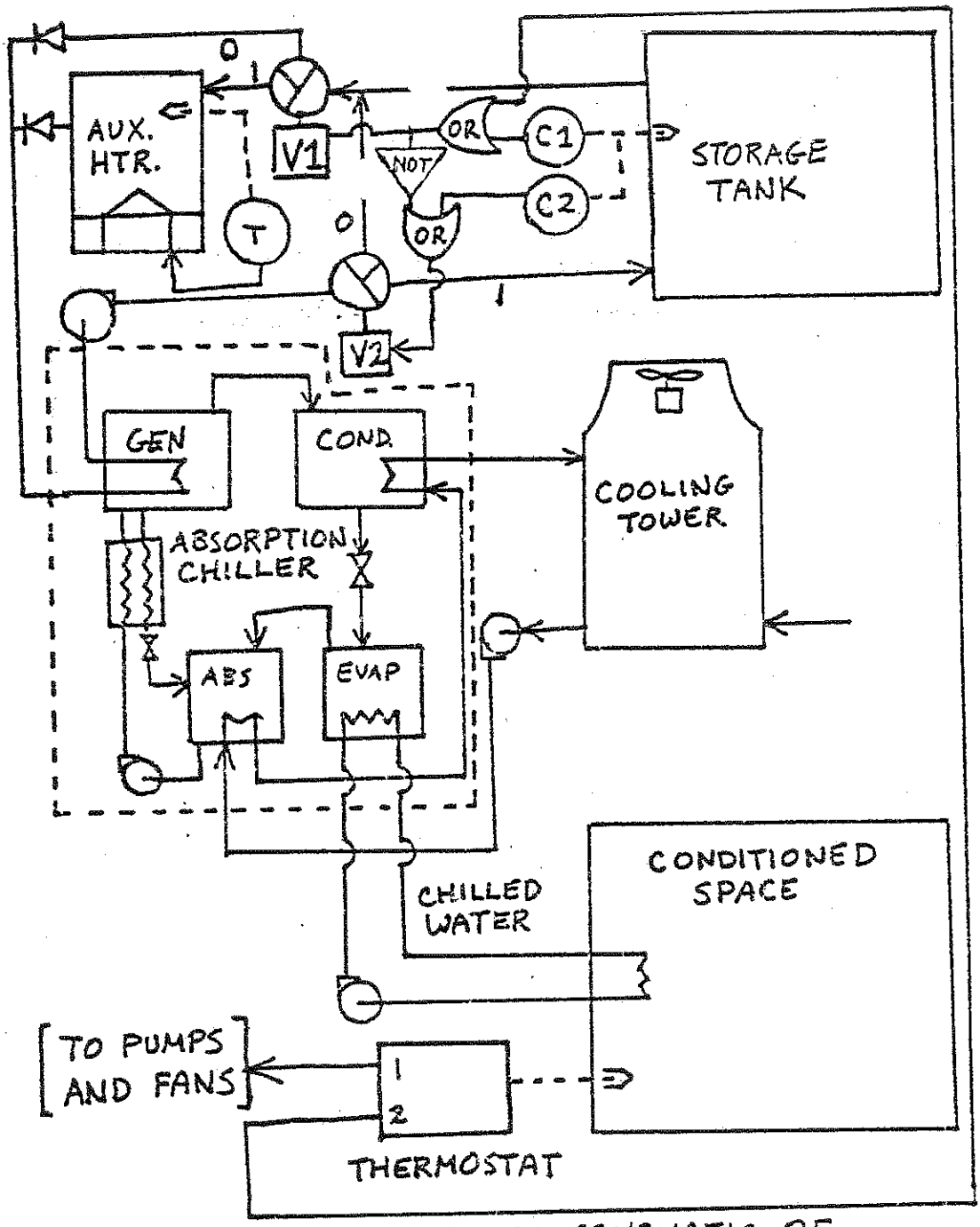

FIGURE 6.1.3 DETAILED SCHEMATIC OF SERIES-PARALLEL HEAT SYSTEM WITH AUXILIARY

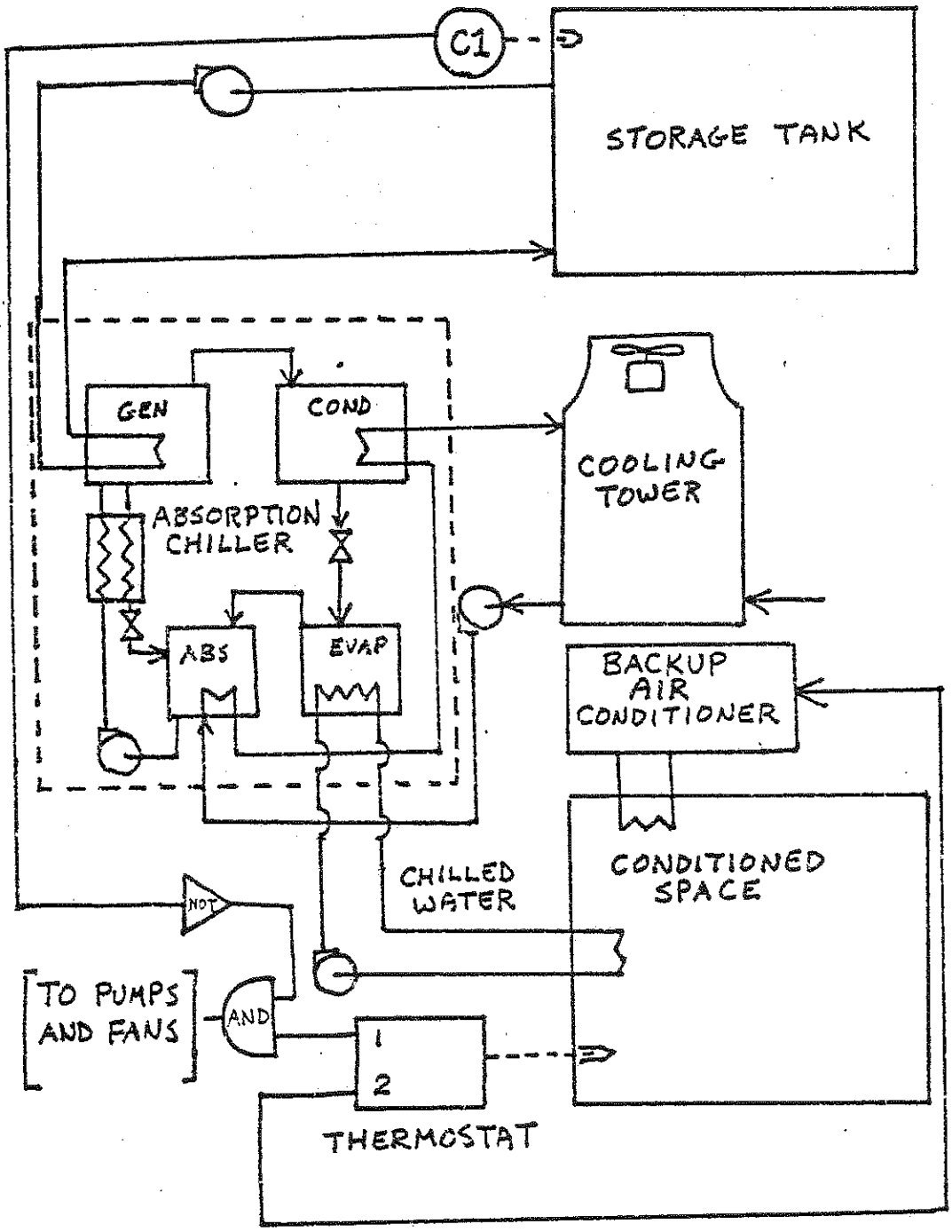

FIGURE 6.1.4 DETAILED SCHEMATIC OF SYSTEM WITH VAPOR-COMPRESSION AUXILIARY

Parallel heat auxiliary is diagrammed in Figure 6.1.2. Auxiliary is called for by controller C1 or the room thermostat, as before. When auxiliary is not needed, valve V1 returns firing water from the generator to storage. When auxiliary is required, valve V1 returns firing water to the auxiliary heater, bypassing storage.

Series-parallel heat auxiliary is diagrammed in Figure 6.1.3. The control system for this auxiliary mode is somewhat more complex than for series or parallel heat auxiliary. The system functions like the parallel heat auxiliary system when the solar source temperature is below a specified changeover temperature, T_{cr}, and like the series heat auxiliary system when the solar source temperature is above T_{cr}.

When auxiliary is not required, valve V1 will be set so as to bypass the auxiliary heater, and valve V2 will be set to return firing water to storage. If auxiliary is called for controller C1 will set valve V1 to route firing water into the auxiliary heater. If auxiliary is commanded and storage is below T_{cr}, controller C2 will cause valve V2 to return firing water to V1. Otherwise, valve V2 will return firing water to storage.

Figure 6.1.4 shows a system without heat auxiliary. In this mode, controller C1 shuts off the chiller when the solar source temperature falls below T_{smin}.

6.2 Comparison of Performance of Four Auxiliary Modes

6.2.1 Comparison of Thermal Performance

To compare the performance of air conditioning systems using the four auxiliary modes described above, simulations were run for Miami, Charleston and Columbia, from April 1 to November 1, 1975. The house, collectors, and absorption chiller were described in Chapter 4. Absorption chiller startup and cooldown time constants were .133 hour and 1.05 hour, respectively. Collector arrays of 60 m^2 were used in Miami and Charleston, and a 30 m^2 array was used in Columbia.

In all simulations, T_{smin} was set at 77°C. Where applicable, T_{aux} was set at 95°C and T_{cr} at 90 °C. The room thermostat called for first-stage cooling when the room temperature exceeded 24.5°C. No deadband was provided on the first stage. The second stage of the room thermostat turned on when the room temperature rose above 25.5°C, and turned off when the room temperature fell below 24.5°C.

In the case where auxiliary heat was not provided for the absorption chiller, a 3.2 ton (40,000 kJ/hr) vapor compression chiller provided backup cooling. The backup chiller was commanded only by the second stage of the room thermostat.

Table 6.2.1 lists seasonally integrated values of Q_u (total solar energy collected), collector efficiency (defined as Q_u divided by the total insolation on the collector array), Q_{aux}, Q_{gen}, $Q_{cool,a}$,

Table 6.2.1

Comparison of Auxiliary Modes

Miami, FL A = 60 m^2 April 1-November 1

MODE:	Series Heat Aux.	Parallel Heat Aux.	Series-Parallel Heat Aux.	Electric Vap.-Comp. Aux.
Q_u (GJ)	105.3	107.5	107.6	108.4
COLLECTOR EFFICIENCY	42.8%	43.7%	43.7%	44.1%
Q_{aux} (GJ)	70.0	65.9	65.5	0
Q_{gen} (GJ)	165.5	165.6	165.7	102.4
$Q_{cool,a}$ (GJ)	106.0	106.6	106.5	64.7
$Q_{cool,b}$ (GJ)	0	0	0	41.9
COP_a	0.640	0.643	0.643	0.632
f	0.577	0.602	0.605	0.607

f defined by equation 5.1.1 or 4.4.1 as applicable

Table 6.2.2

Comparison of Auxiliary Modes

Charleston, SC A = 60 m^2 April 1-November 1

MODE:	Series Heat Aux.	Parallel Heat Aux.	Series-Parallel Heat Aux.	Electric Vap.-Comp. Aux.
Q_u (GJ)	80.7	82.3	82.5	83.1
COLLECTOR EFFICIENCY	37.3%	38.1%	38.2%	38.4%
Q_{uax} (GJ)	37.9	34.5	34.0	0
Q_{gen} (GJ)	106.0	103.8	103.6	70.2
$Q_{cool,a}$ (GJ)	64.8	64.7	64.8	45.3
$Q_{cool,b}$ (GJ)	0	0	0	19.5
COP_a	0.612	0.624	0.625	0.644
f	0.642	0.667	0.672	0.699

f defined by equation 5.1.1 or 4.4.1 as applicable

Table 6.2.3

Comparison of Auxiliary Modes

Columbia, MO A = 30 m^2 April 1-November 1

MODE:	Series Heat Aux.	Parallel Heat Aux.	Series-Parallel Heat Aux.	Electric Vap.-Comp. Aux.
Q_u (GJ)	58.5	60.0	60.0	60.5
COLLECTOR EFFICIENCY	42.3%	43.4%	43.4%	43.7%
Q_{aux} (GJ)	28.2	25.7	25.7	0
Q_{gen} (GJ)	72.2	71.5	71.5	46.1
$Q_{cool,a}$ (GJ)	47.0	47.3	47.3	31.7
$Q_{cool,b}$ (GJ)	0	0	0	15.6
COP_a	0.651	0.662	0.662	0.687
f	0.610	0.641	0.641	0.669

f defined by equation 5.1.1 or 4.4.1 as applicable

COP_a (the average COP of the absorption chiller) and fraction by solar for the four auxiliary modes in Miami.

From Table 6.2.1 it is apparent that series heat auxiliary requires the most auxiliary heat and leads to the lowest collector efficiency and fraction by solar. Parallel heat auxiliary requires approximately 6% less auxiliary energy than does series, and series-parallel requires about 0.6% less auxiliary energy than does parallel.

Vapor compression backup leads to the highest Q_u and fraction by solar, and the lowest COP. This is presumably because the absorption chiller will operate on solar source whenever cooling is required and there is energy available in storage. The other modes allow the chiller to operate on auxiliary when auxiliary is called for by the second stage of the room thermostat, even when storage is above T_{smin}. Storage will thus tend to be at a lower temperature on the average, when vapor compression backup is used, leading to a higher collector efficiency. The lower storage temperature also leads to a reduction in COP, but this is more than compensated for by the higher collector efficiency, leading to a higher fraction by solar.

Tables 6.2.2 and 6.2.3 give the same information for Charleston and Columbia. Again, it is apparent that parallel heat auxiliary gives significantly better performance than series heat auxiliary, and that series-parallel heat auxiliary performs, at best, slightly

better than parallel. As was the case in Miami, vapor-compression auxiliary leads to the highest fraction by solar. In short, the general conclusions that were drawn from Miami also hold true in Columbia and Charleston.

6.2.2 Economic Comparison of Heat and Vapor Compression Auxiliary

A comparison between vapor-compression auxiliary and heat auxiliary will depend on the source of backup heat, the auxiliary heater efficiency, and the average coefficients of performance of the absorption and vapor-compression units. The operating cost per unit of auxiliary cooling delivered by the absorption chiller operating on auxiliary will be

$$C_a = \frac{C_f}{\eta_{ah} COP_a} \qquad (6.2.1)$$

where C_f is the cost of the backup fuel used to fire the auxiliary heater, η_{ah} is the auxiliary heater efficiency and COP_a is the average COP of the absorption chiller. The operating cost per unit of backup cooling by the vapor-compression unit is

$$C_b = \frac{C_e}{COP_b} \qquad (6.2.2)$$

By equating C_a and C_b, a relation between C_f and C_e can be determined such that the auxiliary energy costs are identical for vapor-compression and heat auxiliary:

$$C_e = \frac{COP_b}{\eta_{ah} COP_a} C_f \qquad (6.2.3)$$

As an example, suppose that the average absorption chiller COP were 0.64 (as in Miami with parallel heat auxiliary), the auxiliary boiler efficiency was 0.7, the average COP of the vapor-compression unit were 2.5, and the cost of electricity was 5 cents per kilowatt hour, or $13.85 per GJ. The highest cost of back-up fuel for the auxiliary heater at which heat auxiliary would be less expensive than vapor compression auxiliary, in terms of seasonal energy cost, is

$$C_f = \frac{C_e \eta_{ah} COP_a}{COP_b} = \frac{(13.85)(0.7)(0.64)}{2.5}$$

$$= \$2.48/GJ = \$2.61/Million\ BTU$$

Under these assumptions, unless backup fuel was available for less than $2.61/million BTU (unlikely), vapor-compression backup would cost less to operate.

Note that this rather simple analysis does not take into account the observed fact that the fraction by solar is higher with vapor-compression backup than with heat backup. On the other hand, the analysis does not deal with the relative capital costs of a vapor-compression chiller versus an auxiliary heater. The final decision would need to be made on a life-cycle cost basis which is outside the scope of this thesis.

6.3 Effect of Varying Auxiliary Control Setpoints

6.3.1 Effect of Varying T_{aux}

In the simulations described in Section 6.2, the auxiliary boiler set temperature was 95°C. A series of simulations were performed to examine the effect of varying T_{aux}, and to locate the optimum value.

The usual house, collector and absorption chiller were simulated in Charleston from April 1 to November 1, 1975, using 60 m^2 of collector. Parallel heat auxiliary was provided for the absorption chiller; values of T_{aux} of 80, 85, 90 and 95°C were simulated and compared.

Results are shown in Table 6.3.1. Variations in T_{aux} have a relatively small effect on fraction by solar and auxiliary energy consumption. The maximum spread in Q_{aux}, for instance, is only about 2.5% of the total auxiliary heat supplied.

The highest system COP and fraction by solar, as well as the lowest seasonal Q_{aux}, occur for T_{aux} in the neighborhood of 90°C. This is not particularly surprising in light of the fact that the highest steady-state chiller COP occurs for firing water temperatures in the vicinity of 90°C.

6.3.2 Effect of Varying T_{smin}

To evaluate the effect of T_{smin} on system performance, simulations were run (using the house described in 6.3.1) in which T_{smin} was varied.

Table 6.3.1

Effect of Varying T_{aux}

Charleston, SC A = 60 m^2 April 1-November 1

T_{aux}, °C:	80	85	90	95
Q_{cool} (GJ)	63.0	64.2	64.6	64.7
Q_{gen} (GJ)	105.1	104.4	103.3	103.8
Q_{aux} (GJ)	34.6	34.4	33.8	34.6
f	0.671	0.670	0.673	0.667
COP	0.600	0.615	0.625	0.624
f Q_{cool}	42.3	43.0	43.4	43.2

The optimum value of T_{smin} will depend on the interactions between the collectors, storage and absorption chiller. The chiller COP increases as firing water temperature increases up to about 90°C. On the other hand, collector efficiency decreases and storage losses increase as storage temperature increases. Thus, increasing T_{smin} could be expected to increase the cooling delivered per unit of energy supplied to the generator, while simultaneously decreasing the energy available to the generator.

It would be reasonable to expect that the optimum value of T_{smin} would be affected by the dependence of collector efficiency on storage temperature. To test this hypothesis, additional simulations were run in which U_L, the collector loss coefficient, was halved (U_L = 7.2 kJ/m^{2}hr°C).

Collector area was set at 60 m^2. Auxiliary cooling was provided by a 3.2-ton vapor compression unit when called for by the second stage of the room thermostat. No auxiliary heat was provided for the absorption chiller.

Values of T_{smin} of 77, 80, 85 and 90°C were simulated. No simulations were run with T_{smin} below 77°C, in order to avoid a situation in which the steady-state generator temperature would be below T_{gmin}.

Table 6.3.2 lists the results of simulations in which U_L was equal to 14.4 kJ/m^{2}hr°C. Q_{dump} is the energy dumped by the tank relief valve. Collector efficiency is defined differently than

Table 6.3.2

Effect of Varying T_{smin}: U_L = 14.4 kJ/hr m^2 °C

Charleston, SC A = 60 m^2 April 1-November 1

T_{smin}, °C:	77	80	85	90
Q_u (GJ)	82.6	80.6	77.2	73.8
Q_{dump} (GJ)	7.1	7.3	8.3	11.5
Q_u-Q_{dump} (GJ)	75.5	73.3	68.8	62.3
η_c	0.35	0.34	0.32	0.29
Q_{gen} (GJ)	70.0	67.6	62.6	55.7
$Q_{cool,a}$ (GJ)	44.4	44.0	41.3	36.3
$Q_{cool,b}$ (GJ)	18.7	19.3	22.0	26.6
f	0.703	0.695	0.653	0.577
COP_a	0.633	0.651	0.660	0.652
$\eta_c x COP_a$	0.222	0.221	0.211	0.189

η_c defined by equation 6.3.1

f is defined by equation 4.4.1

in Tables 6.2.1 through 6.2.3, and is given by

$$\eta_c = \frac{Q_u - Q_{dump}}{A \int_{month} H_T dt} \qquad (6.3.1)$$

Equation 6.3.1 defines collector efficiency as the net energy delivered to storage divided by the insolation on the collector.

From Table 6.3.2 it can be seen that the fraction by solar is highest at a T_{smin} of 77°C, and declines steadily as T_{smin} increases. Although COP increases as T_{smin} increases, η_c declines more rapidly. There are two reasons for this decline in collector efficiency. First, the losses from the collector, and hence Q_u, increase as T_{smin} is increased. Furthermore, as T_{smin} is raised Q_{dump} increases quite rapidly. This is due to the fact that the tank temperature is constrained to lie between T_{smin} and 100°C. As T_{smin} gets closer to 100°C, less energy can be stored in the tank and more must be rejected by the relief valve.

Figure 6.3.1 shows the fraction air conditioning by solar as a function of T_{smin} for a U_L of 14.4 kJ/m^{2}hr°C.

Table 6.3.3 lists results of simulations in which U_L = 7.2 kJ/hrm^2°C. Again, the maximum value of f occurs at the minimum value of T_{smin}. The collector efficiency defined in equation 6.3.1 declines more rapidly than COP increases, as T_{smin} is increased. Although Q_u is less sensitive to T_{smin} than was the case with the other collector, this is more than compensated for by the much larger dependence of Q_{dump} on T_{smin}.

Table 6.3.3

Effect of Varying T_{smin}: U_L = 7.2 kJ/hr m^2 °C

Charleston, SC A = 60 m^2 April 1-November 1

T_{smin}, °C:	77	80	85	90
Q_u (GJ)	119.4	118.6	116.9	115.3
Q_{dump} (GJ)	22.9	24.0	28.3	35.2
Q_u-Q_{dump} (GJ)	96.5	94.6	88.6	80.1
η_c	0.45	0.44	0.41	0.37
Q_{gen} (GJ)	91.0	88.9	82.6	73.7
$Q_{cool,a}$ (GJ)	56.6	56.0	53.1	47.7
$Q_{cool,b}$ (GJ)	7.5	8.2	10.9	15.8
f	0.883	0.872	0.829	0.752
COP_a	0.622	0.631	0.644	0.647
$\eta_c x COP_a$	0.262	0.259	0.246	0.221

η_c defined by equation 6.3.1

f defined by equation 4.4.1

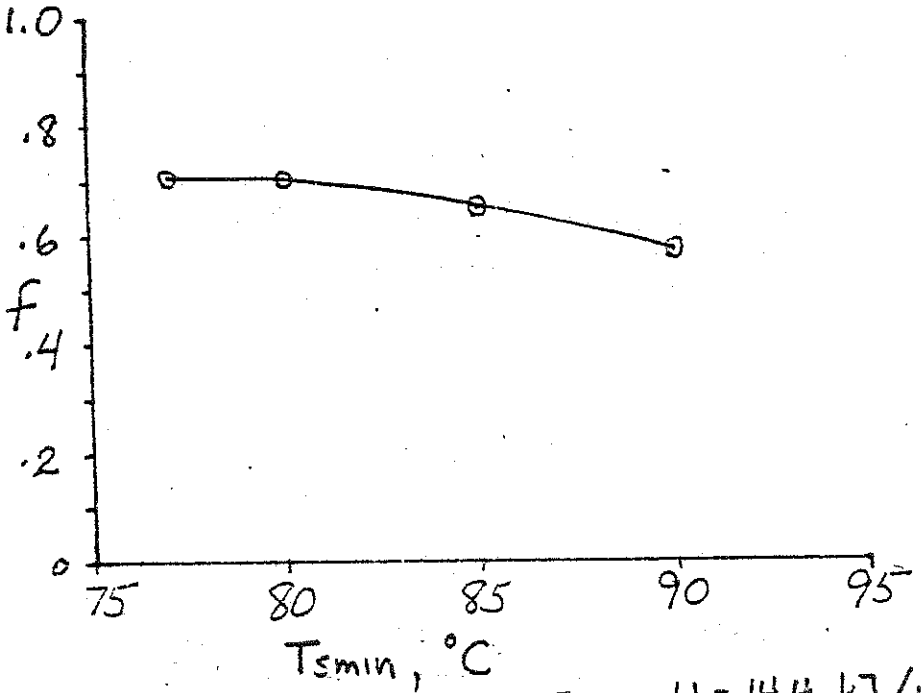

FIGURE 6.3.1 EFFECT OF T_{SMIN}: U_L = 14.4 kJ/HR M^2 °C

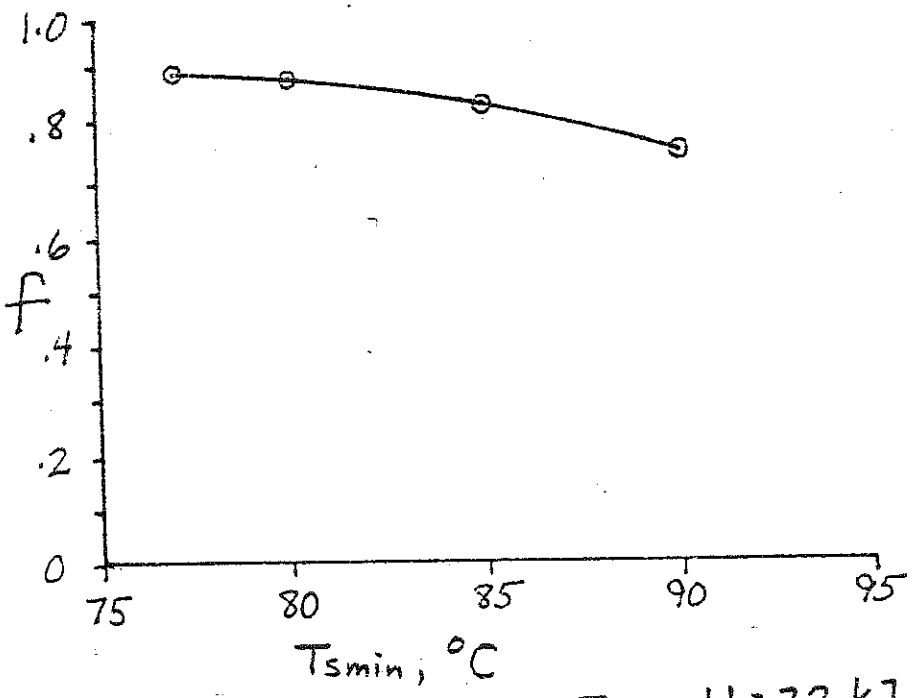

FIGURE 6.3.2 EFFECT OF T_{SMIN}: U_L = 7.2 kJ/HR M^2 °C

Figure 6.3.2 shows f as a function of T_{smin} for U_L equal to 7.2 kJ/hrm^2°C. As was the case for U_L equal to 14.4 kJ/hrm^2°C, the maximum fraction by solar occurs at the minimum value of T_{smin}.

6.4 Summary

Comparison of four auxiliary strategies (series heat, parallel heat, series-parallel heat and vapor-compresson auxiliary) indicates that parallel and series-parallel heat auxiliary lead to lower auxiliary energy requirements than series heat auxiliary. A choice between heat and vapor-compression auxiliary would have to be made on economic grounds. Criteria for comparing the seasonal auxiliary energy costs are given, but no life cycle cost analyses are attempted.

When heat auxiliary was used, the optimum auxiliary boiler set temperature was found to be in the neighborhood of 90°C for the chiller simulated. This value corresponds to the firing water temperature at which the chiller has its highest steady-state COP.

The optimum value of T_{smin} was found to be 77°C, which is very close to the minimum firing water temperature at which the chiller can successfully be operated. The optimum value of T_{smin} was not noticeably affected by changing collector U_L.

CHAPTER VII

Recommendations for Further Study

7.1 Recommendations for Further Simulations With Existing Transient Chiller Model

7.1.1 Ammonia-Water Absorption Chillers

The transient model derived in Chapter 2 should be applicable to any single-effect absorption refrigeration machine. The simulations described in Chapters 4, 5 and 6 have all dealt with a chiller using lithium bromide and water, but the chiller model could easily be extended to single-effect ammonia-water chillers as well.

Absorption chillers using ammonia as the refrigerant and water as the absorbent are commercially available. An ammonia-water chiller could be simulated by using appropriate values of the parameters T_{gmin}, $(UA)_o$, τ_h, τ_c, a_{ij} and b_{ij} in the transient chiller model. Ammonia-water chillers usually require higher firing temperatures than lithium bromide-water chilers, and may be advantageously used with evacuated tube or concentrating collectors.

7.1.2 Phase Change Energy Storage

Phase change energy storage materials may be useful in solar air conditioning systems. Phase change materials could be applied to either "hot side" or "cold side" storage. In hot side storage, energy would be collected and used to melt the phase change material at a temperature appropriate for firing the absorption chiller.

Phase change storage would offer the advantage of providing energy at a constant temperature. A phase change material which melts at a temperature where chiller COP is at a maximum might lead to a significant improvement in air conditioning system performance.

With cold side storage, heat would be transferred from the phase change energy storage to the evaporator of the absorption chiller when the chiller is operated, and from the conditioned space to the phase change energy storage material when space cooling is required. By using this scheme it may be possible to reduce chiller cycling and thereby improve system performance.

7.2 Recommendations For Improvements in the Chiller Model

7.2.1 Interactions Between Chiller and Fan Coil

The chiller model described in Chapters 2 and 3 assumes a constant chilled water delivery temperature. In a real system the absorption chiller delivers chilled water to a fan coil which removes heat (sensible and latent) from an air stream. The actual temperature at which chilled water is delivered will be the temperature at which the rate of heat transfer into the evaporator of the absorption chiller is equal to the rate at which heat is transferred from the air stream to the chilled water at the fan coil.

To realistically model this interaction it would be necessary first to modify the chiller model to express performance as a function of chilled water temperature at evaporator inlet, as well as

condensing water inlet and generator temperatures, i.e.:

$$\dot{Q}_{cool} = f_1 (T_g, T_c, T_{ch,in}) \qquad (7.2.1)$$

$$\dot{Q}_{gen} = f_2 (T_g, T_c, T_{ch,in}) \qquad (7.2.2)$$

$$T_{ch} = T_{ch,in} - \frac{\dot{Q}_{cool}}{(\dot{m}C_p)_{ch}} \qquad (7.2.3)$$

Second, it would be necessary to develop a more detailed fan coil model which calculates the rate of heat transfer and the coil surface temperature as functions of air and chilled water temperatures and flow rates:

$$\dot{Q}_{coil} = f_3 (T_{ch}, \dot{m}_{ch}, T_{air}, \dot{m}_{air}) \qquad (7.2.4)$$

$$T_s = f_4 (T_{ch}, \dot{m}_{ch}, T_{air}, \dot{m}_{air}) \qquad (7.2.5)$$

The total rate of heat transfer at the coil, $\dot{Q}_{coil}$, would be divided into sensible and latent components, $\dot{Q}_{sens}$ and $\dot{Q}_{lat}$, using the straight line law described in Chapter 3. During a simulation, TRNSYS would iterate until $\dot{Q}_{cool}$ was equal to $\dot{Q}_{coil}$.

7.2.2 Part-Load Control Based on Firing Water Flow Rate

In a large multizone air conditioning system, part-load chiller control would probably not be accomplished by an on-off thermostat. A more common form of part-load control would be to reduce the firing water flow rate to maintain a constant air temperature leaving the fan coil, or a constant chilled water delivery temperature.

If the assumption made in Chapter 2 that the firing water

capacitance rate is greater than the weak solution capacitance rate is relaxed, then equation 2.2.1 becomes

$$\dot{Q}_{gen} = \varepsilon_g \, (\dot{m}C_p)_{min} \quad (T_{hw}-T_2) \tag{7.2.6}$$

where

$$\varepsilon_g = \quad ((\dot{m}C_p)_{hw}, \quad (\dot{m}C_p)_{ws}) \tag{7.2.7}$$

and $(\dot{m}C_p)_{min}$ is the lower value of the weak solution of firing water capacitance rates.

Following the analysis of Chapter 2 with equation 7.3.6 inserted instead of 2.2.1 yields new expressions for τ_h and $T_{g,ss}$:

$$\tau_h = \frac{C_g}{\varepsilon_s\varepsilon_g \, (\dot{m}C_p)_{min} + (\dot{m}C_p)_{ws} \, (1-\varepsilon_g)} \tag{7.2.8}$$

$$T_{g,ss} = \frac{\varepsilon_g(\dot{m}C_p)_{min} \, T_{hw} + [(\dot{m}C_p)_{ws} - \varepsilon_g(\dot{m}C_p)_{min}](1-\varepsilon_s)T_a}{\varepsilon_s\varepsilon_g \, (\dot{m}C_p)_{min} + (1-\varepsilon_s)(\dot{m}C_p)_{ws}} \tag{7.2.9}$$

When the firing water capacitance rate is greater than that of the weak solution, equations 7.3.8 and 7.3.9 reduce to equations 2.2.7 and 2.2.8. When the firing water capacitance rate is less than the weak solution capacitance rate, equations 7.2.8 and 7.2.9 indicate that τ_h and $T_{g,ss}$ will depend on $(\dot{m}C_p)_{hw}$.

The only further changes would be to express instantaneous chiller performance as a function of firing water flow rate, and to set the firing water flow rate proportional to an externally provided control signal, i.e.

$$\dot{m}_{hw} = \gamma_{hw}\dot{m}_{hw,max} \tag{7.2.10}$$

$$\dot{Q}_{cool} = f_1\ (T_g,\ T_c,\ T_{ch,in},\ \dot{m}_{hw}) \tag{7.2.11}$$

$$\dot{Q}_{gen} = f_2\ (T_g,\ T_c,\ T_{ch,in},\ \dot{m}_{hw}) \tag{7.2.12}$$

The modifications suggested in Sections 7.2.1 and 7.2.2 would make the chiller model well suited to the study of solar operated central air conditioning in large multizone buildings, as well as in residential applications. Such studies could have a significant effect on the future penetration of solar energy into the air conditioning market.

CHAPTER VIII

Conclusions

8.1 The Transient Chiller Model

A model was developed which predicts the transient performance of a single effect absorption refrigeration unit. The assumptions made in deriving the model lead to a predicted generator temperature history in which generator temperature goes exponentially towards a steady state value. The instantaneous chiller performance is modelled as being a function of the instantaneous condensing water and generator temperatures during chiller operation.

The transient chiller model was incorporated into a subroutine for TRNSYS and used in simulating residential solar air conditioning systems. The model has proven useful in evaluating the effects of startup transients on system performance, and in comparing system performance using different control strategies.

8.2 Effect of Chiller Transients on System Performance

Simulations were run in Miami and Charleston for a three ton chiller using the startup and shutdown time constants of .133 and 1.05 hours, respectively, as estimated for the chiller at CSU House I. The simulations show that chiller transients can lead to a significant reduction in chiller COP. Transients increased the total energy consumption of the chiller by about 3.7% in Miami and 8.2% in Charleston, and decreased the fraction by solar by about 3.7% and 7.2% respectively over the length of a cooling season. The

reduction in COP is most significant under conditions of low cooling load, when the chiller cycles on and off frequently.

When the chiller is controlled by a room thermostat, an increased thermostat deadband will reduce the frequency of cycling and improve the chiller COP. In simulations in Charleston, increaseing the deadband from zero to 2.6°C led to a 6.7% reduction in the total energy requirement of the chiller, and led to a 5% increase in fraction by solar. The optimum thermostat deadband for a given application would be determined by a compromise between energy savings and occupant comfort.

8.3 Control of Auxiliary

A comparison of the series heat, parallel heat, and series-parallel heat auxiliary modes shows that parallel and series-parallel heat auxiliary are preferable to series heat auxiliary. In Miami, over a period from April 1 to November 1, series heat auxiliary required approximately 6% more auxiliary energy than did parallel heat auxiliary. Series-parallel heat auxiliary required about 0.6% less auxiliary than parallel auxiliary in the same location. Any choice between heat and vapor compression auxiliary would have to be based on life cycle costs.

When auxiliary heat is used to operate the chiller, the optimum auxiliary heater set temperature, T_{aux}, was found to be approximately 90°C for the three ton chiller. This value corresponds to the firing water temperature at which that particular chiller had its highest steady state COP.

The optimum value of T_{smin} was found to be 77°C, which is essentially the minimum firing water temperature at which the chiller simulated could successfully be operated. The optimum value of T_{smin} did not appear to depend on collector U_L.

8.4 Summary of Conclusions

The simulations described in this thesis indicate that in Miami, Charleston and Columbia, absorption air conditioning is technically feasible. The graphs of fraction by solar versus collector area in Chapter 4 show that a residence in these locations can achieve a reasonable air conditioning fraction by solar at a reasonable collector area using high performance flat plate collectors with a lithium bromide-water absorption chiller.

System performance is affected by the control strategy employed. Proper choice of room thermostat deadband improves system performance by minimizing chiller cycling. Proper choice of T_{smin} maximizes the solar energy available to run the chiller, and proper choice of T_{aux} minimizes the chiller's auxiliary energy requirements.

The greatest obstacle to solar air conditioning is not technical feasibility, but economics. The economic feasibility of solar air conditioning is outside the scope of this work. From a technical standpoint, however, solar air conditioning seems to hold some promise.

Literature Cited

1. Farber, E.A., Morrison, C.A. and Ingley, H.A. Formulation of a Data Base for the Analysis, Evaluation and Selection of a Low-Temperature Solar Powered Air Conditioning System (NSF/RANN/SE/GI-39323) National Science Foundation, Washington, DC (1974).

2. Auh, P.C., A Survey of Absorption Cooling Technology in Solar Applications (BNL-50704) Brookhaven National Laboratory, Upton, N.Y. (1977).

3. Chung, R., Löf, G.O.G. and Duffie, J.A. "Solar Space Cooling," Chem. Eng. Prog., Vol. 55, No. 4, p. 74 (1959).

4. Butz, L.W. Use of Solar Energy For Residential Heating and Cooling, MS Thesis, University of Wisconsin, Madison, WI (1973).

5. Allen, R.W. and Morse, F.H. Optimization Studies of Solar Absorption Air Conditioning Systems (NSF/RANN/SE/GI-39117/PR/76/2) National Science Foundation, Washington, DC (1976).

6. Löf, G.O.G. and Ward, D.S., Design, Construction and Testing of a Residential Solar Heating and Cooling System (ERDA COO-2577-10), Colorado State University, Fort Collins, CO (1976).

7. Duff, W.S., Evaluation of the Corning and Phillips Evacuated Tubular Collectors in a Residential Solar Heating and Cooling System (ERDA-COO-4012-1), Colorado State University, Fort Collins, CO (1977).

8. Duff, W.S. and Leflar, J.A., Solar Evacuated Tube Collector-Absorption Chiller Systems Simulation (ERDA-COO-2577-13), Colorado State University, Fort Collins, CO (1977).

9. Duff, W.S., Conway, T.M., Löf, G.O.G., Meredith, D.B. and Pratt, R.B. Performance of Residential Solar Heating and Cooling System With Flat Plate and Evacuated Tubular Collectors: CSU House I (ERDA-COO-2577-14), Colorado State University, Fort Collins, CO (1978).

10. Hoover, E.C., Ochs, T. and Bradley, J.O. A Dynamic Simulation Model of LiBr-H_2O Absorption Cooling Devices, Paper presented at DOE System Simulation and Economic Analysis of Solar Heating and Cooling Conference, San Diego, CA (1978).

11. Klein, S.A., Beckman, W.A. and Duffie, J.A. "TRNSYS-A Transient Simulation Program," ASHRAE Transactions, Vol. 32, Part I, p. 623 (1976).

12. Klein, S.A. et al. TRNSYS-A Transient Simulation Program, Engineering Experiment Station Report 38, University of Wisconsin, Madison, WI (1978).

13. ASHRAE Handbook of Fundamentals, American Society of Heating, Refrigeration and Air Conditioning Engineers, New York (1977).

14. ASHRAE Handbook of Fundamentals, American Society of Heating, Refrigeration and Air Conditioning Engineers, New York (1972).

15. Stoecker, W.F., Refrigeration and Air Conditioning (McGraw-Hill Book Company, New York, 1958).

16. ASHRAE Task Group on Energy Requirements, Subroutine Algorithms to Determine Building Energy Requirements, American Society of Heating, Refrigeration and Air Conditioning Engineers, New York (1975).

17. Pawelski, M.J. Development of Transfer Function Load Models and Their Use in Modelling OSU Solar House I, MS Thesis, University of Wisconsin, Madison, WI (1976).

18. Stephenson, D.G. and Mitalas, G.P. "Cooling Load Calculations By Thermal Response Factor Method," ASHRAE Transactions, Vol. 73, Part I (1967).

19. Mitchell, J.W., Personal Communication (1978).

20. Arkla Industries, "Solaire™ 36 Three Ton Absorption Chiller For Solar Air Conditioning," Specification Brochure, Arkla Industries, Inc., Evanston, IN (1976).

21. Ryan, T.A., Joiner, B.L. and Ryan, B.F., MINITAB Student Handbook, Daxbury Press, North Scituate, MA (1976).

22. University of Wisconsin Solar Energy Laboratory, "Weather Tape WDATA." Solar data compiled from National Weather Records Center Card Deck 280 Hourly Record Tape. Surface observations from National Climatic Center TDF-14 (1977).

23. Hottel, H.C. and Woertz, B.B. "Performance of Flat Plate Solar Heat Collectors," TRANS ASME, Vol. 64, pp. 91-104, (1942).

24. Whillier, A. "Design Factors Influencing Solar Collector Performance," Chapter III of Low Temperature Engineering Applications of Solar Energy, ASHRAE (1967).

Appendix A

Transient Chiller TRNSYS Subroutine

```
      SUBROUTINE TYPE7(TIME,XIN,OUT,T,DTDT,PAR,INFO)
      COMMON/SIM/TIMEO,TIMEH,STEP
      DIMENSION XIN(10),OUT(15),PAR(12),INFO(9)
      DIMENSION TGMIN(3),FLOND1(3),CAPMAX(3),CAPY(3),UA(3),THMIN(3)
      DIMENSION B1(3,3),B2(3,3),B3(3,3),C(3,3,3)
      DATA CP/4.19/,CAPY/37930.,139900.,3'6500./,FLOND1
     $ /2420.,10890.,18150./,OAUX/0./
      DATA TGMIN/58.2,55.9,53.6/,CAPMAX/1.,.37,.46,1.2/
     $ ,UA/.0535,.0595,.0503/,THMIN/76.7,73.9,71.1/
      DATA(B1(J,1),J=1,3)/1.405,-3.502344,.100955/
      DATA(B2(J,1),J=1,3)/1.044028,1.883088E-02,-1.3768'9E-03/
      DATA(B3(J,1),J=1,3)/-1.403339E-02,4.01'284E-04,0./
      DATA(B1(J,2),J=1,3)/-22.678,2.17333,-5.455935E-02/
      DATA(B2(J,2),J=1,3)/-.1356349,-4.524715E-03,7.33297'E-04/
      DATA(B3(J,2),J=1,3)/3.1235'9E-05,-2.772443E-04,0./
      DATA(B1(J,3),J=1,3)/-93.452,5.7072277,-9.051727E-02/
      DATA(B2(J,3),J=1,3)/1.453535,-7.537113E-02,1.105583E-03/
      DATA(B3(J,3),J=1,3)/-2.92'935E-03,6.662707E-05,0./
      DATA((C(J,K,1),K=1,3),J=1,3)/5.048,-1.92',4.2906'1E-02,
     $ .4264,1.5227'5E-02,-5.695471E-04,-5.250574E-03,
     $ 1.304397E-04,0./
      DATA((C(J,K,2),K=1,3),J=1,3)/-15.06,-.338853,2.083'E-02,
     $ .69752,-7.5'6229E-03,-2.852'73E-04,-5.37577E-03,
     $ 1.65533E-04,0./
      DATA((C(J,K,3),K=1,3),J=1,3)/2.332,-.684302,
     $ 1.30'80'E-02,.1238894,7.9557'1E-03,-1.858274E-04
     $ ,-2.065043E-03,2.435798E-05,0./
      COP(TG,TC,K)=C(1,1,K)+C(1,2,K)*TC+C(1,3,K)*TC*TC+(C(2,1,K)
     $ +C(2,2,K)*TC+C(2,3,K)*TC*TC)*TG+(C(3,1,K)+C(3,2,K)*TC
     $ +C(3,3,K)*TC*TC)*TG*TG
      AFLAG=0.
      OAUX=0.
      INFO(6)=6
      IF (INFO(7).LT.0)TINIT=PAR(4)
      IF (INFO(7).EQ.0)TINIT=OUT(6)
      IF(INFO(7).GT.0)GO TO 20
      GO TO 25
20    TINIT=OUT(14)
25    INFO(9)=1
      KAPY=PAR(1)
      IF((KAPY.LT.1.OR.KAPY.GT.3).AND.INFO(7).LT.0)CALL TYPECK
     $ (-4,INFO,0,0,0)
      TTMH=PAR(2)
      TTMC=PAR(3)
      THOT=XIN(1)

      TWB=XIN(2)
      TAMB=XIN(3)
      TCOND=TWB+5.55

      IF(TCOND.GT.32.2)GO TO 30
      IAUX=PAR(5)
      BAND=PAR(7)
      TAUX=PAR(8)
      TTMIN=PAR(9)
      IF(TTMIN.LT.THMIN(KAPY))TTMIN=THMIN(KAPY)
      SIZE=PAR(10)
      IF(SIZE.LT.3'6500.)GO TO 28
      KAPY=3
      CAPY(3)=SIZE
      FLOND1(3)=.05735*SIZE
      LOFLAG=1
      OAUX=0.
      IF(INFO(7).EQ.-1)L1=1
      IF (INFO(7).EQ.0)L1=IFIX(OUT(11))
      IF(INFO(7).GT.0)L1=IFIX(OUT(12))
      IF((THOT.LE.TTMIN+BAND).AND.(L1.EQ.0))LOFLAG=0
      IF(THOT.LE.TTMIN)LOFLAG=0
```

```
      ON=1.
      IF((IABS(IAUX).EQ.4).AND.(LOFLAG.EQ.0))ON=0.
      IF(ON.LT.0.5)GO TO 30
      IF(IAUX.LT.0)GO TO 40
      IF(IAUX.EQ.0.OR.IAUX.GT.4)CALL TYPECK(-4,INFO,0,0,0)
      IF(INFO(7).EQ.-1)CALL TYPECK(1,INFO,4,10,0)
      QLOAD=XIN(4)
      FLOAD=QLOAD/CAPY(KAPY)
      IF(QLOAD.GT.0.)GO TO 50
C NO LOAD, UNIT DOES NOT OPERATE
      ON=0.
30    FLOW=0.
      TCOLD=THOT
      TGFIN=TAMB+(TINIT-TAMB)*EXP(-STEP/TIMC)
      QCOOL=0.
      QGEN=0.
      GO TO 3000
40    ON=XIN(4)
      AUXON=XIN(5)
      IF(LOFLAG.EQ.0)AUXON=1.
      IF (IAUX.LT.-4)CALL TYPECK(-1,INFO,0,0,0)
      IF(INFO(7).EQ.-1)CALL TYPECK(1,INFO,5,10,0)
42    IF(ON.LT.0.5)GO TO 30
      FLOAD=CAPMAX(KAPY)
50    FLOW=FLOW1(KAPY)
      TGENIN=THOT
      IF(TGENIN.GT.95.1)TGENIN=96.1
      IF(TCOND.LT.23.9)TCOND=23.9
      A1=B1(1,KAPY)+B1(2,KAPY)*TCOND+B1(3,KAPY)*TCOND**2
      A2=B2(1,KAPY)+B2(2,KAPY)*TCOND+B2(3,KAPY)*TCOND**2
      A3=B3(1,KAPY)+B3(2,KAPY)*TCOND+B3(3,KAPY)*TCOND**2
      IF(IAUX.EQ.4.OR.IAUX.EQ.-4) GO TO 90
      IF(IAUX.LT.0)GO TO 60
      TS=.83*TGENIN+.17*TCOND
      IF(LOFLAG.EQ.0)AFLAG=1.
      IF(A1+A2*TS+A3*TS*TS-QLOAD/CAPY(KAPY))53,53,65
53    IF(TAUX.GT.THOT)AFLAG=1.
      GO TO 65
60    IF(AUXON.GT.0.5.AND.TAUX.GT.THOT)AFLAG=1.
65    IF(IABS(IAUX).EQ.1.OR.(IABS(IAUX).EQ.3.AND.TGENIN.GE.PAR(5)))
     $ QAUX=FLOW*CP*(TAUX-THOT)*AFLAG
      TGENIN=THOT+(TAUX-THOT)*AFLAG
90    CONTINUE
1000  TS=0.83*TGENIN+0.17*TCOND
      IF(ABS(TS-TG1IN(KAPY) ).LE..1)TS=TG1IN(KAPY)+.1
      TGFIN=TS+(TINIT-TS)*EXP(-STEP/TIMH)
      TGAVG=TS+(TIMH/STEP)*(TINIT-TS)*(1.-EXP(-STEP/TIMH))
      IF(ABS(TS-TINIT).LE.1.)GO TO 1040
      IF (TINIT.LT.TG1IN(KAPY).AND.ABS(TS-TG1IN(KAPY)).LT.1.)GO TO 1080
      IF(TGAVG.GT.TG1IN(KAPY).AND.TGFIN.GT.TG1IN(KAPY).
     $ AND.TINIT.GT.TG1IN(KAPY))GO TO 1040
      GO TO 1050
1040  CAPAV=A1+A2*TGAVG+A3*TGAVG**2
      IF(TGAVG.LT.TG1IN(KAPY))GO TO 1095
      IF(CAPAV.GT.CAPMAX(KAPY))CAPAV=CAPMAX(KAPY)
      IF(CAPAV.GT.FLOAD) GO TO 1045
      QNOR1=CAPAV/COP(TGAVG,TCOND,KAPY)
      GO TO 1100
1045  FRAC=FLOAD/CAPAV
      CAPAV=CAPAV*FRAC
      QNOR1=CAPAV/COP(TGAVG,TCOND,KAPY)
      TGFIN=TAMB+(TINIT+(TGFIN-TINIT)*FRAC-TAMB)*EXP(-STEP*(1.-FRAC)/
     $ TIMC)
      GO TO 1100
```

```
'080      IF(TINIT.GT.TGMIN(KAPY).AND.TGFIN.LT.TGMIN(KAPY))GO TO '090
'085    CAPAV=0.
        QNORM=UA(KAPY)*(TGENIN-TGAVG)
        GO TO '100
'090      TIMEOP=-TIMH*ALOG((TGMIN(KAPY)-TS)/(TINIT-TS))
        TAVOP=TS+(TIMH/TIMEOP)*(TINIT-TGMIN(KAPY))*EXP(-TIMEOP/TIMH)
        FRAC=TIMEOP/STEP
'095    CAPAV=A1+A2*TAVOP+A3*TAVOP**2
        IF(CAPAV.GT.CAPMAX(KAPY))CAPAV=CAPMAX(KAPY)
        CAPAV=CAPAV*FRAC
        IF (CAPAV-FLOAD)'096,'095,'097
'097    TGFIN=TS+(TAVOP-TS)*EXP(-TIMEOP*('.-FLOAD/CAPAV)/TIMC)
        CAPAV=FLOAD
'096    Q2=CAPAV/COP(TAVOP,TCOND,KAPY)
        Q1=UA(KAPY)*(1-FRAC)*(TGENIN-TGAVG)
        QNORM=Q1+Q2
'100    QGEN=QNORM*CAPY(KAPY)
        QCOOL=CAPAV*CAPY(KAPY)
        IF(IABS(IAUX).EQ.2.OR.(IABS(IAUX).EQ.3.AND.THOT.LT.PAR(6) ))
     1  QAUX=QGEN*AFLAG
        TCOLD=THOT-(QGEN-QAUX)/(FLOW*CP)
200     GO TO 3000
C SET OUTPUTS
3000      OUT(1)=QCOOL
        OUT(2)=QGEN
        OUT(3)=TCOLD
        OUT(4)=FLOW
        OUT(5)=QAUX
        OUT(14)=TINIT
        OUT(6)=TGFIN
        OUT(11)=FLOAT(LOFLAG)
        OUT(12)=FLOAT(L1)
        RETURN
        END
```

Appendix B

Room Load Model TRNSYS Subroutine

```
C.
      SUBROUTINE TYPE19(TIME,XIN,OUT,T,DTDT,PAR,INFO)
C  THIS ROUTINE MODELS THE INTERIOR OF A SPACE TO BE HEATED
C  OR COOLED. MODE 1 IS COMPATIBLE WITH ENERGY RATE CONTROL
C  AND MODE 2 IS COMPATIBLE WITH TEMPERATURE LEVEL CONTROL.
C  ASHRAE'S TRANSFER FUNCTION METHOD OF DISTRIBUTING
C  TIME DEPENDANT HEAT GAINS IS USED.
      REAL KT
      DIMENSION XIN(10),DTDT(2),T(2),OUT(20),PAR(20),INFO(9),QST(4)
      DIMENSION DIST(4,3,4),W(3,4),Q(4,4),QT(4,4),FC(4)
      COMMON /SIM/TIME0,TFINAL,DELT
      P1(Z)=-7.90298*(Z-1.0)
      P2(Z)=5.02803*ALOG10(Z)
      P3(Z)=-1.3316E-07*(10.**(11.344*(1.-1./Z))-1.)
      P4(Z)=8.1328E-03*(10.**(-3.49149*(Z-1.))-1.)
      P5(Z)=-9.09718*(Z-1.)
      P6(Z)=-3.56654*ALOG10(Z)
      P7(Z)=.873693*(1.-1./Z)
       DATA IUNIT/0/
      DATA Q/16*0.0/
      DATA QT/16*0.0/
      DATA W/1.000,1.000,1.000,   -1.8260,-2.1092,-2.2908,   1.0697,1.46
     106,1.7252,   -0.2005,-0.5331,-0.4277/
      DATA DIST/0.2727,0.3932,0.3173,0.325',0.2217,0.7108,0.2605,0.2574,
     '0.2155,0.7035,0.2430,0.2503,  -0.3400,-1.2017,-0.4507,-0.4267,-0.
     23354,-1.4455,-0.4652,-0.4038,-0.3712,-1.5638,-0.5085,-0.4445,
     30.''69,0.6317,0.2089,0.'524,0.'448,0.9639,0.2819,0.'330,0.'700,1.'
     4373,0.3547,0.2255,-0.0064,-0.''50,-0.0328,-0.0073,-0.0'28,-0.2'08,
     5-0.0579,-0.0'33,-0.0'66,-0.2693,-0.0825,-0.0245/
       IF (INFO(7).GE.0) GO TO 403
       INFO(9) = '
       P8=-2.2'99
        IF (IUNIT.NE.0) CALL TYPECK(6,INFO,0,0,0)
        IUNIT=INFO(1)
       N=INFO(3)
       MODE=PAR(1)
       IF (MODE.LT.1.OR.MODE.GT.2) CALL TYPECK(4,INFO,0,0,0)
       VOL=PAR(2)
       RATE = PAR(3)
       AREA=PAR(4)
       IC = PAR(5)
       CAPAC = PAR(6)
       SUMUA = PAR(7)
       TBASE = PAR(8)
       DEPTH = PAR(9)
       PERIM = PAR('0)
       TGRD=PAR('1)
        GO TO (50',502),MODE
50'     TMIN=PAR('4)
       TMAX=PAR('5)
       TO=PAR('6)
       GO TO 503
502    OMIN=PAR('4)
       EFF=PAR('5)
       CPH=PAR('6)
       CAPHUM=PAR('9)
C      CAPHUM=ROOM MOISTURE CAPAC. IN EQUIV. KG DRY AIR =
C      DERIV OF TOTAL ROOM MOISTURE WRT ROOM ABS. HUMIDITY
503     IFC=PAR('7)
       WDOT=PAR('8)
       GO TO (40',402),MODE
40'     CONTINUE
C.  TYPECK CALLS FOR MODE='
       TRN=PAR('5)
       TROOM=TRN
```

```
      OUT(2)=TRN
      CALL TYPECK(',INFO,N,'8,0)
      INFO(5)=3
      GO TO 403
402   CONTINUE
C.  TYPECK CALLS FOR MODE=2
      CALL TYPECK(',INFO,N,20,2)
      INFO(5)=5
403    CONTINUE
       DO 44 J='1,4
44     FC(J)='1.0
      GO TO ('1,2),MODE
'1     CONTINUE
C.  READ INPUTS
      M=0
      K='1
      IF (N .EQ. 6) K=0
      GO TO 5
    2 M=3
      K='1
      IF (N .EQ. 9) K=0
      THI=XIN(1)
      FLWH=XIN(2)
      QAC=XIN(3)
      TROOM=T(1)
    5 TAMB=XIN(M+'1)
      QST(2)=XIN(M+2)
      QST('1)=XIN(M+3)
      QST(3)=XIN(M+4) + PAR('2)
      QST(4)=XIN(M+5) + PAR('3)*230.0
      RH=XIN(M+5)/'00.
       QSTSUM=0.
       DO 45 J='1,4
45     QSTSUM=QSTSUM+QST(J)
      QL=0.0
      IF (K .EQ. 0) GO TO '0
      L=M+7
      DO 8  I=L,N
    8 QL=QL + XIN(I)
'0     CONTINUE
      REM=ABS(TIME-IFIX(TIME))
      IF (REM.GT.0.00'.OR.INFO(7).GT.0) GO TO 405
      KT=SUMUA/PERIM*0.'6'
       IF (QSTSUM.LE.0.0.OR.IFC.EQ.0) GO TO '14
C.  DEFINE FC COEFFICIENTS FOR AIR CONDITIONING LOADS AS IN ASHRAE
       FC('1)='.0-0.0'9*KT
       FC(2)='.0-0.0'6*KT
       FC(3)='.0-0.022*KT
       FC(4)='.0-0.025*KT
'14    CONTINUE
      DO '4 J='1,4
      DO '2 I='1,3
      K=5-I
      Q(J,K)=Q(J,K-'1)
      QT(J,K)=QT(J,K-'1)
   '2 CONTINUE
      Q(J,'1)=QST(J)
   '4 CONTINUE
   '5 DO 30 J='1,4
      S'=0.0
      S2=0.0
      DO 20 I='1,4
   20 S'=S' + DIST(J,IC,I)*FC(J)*Q(J,I)
      DO 25 I=2,4
   25 S2=S2 + W(IC,I)*QT(J,I)
      QT(J,'1)=S' - S2
   30 CONTINUE
```

```
      QLD=QT(1,1) + QT(2,1) + QT(3,1) + QT(4,1)
405   CONTINUE
C     RELATIVE-TO-ABSOLUTE HUMIDITY PROCESSOR
      TABS=TAMB+273.16
      IF(TAMB)310,310,320
310   Z=273.16/TABS
      PSAT=10.**(P5(Z)+P6(Z)+P7(Z)+P8)
      GO TO 330
320   Z=373.16/TABS
      PSAT=10.**(P1(Z)+P2(Z)+P3(Z)+P4(Z))
330   WAMB=.622*RH*PSAT/(1.-RH*PSAT)
C     LATENT LOAD CALCULATION
      QLAT=(RATE*VOL*1.204*(WAMB-.012)+WDOT)*2468.
      QINFL=RATE*VOL*1.2185*(TAMB - TROOM)
      QBASE=0.
      IF(IBASE) 35,50,40
   35 QBASE=PERIM*2.1633*(TAMB - TROOM)
      GO TO 50
   40 CONTINUE
      QBSWL=PERIM*DEPTH*1.136*((TGRD + TAMB)/2.0 - TROOM)
      QBSFR=AREA*1.135*(TGRD - TROOM)
      QBASE=QBSWL + QBSFR
50    CONTINUE
      QLOAD=QL + QLD + QINFL + QBASE
      IF(MODE.EQ.2) GO TO 205
   55 CONTINUE
      IF(MODE .EQ. 2) GO TO 205
C.    SAVE TROOM FROM PREVIOUS TIMESTEP IN OUT(15)
      IF (INFO(7).GT.0) GO TO 56
      OUT(15)=OUT(2)
   56 CONTINUE
      TROOM=OUT(15)
      TRN=TROOM+QLOAD*DELT/CAPAC
      IF(TRN.LT.TMIN) GO TO 100
      IF(TRN.LE.TMAX) GO TO 130
      TRN=TMAX
      QLOAD=QLOAD+(TROOM-TMAX)*CAPAC/DELT
      GO TO 150
  100 TRN=TMIN
      QLOAD=QLOAD+(TROOM-TMIN)*CAPAC/DELT
      GO TO 150
  130 QLOAD=0.
  150 OUT(1)=QLOAD
      OUT(2)=TRN
      OUT(3)=QBASE
      IF(QLAT.LT.0)QLAT=0.
      OUT(4)=QLAT
      OUT(5)=QLOAD+QLAT
      IF(QLOAD.LE.0.)OUT(5)=QLOAD
C OUT(5)=TOTAL AC LOAD IF POSITIVE AND HEATING LOAD IF NEGATIVE
      RETURN
  205 CONTINUE
      CFLOW=FLWH*CPH
      IF(CFLOW.LT..01) GO TO 210
      QTRAN=CMIN*EFF*(THI-T(1))
      TOUT=THI-QTRAN/CFLOW
      GO TO 220
  210 TOUT=THI
      QTRAN=0.0
  220 IF(INFO(7).GT.-1)GO TO 230
      TCOIL=PAR(20)
      IF(TCOIL)222,222,223
  222 ZC=273.16/(TCOIL+273.16)
      PSC=10**(P5(ZC)+P6(ZC)+P7(ZC)+P8)
      GO TO 224
  223 ZC=373.16/(TCOIL+273.16)
      PSC=10**(P1(ZC)+P2(ZC)+P3(ZC)+P4(ZC))
```

```
224   WCOIL=.622*PSC/(1.-PSC)
      OUT(10)=WCOIL
230   WCOIL=OUT(10)
      IF(T(2).LE.WCOIL)GO TO 233
      QLINE=1.0E2*(TROOM-TCOIL)+2463.*(T(2)-WCOIL)
      GO TO 234
C NO DEHUMIDIFICATION
233   QLINE=1.0E2*(TROOM-TCOIL)
234   SRATIO=1.0E2*(TROOM-TCOIL)/QLINE
      QACS=SRATIO*QAC
      QACL=(1.-SRATIO)*QAC
      QEXS=QLOAD+QTRAN-QACS
      DTDT(1)=QEXS/CAPAC
      DTDT(2)=(RATE*VOL*1.204*(WAIB-T(2))+WDOT-QACL/2468.)/CAPHUM
300   OUT(1)=TOUT
      OUT(2)=FLWH
      OUT(3)=QEXS
      OUT(4)=TROOM
      OUT(5)=QTRAN
      OUT(6)=QBASE
      OUT(7)=T(2)
C T(2) IS ROOM ABSOLUTE HUMIDITY
      OUT(8)=QACS
      OUT(9)=QACL
      RETURN
      END
```

Appendix C

Typical TRNSYS Simulation Deck

```
SIMULATION 2'62 7295 .25
UNIT 1 TYPE 9 DATA READER
PARAMETERS 7
6 ' 2 3.6 0 '0 '
(1X,T'4,F2.0,T20,F4.0,T28,F2.0,1X,2F6.',T49,F3.0)
UNIT 2 TYPE '6 RADIATION PROCESSOR
PARAMETERS 20
' 90 32.8 4870 .3 0 32.8 0 90 0 90 90 90 '80 90 -90 25 '80
25 0
INPUTS '
',2
0
UNIT 3 TYPE ' COLLECTOR
PARAMETERS 7
' 35 .9 4.'9 .95 '4.4 .95
INPUTS 4
6,' 6,2 ',4 2,'
90 0 22 0
UNIT 4 TYPE 4 2-NODE STORAGE TANK
PARAMETERS 5
2.625 '5 4.'9 '000 '
INPUTS 5
5,' 5,2 20,' 20,2 ',4
22 0 22 0 22
DERIVATIVES 2
95 90
UNIT 5 TYPE '3 RELIEF VALVE
PARAMETERS 2
'00 4.'9
INPUTS 3
3,' 3,2 3,'
22 0 22
UNIT 6 TYPE 3 PUMP
PARAMETERS '
'750
INPUTS 3
4,' 4,2 7,'
90 0 0
UNIT 7 TYPE 2 PUMP CONTROLLER
PARAMETERS 3
```

```
4 0 0
INPUTS 3
3,1 4,1 7,1
22 90 0
UNIT 8 TYPE 7 ABSORPTION CHILLER
*3 TON, IAUX=-2
*TIMH=.133 HR, TIMC=1.05 HR
PARAMETERS 10
1 .133 1.05 22 -2 90 3. 95 77 0
INPUTS 5
4,3 1,5 1,4 25,1 14,1
95 20 22 0 0
UNIT 17 TYPE 11 FLOW SPLITTER
PARAMETERS 1
2
INPUTS 3
4,3 4,4 13,3
95 0 0
UNIT 18 TYPE 3 SPACE HEATING PUMP
PARAMETERS 1
1200
INPUTS 3
17,1 17,2 13,1
95 0 0
UNIT 19 TYPE 15 PARALLEL AUX SPACE HEATER
PARAMETERS 5
-1 40000 0 1 -3
INPUTS 1
13,2
0
*40000 KJ/HR
UNIT 20 TYPE 11 TEE PIECE
PARAMETERS 1
1
INPUTS 4
8,3 8,4 12,1 12,2
95 0 95 0
UNIT 9 TYPE 17 4 WALLS
PARAMETERS 25
2 .3 .3 4 2 44.6 44.6 44.6 44.6 .8 1 .12 .12 .12 .12 0 0 0 0
.02069 .05369 .013 1 .0000
-.5387 .06334
INPUTS 7
1,4 2,8 2,9 2,10 2,11 1,3 12,4
22 0 0 0 0 3 22
UNIT 10 TYPE 18 ROOF
PARAMETERS 13
1 1 .3 .3 42.8 17.7 42.8 17.7 98 80 2 25 25
INPUTS 8
1,4 2,13 2,9 2,12 2,11 1,3 3,1 12,4
```

```
22 0 0 0 0 3 22 22
UNIT 12 TYPE 19 ROOM WITH LATENT LOAD
PARAMETERS 20
2 408 .5 83.7 ' '5000 '0'6 0 0 '78.4 2' 2450 4 5023 .6 4.'9 0 .5 5000 7.
INPUTS 10
'8,' '8,2 8,' ',4 '',' 9,3 0,0 0,0 ',6 '9,'
20 0 0 20 0 0 0 0 90 0
DERIVATIVES 2
22 .007
UNIT '3 TYPE 8 THERMOSTAT (2 STG HT +'ST STG COOL)
PARAMETERS 6
4 ' 0 24.5 20 '9
INPUTS 2
12,4 4,3
23 95
UNIT '4 TYPE 2 SECOND STAGE COOLING CONTROLLER
*TURNS ON AT 26 C
PARAMETERS 3
4 0 0
INPUTS 3
'2,4 0,0 '4,'
23 26.0 0
UNIT '' TYPE '5 CONDUCTION SUMMATON
PARAMETERS '
3
INPUTS 2
9,2 '0,2
0 0
UNIT '6 TYPE 25 PRTINTERRERER
PARAMETERS '
0
INPUTS '0
',4 ',6 '2,3 '2,4 '2,7 8,' 8,2 '2,5 '9,2 4,7
TAMB RH QEXS TRN WRM QCOOL QGEN QTRAN HTAUX DELTAE
UNIT 22 TYPE 28 SUMMARY
PARAMETERS 24
-' 2'62 '0000 0 -'' -4 -'2 -4 -'3 -4 -'4 -4 -'5 -4 -'6 -4 -'7 -4 -'8 -4
-'9 -4 -20 -4
INPUTS '0
8,2 8,' 8,5 3,3 4,5 4,6 5,3 '3,3  '2,8 '2,9
LABELS '0
QGEN QCOOL QAUX QU QLOSS QDELIV QDUMP TIMEAC QACS QACL
UNIT 30 TYPE 28 HEATING SUMMARY
PARAMETERS 8
-' 2'62 '0000 0 -'' -4 -'2 -4
INPUTS 2
'2,5 '9,3
LABELS 2
QHT QHTAUX
UNIT 2' TYPE 27 HISTOGRAM
PARAMETERS ''
' 5'36 '0000 2'62 '0000 '9 35 '6 68 '00 '6
INPUTS 2
'2,4 4,3
23 90
*TROOM,TTANK
LIMITS '5 4
TOLERANCES .005 .005
UNIT 25 TYPE 2 FIRST STAGE COOLING CONTROLLER WITH DEADBAND
PARAMETERS 3
4 0 0
INPUTS 3
'2,4 0,0 25,'
23 24.5 0
*SETPOINT=XIN(2)+PAR(2).COOLING IS COMMANDED UNTIL ROOM TEMP
*FALLS BELOW XIN(2)=SETPOINT-DEADBAND.  PAR(2)=DEADBAND
END
```

Appendix D

Manufacturer's Performance Data for Arkla WF-36

PERFORMANCE DATA
MODEL WF 36

Hot Water Flow ..... 11.0 GPM
Condensing Water Flow ..... 12.0 GPM
Chilled Water Flow ..... 7.2 GPM
Chilled Water Leaving Temperature ..... 45° F

HOT WATER INLET TEMP	HOT WATER OUTLET TEMP	ENERGY INPUT BTU/H	INLET COND. WATER TEMP	DELIVERED CAPACITY BTU/H	DELIVERED CAPACITY TONS	REJECTED HEAT BTU/H
170° F	167.0	15,400	80° F	9,700	0.81	26,100
	167.4	14,500	85° F	6,400	0.53	20,900
	*	*	90° F	*	*	*
175° F	170.7	23,800	80° F	17,300	1.44	41,100
	171.1	21,600	85° F	13,100	1.09	34,700
	*	*	90° F	*	*	*
180° F	174.3	31,200	80° F	24,400	2.03	55,600
	174.8	28,800	85° F	19,400	1.62	48,200
	175.7	23,800	90° F	14,200	1.18	38,000
185° F	178.0	38,400	80° F	31,100	2.59	69,500
	178.5	35,900	85° F	25,600	2.13	61,500
	179.4	30,600	90° F	19,300	1.61	49,900
190° F	181.7	45,800	80° F	36,800	3.07	82,600
	182.2	42,900	85° F	31,300	2.61	74,200
	183.2	37,500	90° F	23,800	1.98	61,300
195° F**	185.3	53,100	80° F	40,600	3.38	93,700
	185.9	50,000	85° F	36,000	3.00	86,000
	186.9	44,300	90° F	27,600	2.30	71,900
200° F	189.3	58,800	80° F	41,800	3.48	100,600
	189.8	56,000	85° F	40,200	3.35	96,200
	190.7	51,000	90° F	30,500	2.54	80,500
205° F	193.4	63,800	80° F	42,000	3.50	105,800
	193.9	60,800	85° F	42,000	3.50	102,800
	194.8	56,200	90° F	32,500	2.71	88,700

*Unit operation unstable in these areas. **Lighter area represents conditions for rated capacity.

MODEL WF 36
Pressure Drops vs Water Flows
For Pump Sizing

FLOW, GPM	PRESSURE DROP, FEET OF WATER		
	CHILLED WATER	HOT WATER	CONDENSING WATER
4	1.7 Min.		
5	2.5	2.6 Min.	
6	3.4	3.7	
7	4.4	4.7	
7.2	4.6		
8	5.5	5.9	
9	6.8	7.1	5.8 Min.
10	8.1	8.4	7.0
11	9.4	9.8	8.3
12	10.9	11.2	9.6
13	12.5 Max.	12.8	11.0
14		14.4	12.5
15		16.1	14.2
16		17.8	15.8
22		29.9 Max.	27.4
25			33.9 Max.

ARKLA

Where Progress Is Built On Quality

Arkla Industries Inc.
P.O. Box 534
Evansville, IN 47704

FORM NO. SP 611T-1, NOV. 1976

PRINTED IN USA